

INVESTIGATIONS CONCERNING THE  
NUCLEI OF RaC AND RaC'.

A

THESIS

submitted by

IAN R. CAMERON, B.Sc.

for the degree of

DOCTOR OF PHILOSOPHY.

University of Edinburgh.

April 1958.



## CONTENTS.

### Chapter I.

#### INTRODUCTION.

- |                               |         |
|-------------------------------|---------|
| § 1. General                  | page 1. |
| § 2. The decay of RaB and RaC | page 4. |

### Chapter II.

#### THE DOUBLE $\beta$ -RAY SPECTROMETER.

- |   |          |
|---|----------|
| § 1. Introduction   | page 18. |
| § 2. Description of the spectrometer and associated equipment | page 21. |
| § 3. Calibration of the instrument                            | page 28. |
| § 4. Measurement of the coincidence resolving time            | page 32. |
| § 5. Determination of detector characteristics                | page 33. |

### Chapter III.

#### THE SOURCE PREPARATION.

- |  |          |
|--|----------|
| § 1. General   | page 35. |
| § 2. The source preparation apparatus                            | page 37. |
| § 3. Verification of the "surface layer" character of the source | page 42. |



## Chapter IV.

### THE MEASUREMENTS ON THE $\beta$ -RAY SPECTRA OF RaB AND RaC.

- |   |          |
|---|----------|
| § 1. Summary of techniques  | page 45. |
| § 2. The coincidence measurements on the<br>RaB $\rightarrow$ C transition  | page 46. |
| § 3. The measurements on the continuous<br>spectrum                         | page 52. |
| § 4. The coincidence measurements on the<br>RaC $\rightarrow$ C' transition | page 58. |

## Chapter V.

### THE CONSTRUCTION OF DECAY SCHEMES FOR RaC AND RaC'.

- |   |          |
|---|----------|
| § 1. The RaB $\rightarrow$ C decay  | page 61. |
| § 2. The RaC $\rightarrow$ C' transition                                  | page 71. |
| § 3. Collective and particle excitations<br>in the nuclei of RaC and RaC' | page 92. |

- |                  |           |
|------------------|-----------|
| ACKNOWLEDGEMENTS | page 104. |
| REFERENCES       | page 105. |
| APPENDIX         | page 111. |

CHAPTER I.  
Introduction.

§1. General.

Since the discovery of natural radioactivity among the heavy elements at the end of the periodic table, a considerable volume of research has been devoted to the precise measurement of the energies and relative intensities of the nuclear radiations involved in the disintegration chains. The data obtained from such measurements are of value in providing a systematic basis for evaluation of the factors influencing the binding energies and level structures of the heavy nuclei. In particular spin and parity assignments may be derived from an application of the selection rules for  $\beta$ - and  $\gamma$ -transitions and by use of the results obtained from measurements of the internal conversion coefficients or K/L conversion ratios of the  $\gamma$ -radiation; other measurable effects of the multipolarity of the  $\gamma$ -transition are the mean life of the transition and the angular correlation between successive  $\gamma$ -quanta emitted from the same nucleus.

The binding energies of the nuclei depend on such factors as proximity to the magic numbers 82 and 126, and the odd-evenness of neutron and proton numbers. Consequently, accurate values of the binding energies are essential as an experimental criterion of the

## 2.

effectiveness of any nuclear model in taking account of the basic details of nuclear structure. In particular, the knowledge both of binding energies and of the characteristics of nuclear levels may assist in clarifying the relationship between the nuclear shell model and the effects of collective motion of the nucleons. The simple shell model successfully accounts for the spins and parities of many nuclear levels, and with the assumption of a strong spin-orbit coupling, provides values of the magic numbers which correspond to the values predicted from the sudden changes in the fairly smooth variation of binding energy with neutron and proton number. The introduction of an additional collective motion, however, is necessary to account for the low-lying rotational levels found in regions far away from the closed shells.

Much of the earlier work on the level structures of nuclei was concerned with the study of the fine structure of the  $\alpha$ -particle spectra arising from the transformations. Since each group of  $\alpha$ -particles is effectively monoenergetic, the determination of the energy levels of the daughter nucleus is relatively simple. The continuous nature of the  $\beta$ -spectra, on the other hand, introduced an obvious difficulty, and the earlier investigations of  $\beta$ -active nuclei were concentrated mainly on the examination of the line

### 3.

spectra associated with the continuous component. The line spectra were considered initially to arise from photo-electrons expelled from the atomic electron orbits by monoenergetic  $\gamma$ -quanta emitted from the nucleus, but were later interpreted as due to a direct interaction between the excited nucleus and the atomic shells, without intermediate  $\gamma$ -emission.

For the continuous  $\beta$ -spectrum, in addition to the problems associated with its continuous nature, a further complication arises from the fact that an unfavourable spin change in a  $\beta$ -transition has a much more inhibiting effect than the corresponding change in  $\alpha$ -decay. As a result the daughter nucleus after  $\beta$ -decay generally has a more complicated  $\gamma$ -decay scheme than the daughter nucleus after  $\alpha$ -disintegration. Another effect tending to produce complexity in the level scheme of the daughter nucleus is the much less critical dependence of disintegration constant upon transition energy in  $\beta$ -decay when compared with  $\alpha$ -emission. The ground-to-ground transition may be completely inhibited, and a detailed knowledge of both the  $\beta$ -feeds and the following  $\gamma$ -rays is necessary for the determination of the total disintegration energy.

## § 2. The decay of RaB and RaC.

One of the best-known examples of the complexity arising in the decay of a natural radioelement is the decay chain  $\text{RaB} \rightarrow \text{RaC} \rightarrow \text{RaC}'$  ( ${}^{214}_{82}\text{Pb} \rightarrow {}^{214}_{83}\text{Bi} \rightarrow {}^{214}_{84}\text{Po}$ ). Since it occurs near the end of a radioactive series, the uncertainty in disintegration energy affects the accuracy with which binding energies could otherwise be calculated in the series. One of the earliest detailed surveys was carried out by Rutherford, Lewis and Bowden (1) on the long-range  $\alpha$ -particles of RaC'. Since the long-range  $\alpha$ -particles originate from excited levels of the RaC' nucleus, comparison of the long-range  $\alpha$ -particle energies with the energy of the much more intense transition between the ground states of RaC' and RaD gives a direct indication of the positions of the levels of RaC'. Using a magnetic spectrograph with a source of the radium active deposit formed by the decay of  ${}^{222}\text{Rn}$ , Rutherford and his co-workers demonstrated the existence of twelve groups of long-range  $\alpha$ -particles from RaC'. It was found possible to correlate the more prominent  $\gamma$ -rays known from the conversion electron measurements of Ellis and Aston (2) with the levels postulated from the  $\alpha$ -particle scheme, although it was found necessary to introduce four other levels not subject to de-excitation by the emission of

long-range  $\alpha$ -particles. \*

The first investigations of the internal conversion lines from Ra(B + C) were those of Baeyer, Hahn and Meitner (3), and Rutherford and Robinson (4), but the most detailed survey was carried out over a period of thirteen years by C.D. Ellis and various co-workers. The method used was the spectrometric comparison of the natural spectrum of Ra(B + C) with the corresponding photo-electron spectrum excited in platinum. The final results of this survey (5) contain evidence of 30 internal conversion lines in the spectrum of RaB and 67 in that of RaC.

The measurements of Ellis remained the standard work on the  $\gamma$ -rays of Ra(B + C) until a detailed spectroscopic investigation by G.D. Latyshev and others (6) of the phenomena associated with the interaction of hard  $\gamma$ -rays with matter suggested the existence of  $\gamma$ -transitions not observed by Ellis. The results of Latyshev were based on measurements of (a) Compton electrons liberated from thin radiators; (b) internal conversion electrons; (c) the positrons produced by internal pair production in an ionised atom, the

---

\* The level structure postulated by Rutherford et al., together with the decay schemes of more recent workers, is discussed in greater detail in Chapter V.

electron occupying the formerly unoccupied state, and the positron carrying away the whole of the remaining energy. A great deal of experimental work followed in an attempt to confirm the new features of the decay scheme found by Latyshev. Mann and Ozeroff (7), as a result of measurements on the photo-electrons from a thin Pb radiator by a magnetic spectrometer, found no transitions other than those of Ellis, and Whyte (8) found results in better agreement with Ellis and Aston than with Latyshev. On the other hand, Mladjenovic and Hedgran (9), investigating the Compton electrons ejected from a thin Al radiator, confirmed the existence of all but one of the Latyshev  $\gamma$ -transitions, and Pearce and Mann (10) also found several of the new transitions. Cork et al. (11) carried out a survey of the internal conversion lines from radium, but found only half the lines of Ellis in addition to several new lines; they also failed to detect some of the higher energy  $\gamma$ -rays of Latyshev, probably due to a lack of sensitivity of measurement in that region. A survey by Mladjenovic and Slatis (12) gave better agreement, particularly in respect of intensity, with Ellis than with Cork.

The table overleaf shows the relative intensities quoted by several authors for the more intense  $\gamma$ -rays, the energy values given being those due to Mladjenovic

## 7.

and Slatis, with the exception of the 2.432 MeV  $\gamma$ -ray, found by Mladjenovic and Hedgran (13). The intensities have been normalised to give a value of unity for the 2.2042 MeV  $\gamma$ -ray.

Energy of $\gamma$ -ray (MeV)	Relative Intensity						
	1	2	3	4	5	6	7
0.6093	8.9	-	2.96	-	5.13	-	4.64
0.7687	0.88	-	0.52	-	1.11	-	0.70
0.9348	0.91	-	-	-	0.54	-	0.52
1.1204	2.78	2.41	1.32	-	3.9	-	2.06
1.2383	0.85	0.56	-	-	1.42	-	0.88
1.3782	0.86	1.19	0.92	-	1.66	-	0.72
1.5093	-	0.71	-	-	0.56	-	0.43
1.7644	3.49	2.42	4.0	-	3.14	3.22	2.52
1.8485	-	0.41	-	-	0.33	-	0.28
2.2042	1.0	1.0	1.0	1.0	1.0	1.0	1.0
2.432	-	0.5	-	0.38	0.36	0.48	0.41

The values of the relative intensities quoted in columns 1 - 7 are from the following authors:

1. Ellis and Aston (2)
2. Latyshev (6)
3. Mann and Ozeroff (7)
4. Wolfson (14)
5. Mladjenovic and Hedgran (13)
6. Backenstoss and Wohlleben (15)
7. Dzelepov and Sestopalova (16).



The last of these papers, which was based on measurements on the Compton spectrum of  $\text{RaC}$ , appeared after the present investigation was begun. The authors proposed modifications to the tables of Mladjenovic and Slatis, and confirmed that the totally internally converted  $\gamma$ -ray of 1.414 MeV arose from a  $0 \rightarrow 0$  transition, as first suggested by Fowler (17).

In the determination of the end-points of the  $\beta$ -particle spectra involved in the disintegration of the  $\text{RaC}$  nucleus, a similar degree of uncertainty exists. The original absorption measurements of Sargent (18) gave an end-point energy for the hardest component of 3.15 MeV. A rough analysis of the  $\beta$ -spectrum of  $\text{RaC}$  by Latyshev (6) gave two partial spectra of end-points 3.17 MeV (23%) and 1.65 MeV (77%). The measurements of Kageyama (19) led to the postulation of  $\beta$ -feeds of maximum energies 1.00 MeV (20%), 1.65 MeV (57%), and 3.20 MeV (23%).

Wapstra (20) carried out  $\beta$ - $\gamma$  coincidence-absorption measurements on  $\text{Ra(B + C)}$  and ~~found two  $\beta$ -groups of end point energies 3.173 and 1.65 MeV.~~ <sup>claimed support for</sup> Latyshev's analysis yielding end-points at 3.17 MeV. and 1.65 MeV. In addition, two other  $\beta$ -feeds of energies 1.408 MeV and 1.445 MeV (each of  $\sim 25\%$  intensity), the existence of which was not inconsistent with the absorption measurements, were postulated to account for the known  $\gamma$ -transitions in the daughter nucleus. The  $\beta$ - $\gamma$

coincidence measurements for the 3.173 MeV  $\beta$ -group suggested that any following  $\gamma$ -transition must have an energy  $< 150$  keV. Since the excitation energies of the first excited states of even-even nuclei in this region are considerably higher than 150 keV, this energy varying smoothly with proton and neutron number, Wapstra concluded that the 3.17 MeV transition was the  $RaC \rightarrow C'$  ground-to-ground state transition. This conflicted with the level scheme suggested by Ellis (21), where the 3.17 MeV  $\beta$ -transition led to the 609 keV first excited state, but was in accord with the conclusions of Bothe and Maier-Leibnitz (22). No long-range  $\alpha$ -particle lines have been found corresponding to the three excited levels postulated in the decay scheme of Wapstra (fig. (1)). The author suggested that this was not unreasonable, as the most intense  $\gamma$ -emission would arise from the levels with the shortest half-lives, and thus a weak  $\alpha$ -branching. It must be borne in mind, however, that the probability of  $\alpha$ -emission increases rapidly with energy, as given by the formula due to Feather (23). For a hypothetical  $2+$  state at 1700 keV, for example, the lifetime for de-excitation by  $\alpha$ -emission is less by a factor of the order of 400 than that of the 609 keV state. But even when the ratio of probabilities for de-excitation of a given state by  $\alpha$ - and  $\gamma$ -emission may appear to be

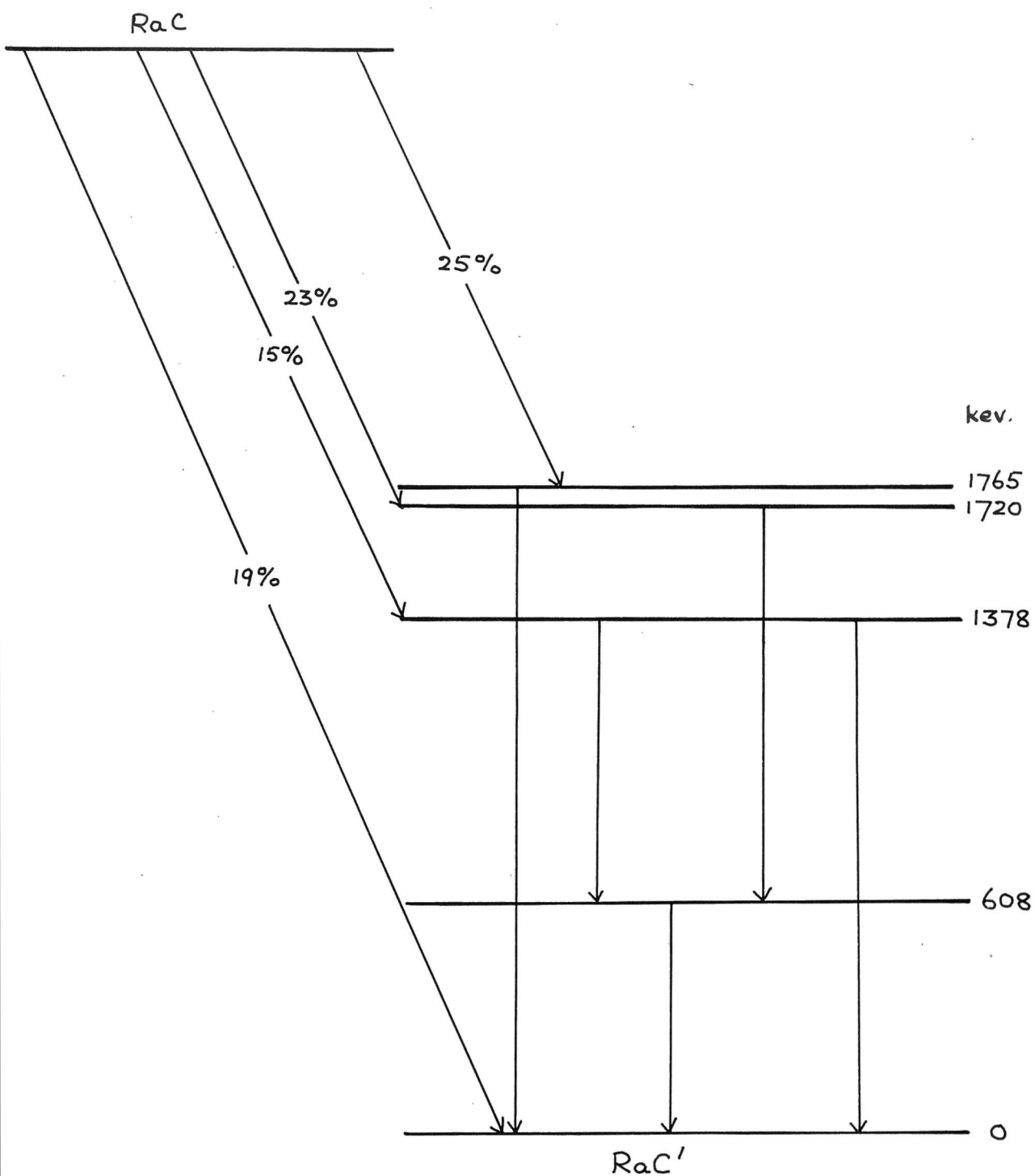


Fig.(1). Decay Scheme of Wapstra for  $RaC$ .

such that an  $\alpha$ -particle group of detectable intensity would be expected to occur, the absence of  $\alpha$ -radiation can be explained by adopting a spin and parity assignment for the state of the form  $(2n) -$  or  $(2n + 1) +$ . Such an assignment would automatically preclude the possibility of  $\alpha$ -particle emission leading to the  $0 +$  ground state of the even-even nucleus of  $\text{RaC}'$ .

Results in disagreement with those of Wapstra were given by Demichelis and Malvano (24) in a series of papers describing  $\gamma$ - $\gamma$  coincidence measurements on  $\text{RaC}'$ . Confirmation appeared to have been obtained for three of the  $\gamma$ -cascades postulated in the Rutherford decay scheme - those of  $0.933 - 1.761$  MeV,  $1.376 - 0.760$  MeV, and  $1.12 - 1.76$  MeV. No evidence was found for the existence of the other two cascades - those of  $1.241 - 0.426$  MeV and  $0.499 - 2.198$  MeV. The existence of the  $1.12 - 1.76$  MeV cascade is in conflict with the results of Wapstra, who failed to find evidence for such a feature in the coincidence-absorption measurements. It had been previously pointed out by Feather and Richardson (25) that the assumption of the existence of the  $1.12 - 1.76$  MeV  $\gamma$ -cascade led to difficulties if the  $3.17$  MeV  $\beta$ -feed were taken to represent the ground-to-ground state transition. If the assumption were made that the  $1.12$  MeV and  $1.76$  MeV  $\gamma$ -rays were in cascade from the  $2.88$  MeV level known from the

measurements of Rutherford, the excitation of this level must arise from a partial  $\beta$ -spectrum of only 0.29 MeV end-point energy. Relating this to the Sargent diagram, it was seen that the maximum possible intensity for the  $\beta$ -feed (allowed transition) was only about 1.5%. The degree of excitation of the 2.88 MeV state required to give the correct intensity for the  $\gamma$ -cascade was  $\sim 20\%$ . If, on the other hand, it was assumed that the 3.17 MeV  $\beta$ -transition led to the first excited state at 609 keV, the maximum energy of the partial  $\beta$ -spectrum became  $\sim 0.90$  MeV, giving an intensity of the correct magnitude if the appropriate spin change were selected. Additional support for the supposition that the 3.17 MeV  $\beta$ -transition reaches the 609 keV excited state was provided by the results of Muller et al. (26), assigning an intensity of approximately 1 quantum per disintegration to the 609 keV  $\gamma$ -transition, although the degree of accuracy of their results does not preclude the possibility of a weak ( $\sim 10\%$ ) ground-to-ground transition.

For the disintegration  $\text{RaB} \rightarrow \text{C}$  ( ${}^{214}_{82}\text{Pb} \rightarrow {}^{214}_{83}\text{Bi}$ ), the postulated decay schemes are much less complex, but some degree of uncertainty does exist, particularly in the assignment of spin and parity to the  $\text{RaC}$  ground state. The initial measurements on the  $\beta$ -spectrum of  $\text{RaB}$  were made by Gurney (27), who obtained a value of

$\sim 650$  keV for the end-point energy; Ellis (21), on the basis of measurements of the  $\gamma$ -rays and conversion electrons, proposed a level scheme for the nucleus of RaC with four excited levels, associated with the well-known  $\gamma$ -transitions. The analysis of Latyshev (6) suggested the existence of a harder  $\beta$ -component of end-point energy in the region of 720 keV. A repeated Fermi analysis by Kageyama (19) suggested the existence of  $\beta$ -particle groups of end-point energies  $650 \pm 10$ ,  $590 \pm 10$  and  $360 \pm 20$  keV, although the author remarked that the actual existence of the last component was doubtful.

The level scheme of Ellis is shown in fig. (2). According to this scheme the  $\text{RaB} \rightarrow \text{C}$  ground-to-ground state  $\beta$ -transition is "unobserved". Some doubt was cast on this conclusion by the results of Gray (28), but the analysis of Feather and Richardson (25) supported the conclusion of Ellis. The argument of Feather and Richardson was based on the assumption that whether the 3.17 MeV  $\text{RaC} \rightarrow \text{C}'$   $\beta$ -transition were taken as representing the ground-to-ground state transition or a transition to the first excited state at 609 keV, ~~it~~ <sup>the ground-to-ground state transition</sup> could be regarded as at least second forbidden. The representative points for the  $\text{RaB} \rightarrow \text{C}$  and  $\text{RaC} \rightarrow \text{C}'$  ground-to-ground transitions must lie on the same band in the Sargent diagram, since the initial and final

	kev.		Excitation.
_____	350	0+	52%
_____	290	0+	47%
_____	257	2+	1%
_____	53	2+	0
_____	0	2+	0

Fig.(2). Level scheme of Ellis for RaC.

states in such a disintegration would both have  $I = 0$  and even parity. Hence it was deduced that the degree of forbiddenness of the  $RaB \rightarrow C$  ground-to-ground state transition was much higher than <sup>corresponded to</sup> the experimental upper limit set for its intensity.

In the decay scheme of Ellis, the four main  $\gamma$ -rays, of energies 53, 242, 295 and 352 keV respectively are now known to be almost pure M1 transitions. The multipole order was given by Mladjenovic and Slatis (12) as M1 with possible E2 admixture, but E2 admixtures of  $> 10\%$  were excluded on account of the absence of  $L_{III}$  conversion lines, since E2 radiation would be strongly converted in the  $L_{III}$  subshell. According to the argument of Feather (29), if the two  $\beta$ -transitions to the levels at 352 keV and 295 keV are accepted as allowed transitions, the ground state of the  $RaC$  nucleus must have even parity and spin 0, 1 or 2. Since a spin of either 0 or 1 would imply the existence of an allowed  $\beta$ -transition from the 0 + ground state of  $RaB$  to the ground state of  $RaC$ , these assignments were unacceptable. A spin value of 2 would have given an allowed transition to the 2 + first excited state of  $RaC'$ , which was again in conflict with the experimental results. It was pointed out that after rejection of all three possibilities, the only assignment consistent with the measured K-conversion coefficient of all four



$\gamma$ -rays was that of 3 - for the ground state. The 53 keV state had then to be considered as a 3 - state also, to preserve the M1 character of the de-excitation radiation. The two upper states were then classified as 0 + states, leading to an E3 character for the higher energy  $\gamma$ -rays, an assignment which disagreed with the experimental K/L ratios.

Wapstra (20) on the other hand, assigned a value of 2 - to the RaC ground state, basing his suggestion on a calculation of the function  $\log (w_0^2 - 1) ft$  ( $w_0$  = transition energy in relativistic units, plus one), for the 3.17 MeV transition in RaC  $\rightarrow$  C' (assumed ground-to-ground) and the 1.75 MeV transition to the 1.414 MeV excited state. The values of this function obtained for both transitions were such as to suggest that they both belonged to the special class of first forbidden transitions characterised by the spin and parity changes  $\Delta I = 2$ , 'yes'. If this conclusion were accepted, the value of  $\log (w_0^2 - 1) ft$  for the 2.56 MeV transition (see fig. (1)) was somewhat high, but it was pointed out by Wapstra that this was also known to occur in some similar cases.

Additional evidence for the 2 - allocation appeared in the measurements of Demichelis and Radicati<sup>(30)</sup> on the angular correlation between the 2.56 MeV  $\beta$  - transition and the 0.609 MeV  $\gamma$ -ray.

Johansson (31), on the other hand, from  $\beta - \gamma$  coincidence measurements on  $\text{Ra}(\text{B} + \text{C})$ , allocated the value  $0 -$  to the ground state of  $\text{RaC}$ , a result in agreement with the value obtained by an application of the method of Nordheim (32) for combination of the spins of individual particles. Johansson derived  $\log ft$  values for the 3.17 MeV  $\beta$ -group and the  $\beta$ -feed to the 609 keV level, and hence estimated the degree of forbiddenness of the two transitions. Taking the ground state of  $\text{RaC}'$  as  $0 +$ , and the 609 keV state as  $2 +$ , the  $\text{RaC}$  ground state must then have the assignment  $0 -$ .

A further possible value for the  $\text{RaC}$  ground state was given in the tables of King (33), where the assignment  $1 -$  was made. This assignment appears to be supported by the  $\beta - \gamma$  coincidence absorption measurements of Ricci and Trivero (34). These authors observed the 2.56 MeV  $\beta$ -branch from the ground state of  $\text{RaC}$  to the 609 keV first excited state of  $\text{RaC}'$ , and obtained a  $\log ft$  value of 7.9 for the transition. In addition they obtained  $\log ft = 7.9$  for the 3.17 MeV ground-to-ground transition. Assuming that both transitions were normal first forbidden, the ground state of  $\text{RaC}$  would have the assignment  $1 -$ . The authors pointed out, however, that if the 3.17 MeV transition were taken as belonging to the special class

of first forbidden transitions ( $\Delta I = 2$ , 'yes') the results were consistent with the assignment 2 - for the ground state of RaC.

The position at the start of the present investigation appeared to be that no direct measurements of the  $\beta$  -feeds to the excited levels of the RaC' nucleus had been performed in sufficient detail to provide a direct correlation with the numerous levels postulated on the basis of the measurements of the  $\gamma$ -rays and long-range  $\alpha$ -particles. After the measurements on the continuous spectrum associated with the RaC  $\rightarrow$  C' transition had been almost completed, papers were published by Daniel and Nierhaus (35), giving the results of a repeated Fermi Analysis of the continuous  $\beta$  -spectrum of RaC, and postulating a decay scheme based on coincidence measurements between the  $\beta$  -particles of the continuous spectrum and the  $\gamma$ -rays or conversion electrons. Discussion of this decay scheme will be deferred to Chapter V, but a satisfactory degree of agreement was obtained with the results of the present investigation, especially in regard to the end-point energies of the component  $\beta$  -spectra.

Recently published results on measurements of coincidences and internal conversion coefficients by Nielsen et al. (36) have also appeared since the present work was begun. Decay schemes for both the

RaC and RaC' nuclei have been constructed on the basis of these measurements. In Chapter V an attempt will be made to correlate the results of the present work with the measurements of Nielsen and also with the decay scheme suggested by Feather (37) on the basis of the  $\alpha$ -particle measurements of Rutherford.

CHAPTER II.The Double  $\beta$ -Ray Spectrometer.§ 1. Introduction.

The investigation was carried out with a modified form of the semi-circular focusing double  $\beta$ -ray spectrometer described by Feather, Kyles and Pringle (38); in its original form the instrument employed Geiger counters as particle detectors, and was used in a survey of the thorium active deposit. Later, in order to facilitate coincidence counting by reducing the resolving time of the apparatus, the Geiger counters were replaced by scintillation counters, and the electronic circuits modified to take advantage of the shorter pulses supplied by the photomultipliers. The redesigned instrument was used in an investigation of the  $\beta$ -particle spectrum of mesothorium by Kyles, Campbell and Henderson (39), and for coincidence measurements on the  $\text{ThC}'' \rightarrow \text{D}$  transition by Knight (40).

The basic problem of  $\beta$ -spectroscopy is the provision of a high degree of resolution while retaining sufficient intensity to achieve a reasonable statistical accuracy in the results. Although the collecting power of the semi-circular instrument cannot compare with that of the magnetic lens spectrometer, it has advantages which compensate for the lower intensity.

The use of a steady magnetic field provided by a permanent magnet enables a very accurate determination of field strength to be made at leisure, and facilitates comparison with standard sources under identical field conditions. Further advantages are the relatively simple way in which the resolution may be changed by variation of slit widths, and the accuracy with which line profiles can be determined due to the small increments in radius of curvature which can be accurately measured. The variable field spectrometer, on the other hand, can be designed to provide the detectors with a greater degree of screening from unwanted  $\gamma$ -radiation, but the effect of  $\gamma$ -ray background was reduced in the present instrument by the use of the proportional properties of the scintillation counters.

The double  $\beta$ -ray spectrometer consists effectively of two single semicircular focusing spectrometers arranged to focus independently electrons emitted from a central source common to both instruments. Each of the crystal detectors is movable through a traverse sufficient to scan a reasonably wide range of electron momenta for a given setting of the magnetic field. For an instrument of this type, the incorporation of movable detectors with a fixed magnetic field is obviously simpler than the use of a fixed geometry system with independently variable fields requiring careful

shielding from each other.

The chief advantage of the instrument lies in its capabilities for clarifying complicated decay schemes by the study of coincidences between either  $\gamma$ -quanta and  $\beta$ -particles or between  $\gamma$ -quanta of different energies. If the  $\gamma$ -ray is sufficiently strongly internally converted, it is possible to focus the appropriate conversion line on one of the detectors, leaving the counter on the other side of the instrument free either to accept the conversion line of another  $\gamma$ -ray, or to scan the portion of the continuous  $\beta$ -spectrum within the momentum range corresponding to the field setting. The latter technique enables one to obtain the end-point energy of a partial  $\beta$ -spectrum in coincidence with a given  $\gamma$ -ray. The study of  $\gamma$ - $\gamma$  coincidences is of value in building up complicated decay schemes by deciding whether a given pair of  $\gamma$ -transitions are competitive or in cascade. One essential condition for the coincidence measurements is that the lifetimes of the excited states from which the  $\gamma$ -rays originate should not be greater than the resolving time of the coincidence set.

In addition to its use for coincidence measurements, either half of the instrument can be used alone for measurements on the continuous spectrum and conversion lines of the source, and when used for this purpose a

high degree of resolution can be obtained by the use of a narrow source and of very fine source and detector slits.

## § 2. Description of spectrometer and associated equipment.

### (a) The Magnet.

The design of the instrument is illustrated in fig. (3). The vacuum box was mounted between the flat rectangular pole pieces of a large permanent cobalt steel magnet originally designed by Cockcroft, Ellis and Kershaw (41). The strength of the field was adjustable by passing current from 230V. D.C. mains through a reversing switch and variable resistance in series with the six energising coils surrounding the laminated steel magnet arms. A current of 15 amps. in each coil provided a field of the order of 2000 oersteds in the air gap between the pole-pieces. In the course of an investigation of a complete spectrum several changes of field were necessary. The existing field was reduced to zero by passing a suitable demagnetising current, and a current of the magnitude required to produce the new field was then passed in the original direction. It was found that the field, once set, showed no detectable variation over periods sufficient for even the longest coincidence runs.



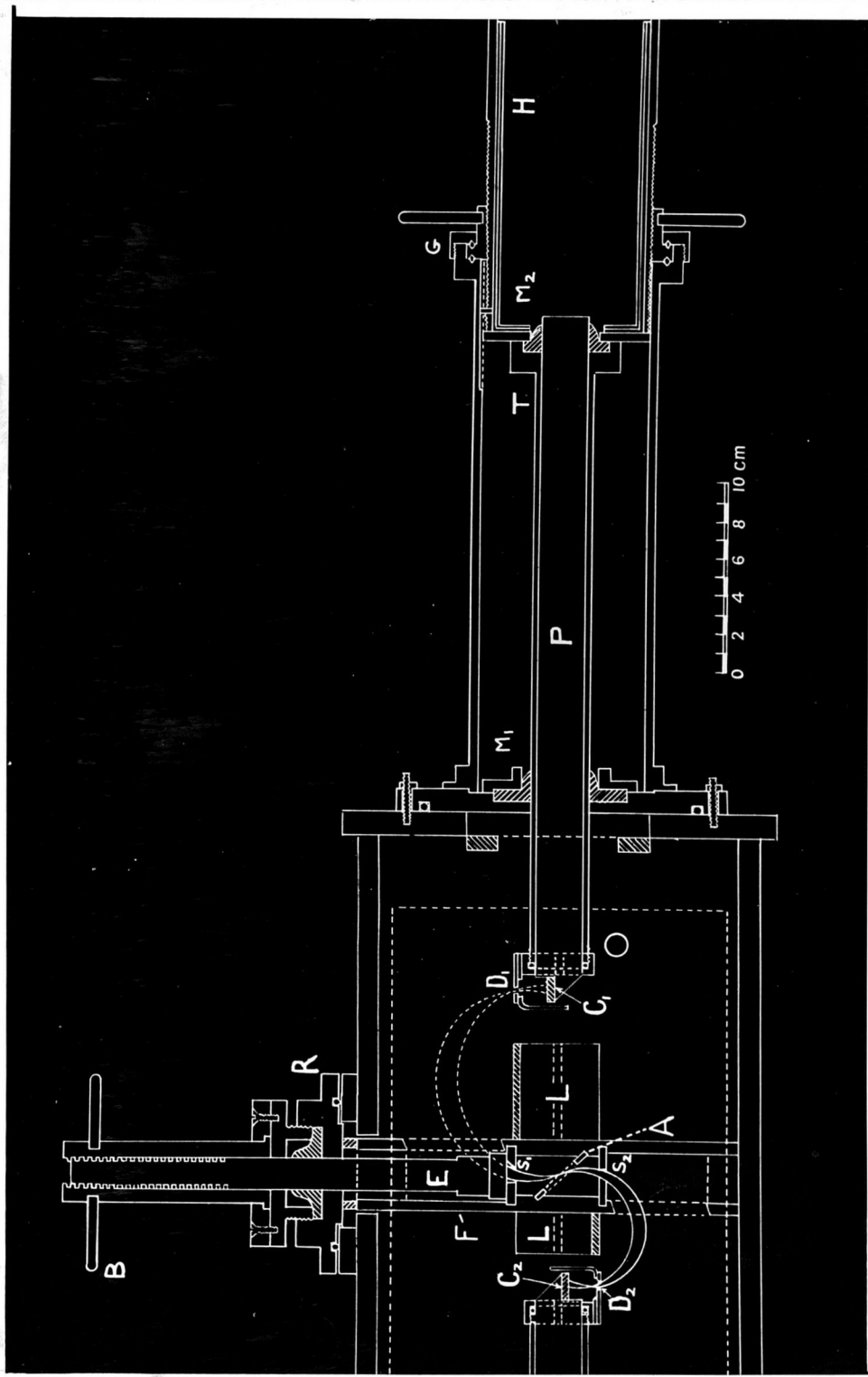


Fig. (3). The double  $\beta$ -ray spectrometer.

(b) The Vacuum Box.

This was a flat, rectangular brass box, lined internally with aluminium, clamped in position between the magnet poles, and evacuated continuously by a two-stage diffusion pump to a pressure of  $10^{-4}$  mm. Hg. The magnetic lines of force are perpendicular to the plane of the diagram. The source, consisting of radon embedded in thin aluminium foil, was mounted on the aluminium frame, A, which fitted into grooves on the source holder F. In the measurements where a high resolving power was of primary importance, the frame A was mounted to give an emission angle of  $45^{\circ}$ , thus ~~increasing~~ <sup>improving</sup> the effective resolution. The source holder, F, (illustrated in plate ( I )), was an aluminium frame of square cross-section fitting into a porthole on the top of the box, and located by lugs sliding in grooves cut in the walls. The source slits  $S_1$  and  $S_2$  selected two sheaves of  $\beta$ -particles which were focused in the planes of the detector slits  $D_1$  and  $D_2$ . The source slits were placed in grooves cut in the sides of the holder F, facilitating the interchange of slits to suit the resolution required. The detector slits were readily adjustable to any desired value. The square porthole was sealed by a neoprene ring fitting into a circular groove in the brass disc, R, which carried an aluminium shutter E. The shutter could be

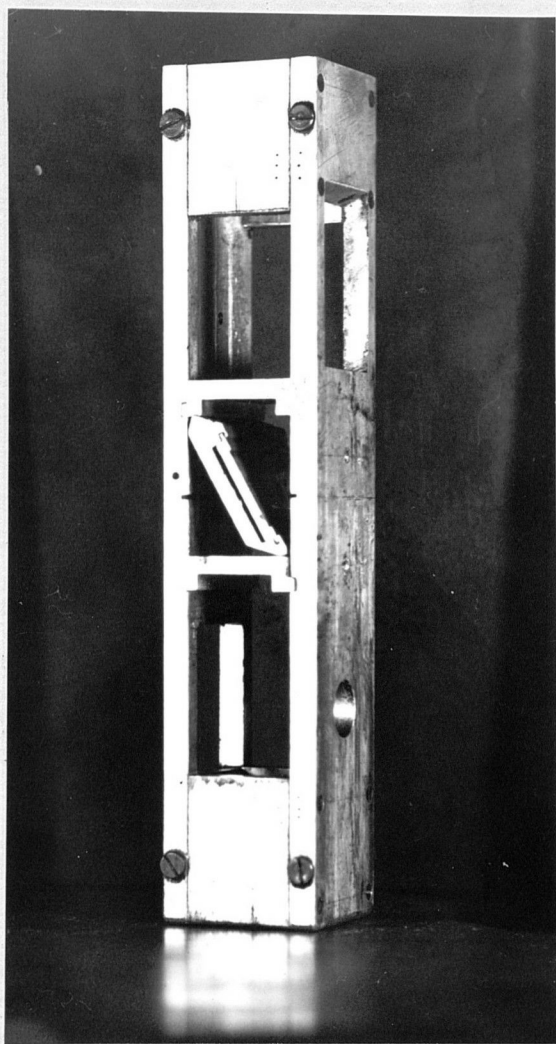


Plate I. The source holder.

raised or lowered by rotation of the arms B and in the lower position covered the slit  $S_1$  and prevented electrons from reaching the detector crystal,  $C_1$ . Lead blocks, L, covered with perspex to reduce scattering, were used to shield the detectors from  $\gamma$ -rays emitted from the source. To avoid build-up of static charge the perspex was covered with aquadag.

(c) The Detectors.

Anthracene crystals were used as detectors, on account of their high light yield for  $\beta$ -particles, and the short decay time of the pulses produced. Anthracene had the additional advantage that large single crystals were obtainable, giving efficient light collection. The crystals were cut to a thickness of 0.4 cm. The vapour pressure of anthracene is low enough to ensure that the dimensions of the crystals were not appreciably decreased by evaporation over the periods required for the coincidence counting.

The mechanical arrangement of the counter movement is also illustrated in fig. (3) and in plate (II). The crystal,  $C_1$ , was mounted on a horizontal shelf cut in the perspex light-guide, P, optical contact being maintained through a thin layer of white petroleum jelly. A plane reflecting surface, cut at  $45^\circ$  to the perspex rod, assisted in the transmission of light along the



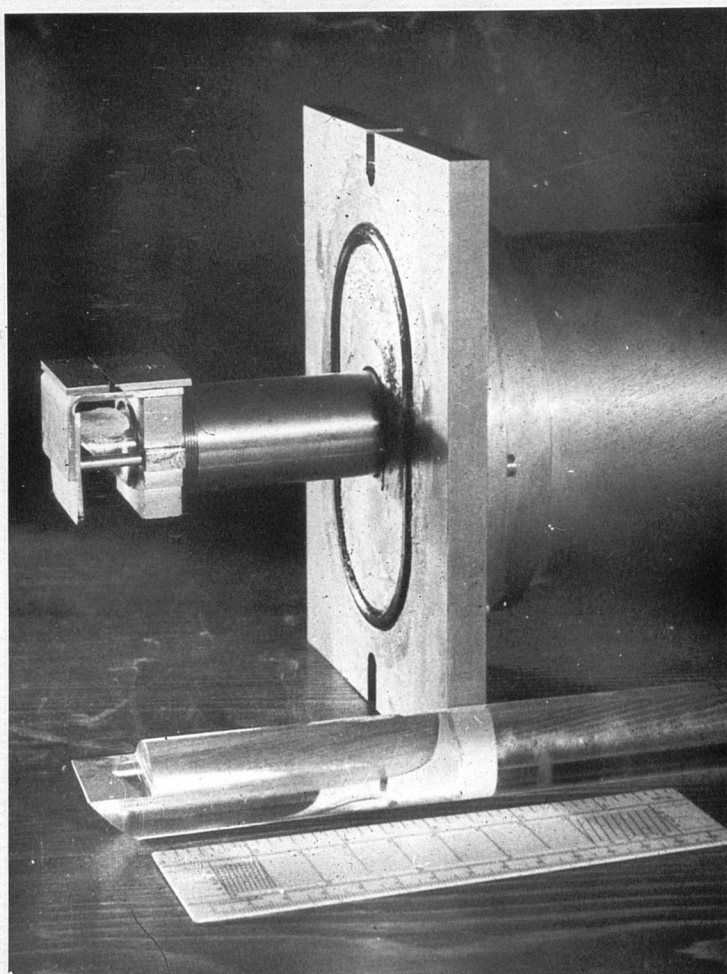


Plate II. The crystal detector.

rod by total internal reflection. The plane end of the rod was in optical contact with the end of the spring-mounted photomultiplier tube (E.M.I. type 4045), both photomultipliers being encased in double-walled mu-metal cans to provide screening from the magnetic field. Since the cathode was at a high negative potential the photomultipliers were periodically removed and coated with paraffin wax to reduce the possibility of electrical discharge from the high-voltage electrode to the screening can.

The detector movement was effected by a screwed flange, G, which engaged in an accurately cut double-start thread on the outer surface of the photomultiplier case. Rotation of the arms attached to the flange moved the complete assembly of detector, light-guide and photomultiplier into or out of the vacuum box, rotation of the light-guide being prevented by lugs which were attached to the outer surface of the light-guide tube, and fitted into grooves on the vacuum box. The perspex light-guide fitted into a brass tube, T, and vacuum sealing of the system was provided by the hat-packings  $M_1$  and  $M_2$ , and the neoprene ring, O. The setting of the counter slit was determined in terms of the number of turns on the setting screw thread, and a range of radius of curvature of electron path from 2.7 cm. to 6.3 cm. was obtainable.

The collecting power and resolution of the instrument both varied with detector position, the former being greatest when the detector was nearest to the source, and the latter when the detector was fully withdrawn. In the innermost position, with suitable slit widths, a solid angle of 1% of  $4\pi$  could be obtained with a resolution of 3%; with the detector fully withdrawn the solid angle decreased to  $\frac{1}{3}$ % of  $4\pi$ , with a resolution of 1.5%.

(d) The Electronic Equipment.

A block diagram of the electronic circuits is given in fig. (4). The discriminator and amplifier units have been fully described by Wells (42), and will not be given here in detail.

The advantage in the use of scintillation techniques lies in the very short rise time of the pulse produced in the phosphor, which permits the use of a coincidence set with a very short resolving time. With Geiger counters, the statistical time lag between the entry of an ionising particle and the production of a pulse at the counter electrode places a lower limit on the resolving time which can be employed. The use of resolving times below  $\sim 5 \times 10^{-7}$  sec. results in the loss of genuine coincidences. On the other hand, when coincidence measurements are being carried out on conversion lines superimposed on a relatively high

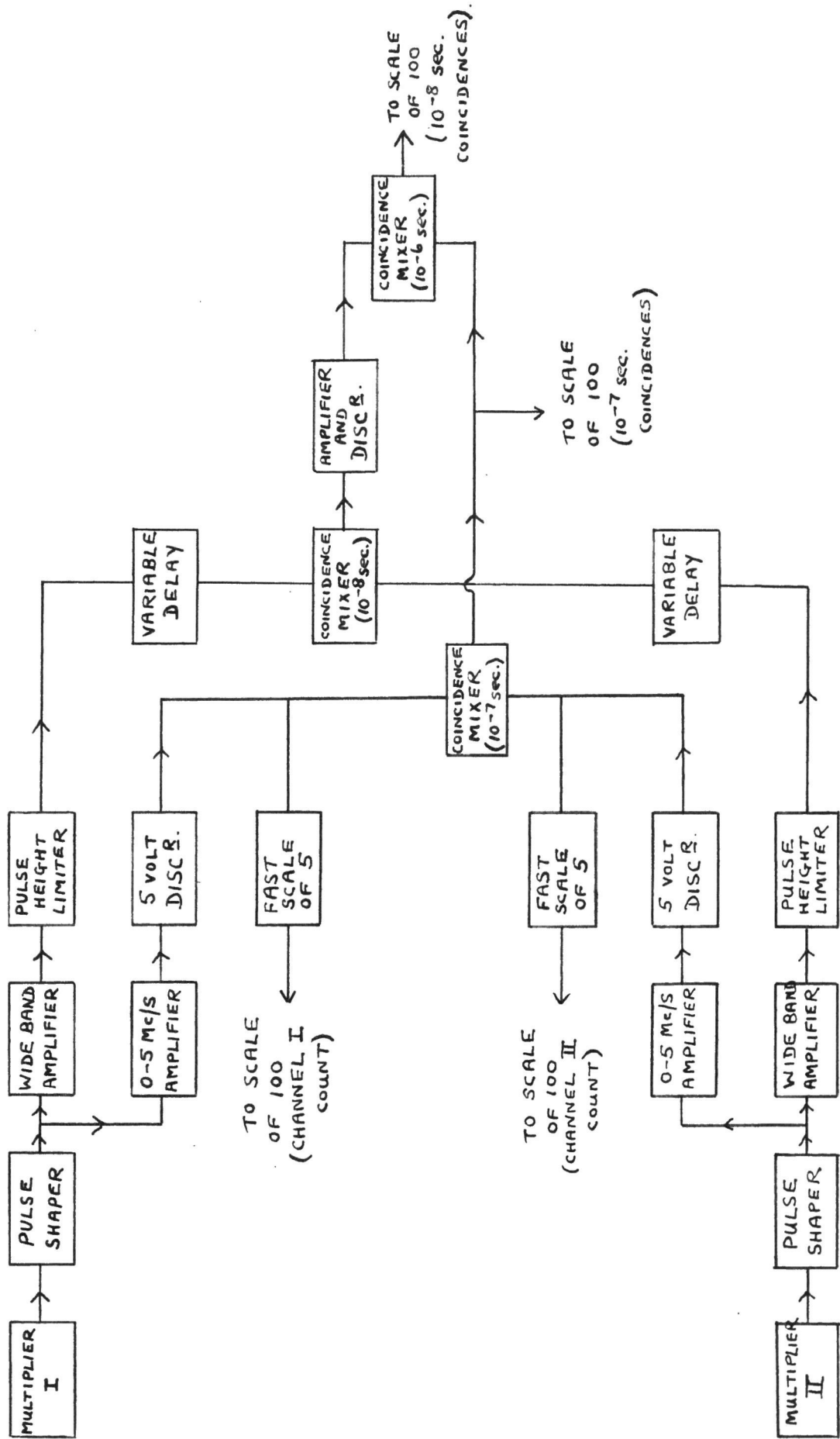


Fig. 4. BLOCK DIAGRAM OF ELECTRONIC CIRCUITS



continuous background, the use of resolving times of such an order inevitably results in the recording of a high level of chance coincidences. With the scintillation counters employed in the present investigation, it was possible to use a coincidence resolving time of the order of  $10^{-8}$  sec. without the loss of genuine coincidences.

To reduce coincidences between noise pulses, some form of pulse height discrimination must be incorporated in the circuit, but no discriminator exists with a sufficiently high bandwidth (0 - 100 Mc/s). This difficulty was overcome by the "fast-slow" coincidence system shown in the figure. The pulses from both multipliers passed through wide-band amplifiers to the coincidence set with a resolving time of  $10^{-8}$  sec. Simultaneously the pulses were amplified at a bandwidth of 5 Mc/s, and, after passing through 5 volt discriminators, were mixed in the second coincidence unit with a resolving time of  $10^{-7}$  sec. The outputs from the two separate coincidence units were then passed into a third mixer with a resolving time of  $10^{-6}$  sec. This system combined the advantages of the short resolving time of the  $10^{-8}$  sec. unit, which reduced accidental coincidences to a minimum, with the use of pulse height discrimination to reduce noise coincidences in the  $10^{-7}$  sec. channel. The true coincidence rate could be

derived by subtraction of the chance coincidences from the total coincidence rate recorded. Since the final mixer recorded coincidences with an effective resolving time of  $10^{-8}$  sec., the chance coincidence rate could be calculated from a knowledge of the single-channel rates and the accurately measured resolving time of the  $10^{-8}$  sec. mixer.

The pulse shaping circuits were incorporated to eliminate the effects of the slow decay ( $\approx 10^{-6}$  sec.) of the pulses supplied by the preamplifier. The pulse was reflected in a 20 ft. cable, and the output pulse had a duration of  $5 \times 10^{-8}$  sec., with an approximately rectangular shape. The 5 Mc/s amplifiers were conventional, but the 100 Mc/s amplifiers were of the "distributed amplifier" type where a high apparent gain-bandwidth product was obtained by using a sequence of parallel pentodes with delay lines in grid and anode circuits. Since a certain amount of mismatching might occur between the two channels leading into the  $10^{-8}$  sec. mixer, due to the difference in photomultiplier characteristics or the amplifier delays in each channel, variable delay lines were incorporated before the coincidence mixer to compensate for this effect.

All three coincidence mixers were of the "delay line" type, in which the incoming pulses were reflected, with change of phase, from the short-circuited

termination of a coaxial cable; the time ( $\tau$ ) taken for the pulses to travel to and fro along the cable determined the resolving time of the mixer. If the leading edges of pulses from each channel occurred within a time  $\tau$  of each other, they would overlap and produce a resultant pulse which operated the coincidence unit. The nominal resolving time of the unit could be varied by selecting one of a group of coaxial cables of differing lengths. The gain of the amplifier following the  $10^{-8}$  sec. mixer, and the level of the discriminator bias could be adjusted so that only the pulses produced by the superposition of two single-channel pulses in the mixer were counted.

### § 3. Calibration of the Instrument.

#### (a) The Magnetic Field.

For the measurement of magnetic field strength the source-holder could be removed and replaced by a search coil attached to a Grassot fluxmeter. To ensure that the coil was always aligned properly in the field, it was free to rotate between locating pins on a holder which fitted into a set position on the vacuum box. When rotated through  $180^\circ$ , the coil produced a galvanometer deflection proportional to the field strength. Since the radius of <sup>path</sup>~~curvature~~ of a  $\beta$  - particle leaving the source and striking the detector

could be calculated from a knowledge of the geometry of the system, it was possible to calibrate the search coil by reference to certain of the well-known internal conversion lines, the  $H\rho$  values of which had been determined by Mladjenovic and Slatis (12). The conversion from detector position to radius of curvature was made by reference to a set of tabulated values which had been corrected to allow for the slight variation in field strength occurring from the central regions to the periphery of the gap between the poles. To cover the range of field values up to the maximum of 2000 oersteds, two coils with different numbers of turns were used, and as far as possible the field settings were also checked by direct reference to convenient internal conversion lines, emitted either by the radium source being used, or by a source of the thorium active deposit.

In the calibration by the internal conversion lines, assymetric placing of the source foil in its holder would give rise to error in the calculation of the value of  $\rho$  corresponding to the peak of the line. To correct for this, the source holder was rotated through  $180^\circ$  about the vertical axis, and the mean of the two detector positions corresponding to the peak of the conversion line was taken.

(b) The Normalising Factors.

In obtaining a momentum spectrum of the  $\beta$  - particles emitted from the source, measurements were taken with chosen source and detector slit widths of the counting rate at set positions of the detector. In addition to the "true" variation of counting rate with the chosen momentum band, the counting rate depends upon two instrumental variables:

(a) the solid angle of acceptance of the detector, which decreases as the counter moves further from the source.

(b) the magnetic field, which had in general to be varied several times in order to scan a complete spectrum, since only a limited range of  $H\rho$  values is focused for a given field setting. If the field strength be increased by a certain factor, the number of  $\beta$  -particles in a given solid angle will increase in the same ratio, due to the increase in the magnitude of the momentum band accepted. Thus when the survey of a complete spectrum involved the combination of several portions taken at different field values, each set had to be divided by a factor proportional to the field strength.

While it is possible to derive the normalising factors required to correct for the solid angle effect from theory, the amount of calculation involved is so

great that an experimental determination is preferable. In addition the practical derivation takes account of such factors as the possible variation of the number of electrons scattered by the detector slit with the angle at which the electrons arrive in the slit plane, which depends on the detector setting.

The method used was to observe the counting rate for electrons of a specific  $H_p$  band, selected as being on a flat portion of the momentum spectrum, and as far as possible from the neighbourhood of internal conversion lines. A set of field values was selected, such that the chosen momentum band was moved at intervals along the complete range of detector positions. At each point, an additional count was taken with the shutter down to eliminate the effect of  $\gamma$ -rays and of noise pulses in the photomultiplier. After correction for decay, the normalising factors were given by the ratio of  $H/N$  at each point,  $H$  being the magnetic field strength and  $N$  the corresponding  $\beta$ -particle counting rate.

This procedure was repeated for each of the combinations of source and detector slits used in the experiment. A typical curve illustrating the variation of normalising factor with detector position is shown in fig. (5). A factor of unity at 7 turns has been arbitrarily chosen.

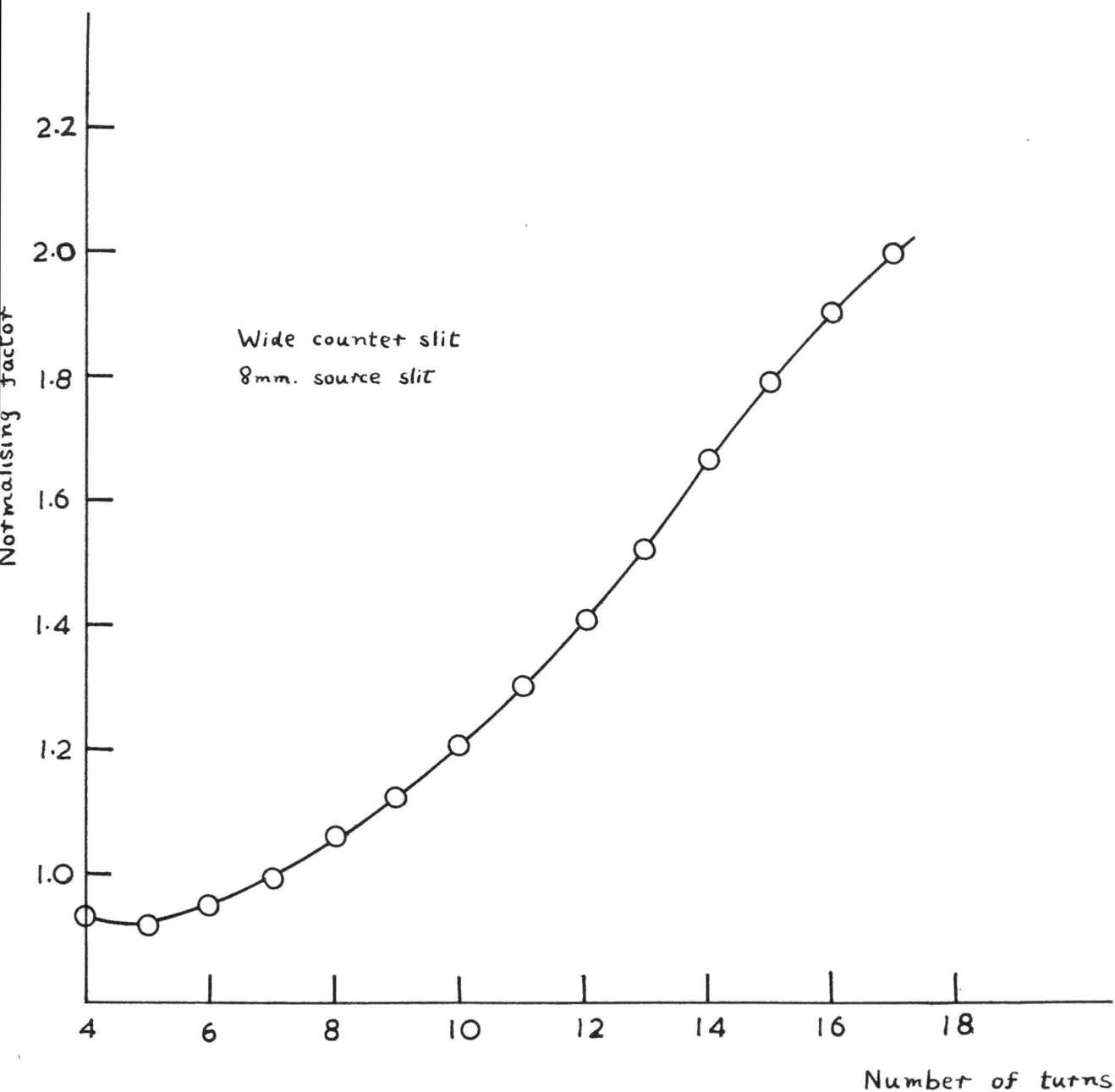


Fig. (5). The normalising factors.

A useful check on the correctness of the normalisation was provided by the consistency of the partial spectrum curves obtained in a complete analysis of the radium active deposit up to  $H_p \sim 12,000$  oersted-cm. It was found that the separate portions of the spectrum, each corresponding to a different field setting, fitted together satisfactorily.

#### §4. Measurement of the Coincidence Resolving Time.

In order to estimate the number of chance coincidences, an accurate value for the coincidence resolving time was required. This was obtained by measuring the coincidence rate between the pulses from two completely independent  $\gamma$ -ray sources, so that the recorded rate was due to chance coincidences alone. The detectors were moved as far apart as possible, and the two sources ( $^{60}\text{Co}$  and  $^{226}\text{Ra}$ ) were fixed to the outside of the spectrometer in such a way that each detector was influenced by only one of the sources. This was checked by moving each source in turn into position, and verifying that no effect was produced on the farther counter. The chance coincidence rate  $N_{12}$  was then related to the single-channel counting rate by the formula

$$N_{12} = 2N_1N_2\tau$$

where  $\tau$  was the resolving time of the mixer.



Since the resolving time varied slightly with the voltage on the photomultipliers, presumably due to a change in the shape of the output pulses, it was necessary to determine the value of  $\tau$  after every change in photomultiplier voltage.

The optimum conditions for coincidence measurements are attained when the rate of occurrence of accidental coincidences is equal to the genuine coincidence rate, and this condition was usually approximately realised initially with most of the sources prepared by the evaporation method.

Additional checks had to be carried out to ensure correct matching in time between the channels leading to the fast coincidence set, and this was done by switching various delays into each channel until the genuine coincidence rate was a maximum.

### §5. Determination of Detector Characteristics.

For each band of  $\beta$ -particle energies, it was necessary to determine the position of the plateau in the curve of  $\beta$ -particle counting rate against photomultiplier voltage. Measurements were taken of the total counting rate and the background counting rate (with shutter down to cut off  $\beta$ -particles). A typical plot of  $\beta$ -particle counting rate against photomultiplier voltage is given in fig. (6), showing

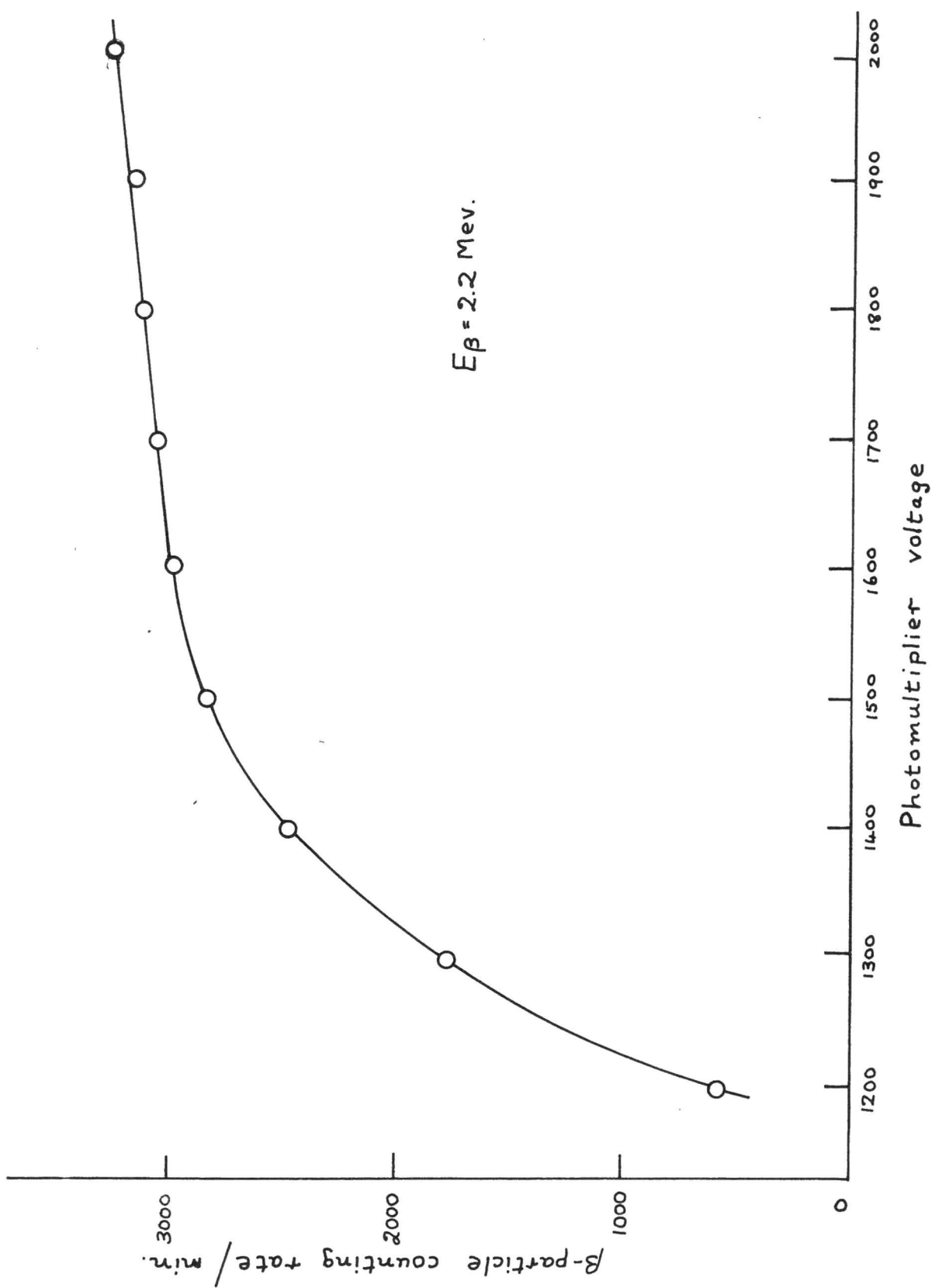


Fig.(6) Voltage characteristic for photomultiplier.

an almost level plateau of gradient 0.02% per volt. Since the counting rate due to  $\gamma$ -radiation and electronic noise increased with photomultiplier voltage, the detector was always operated at the lowest voltage necessary to ensure that the  $\beta$ -particles were counted with maximum efficiency. As indicated by Bell (43), the maximum efficiency will be less than 100%, since about 8% of the  $\beta$ -particles entering the anthracene will scatter out of the crystal before being stopped, and thus will produce smaller pulses than they should. A further reason for the choice of anthracene rather than NaI (Tl) as a scintillator lies in the fact that the corresponding scattering figure for NaI (Tl) is as high as 80 - 90%.

CHAPTER III.The Source Preparation.§1. General.

The majority of the work on the  $\beta$ -particle spectrum of Ra(B + C) has been performed either with enclosed sources of  $^{222}\text{Rn}$  or with sources of the radium active deposit formed after the radon decay. With sources of the first type, errors are introduced by absorption of the  $\beta$ -radiation in the walls of the containing ampoule. A typical value for the wall thickness of the glass container is 3 mgm./cm.<sup>2</sup>, which is large enough to cause appreciable distortion of the spectral shape, particularly at low energies. Since the transient half-life of the short-lived part of the disintegration chain from RaB onwards is only 26.8 minutes, sources of the second type raise obvious difficulties when used in coincidence measurements requiring counting periods of several hours. Due to the closeness of the decay periods of RaB and RaC (26.8 min. and 19.7 min. respectively), the RaC component will decay in a complicated manner for several hours after a source is taken off. Where the RaB and RaC spectra overlap, it is impossible to correct for decay unless the relative proportions of the two substances are known. Additional difficulty arises since the  $\gamma$ -ray

background is similarly affected by the complicated decay. The complexity of the decay, and the sensitive dependence of the radiation intensity on the relative proportions of the two substances, can be utilised as a means for distinguishing to which of the two a radiation of given energy belongs, by studying the variation of its intensity with time. For straightforward coincidence measurements, on the other hand, the short decay period has the effect that by the time the source has finally settled down to a steady decay rate, it is almost certainly too weak to use.

In consequence of the difficulties arising in the use of the types of sources described above, it was decided to experiment with sources of radon embedded in thin aluminium foil, using the discharge method of preparation described by Momyer (44). Since the half-life of radon is of the order of 3.8 days, it was hoped that this type of source would enable several days of counting to be done with a single source without excessive correction for decay. It was also hoped that it would be found possible to obtain radon sources on foil so thin that absorption effects would be negligible.

## § 2. The Source Preparation Apparatus.

The apparatus used for preparation is shown in fig. (7). A slow stream of nitrogen was passed for 30 minutes through a 5 mC. solution of radium in hydrochloric acid. Radon was swept out of the solution by the nitrogen flow, and the gas stream was then passed through a bath of sodium hydroxide to remove hydrochloric acid, the cleansing process being made more efficient by the introduction of a sintered disc to break the gas flow up into fine bubbles. The gas then flowed through two carbon-dioxide-acetone traps to remove moisture, and thence into the two liquid nitrogen traps where the radon was condensed. The system was evacuated with a mercury diffusion pump, and the nitrogen traps allowed to heat up in sequence, the radon being finally condensed in the discharge tube by liquid nitrogen cooling.

The electrode system in the discharge tube is shown in fig. (8). The cathode was a flat brass plate, A, embedded in an ebonite block, B, the top of the plate being flush with the upper surface of the block. The brass plate was joined to a brass rod, C, which ran through an ebonite cone, D, designed to fit the inside of the ground glass joint inserted in the socket of the discharge tube. (For clarity in the diagram, the rod C is shown withdrawn some little way from the ebonite

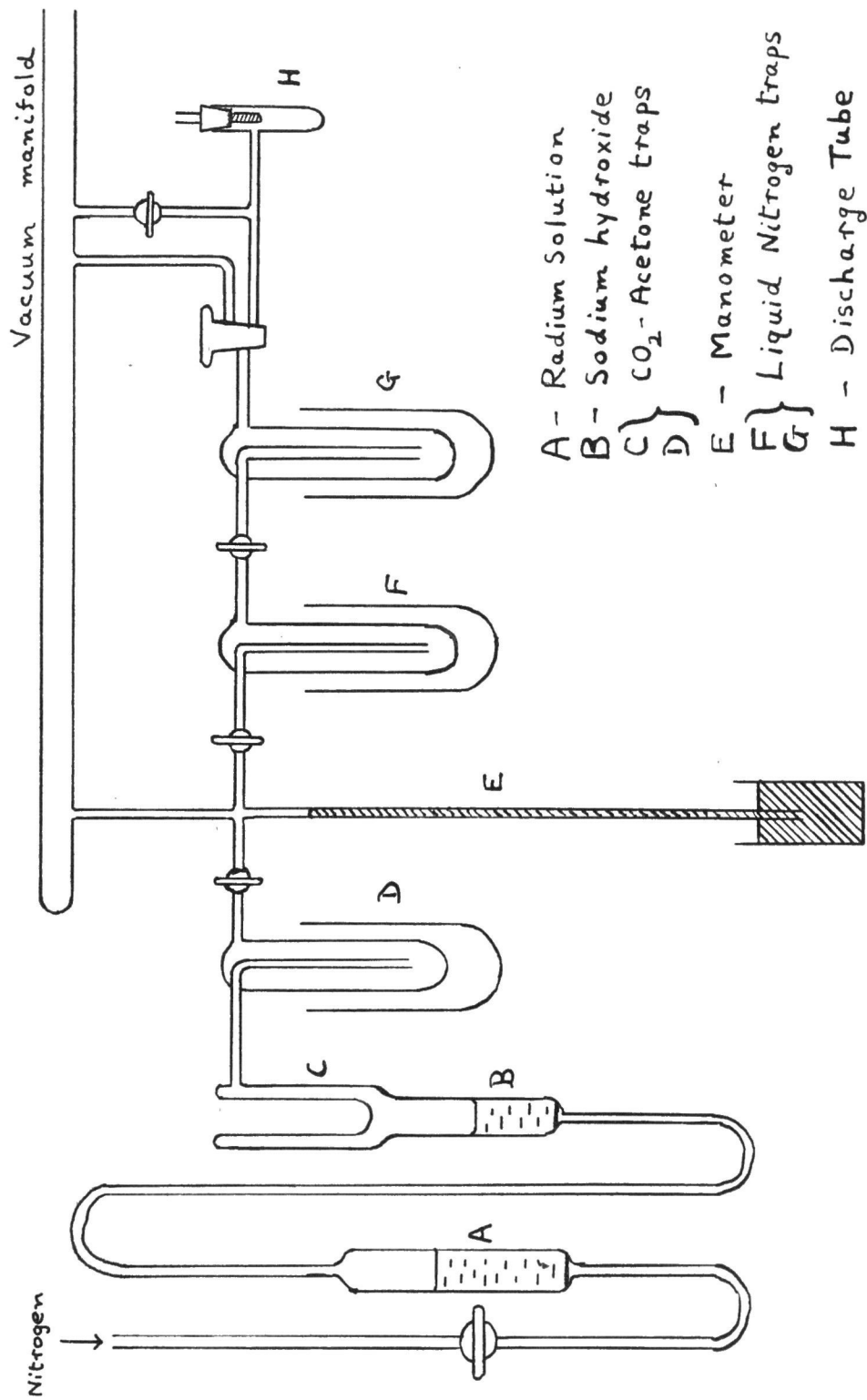


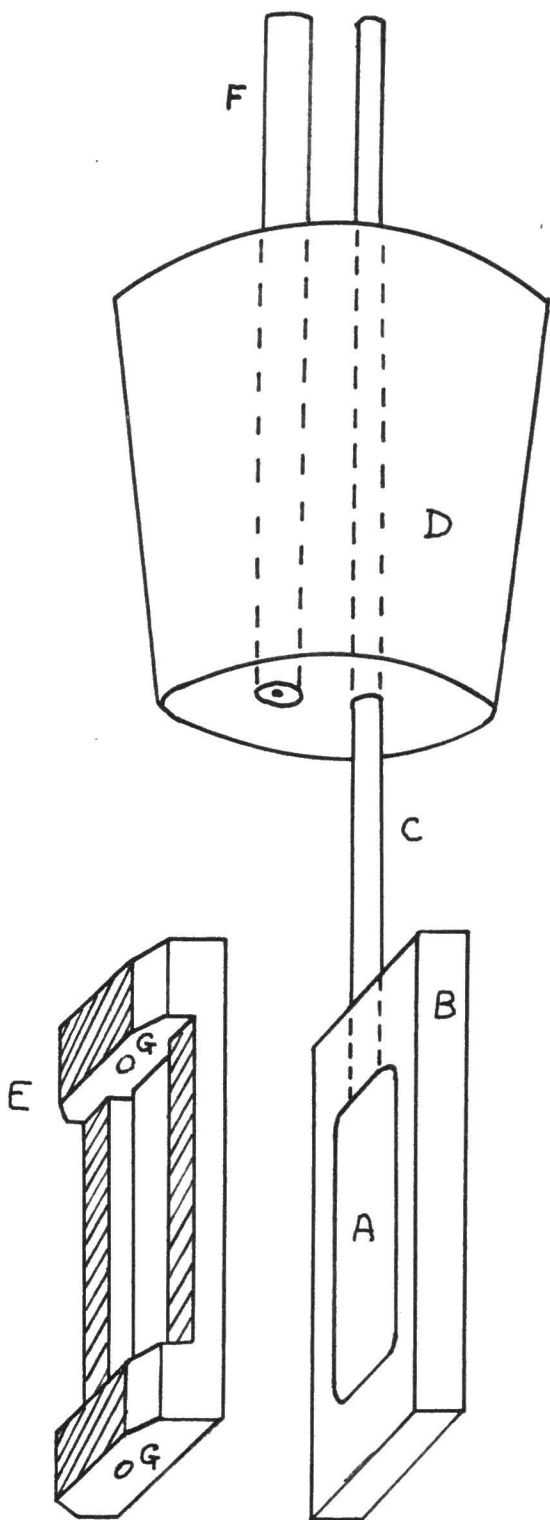
Fig.(7). The source preparation apparatus.

cone, but in operation the upper face of B was flush with the lower face of D). The thin aluminium foil was laid over the plate A, and the ebonite frame, E, placed on top of it. A rod screwed at one end was fitted through the holes, G, to hold the ebonite in position, and act as the anode for the discharge. Electrical contact was made by screwing this rod into another brass rod, F, which passed through the ebonite cone. A fair degree of vacuum tightness was ensured by making the brass rods C and F of such dimensions that they just fitted the holes in the ebonite when cooled in liquid air. In practice, it was found necessary to apply black wax to achieve complete vacuum-tightness. The ebonite cone D was waxed on to the interior of the glass cone.

In the original version of the electrode system the anode was equipped with a series of sharp spikes to concentrate the discharge. It was found, however, that this system tended to produce local discharges of such intensity that holes were frequently burnt in the aluminium foil. In consequence the pointed anode was replaced by the screwed rod which gave a more uniform discharge.

The D.C. voltage used in the discharge process was between 700 and 1000 volts, and the total running time was 30 minutes. By trial and error it was found that





- A - Cathode
- B - Ebonite block
- C - Brass Rod
- D - Ebonite Cone
- E - Ebonite frame
- F - Brass Rod
- G - Holes for anode

Fig.(8)

The Electrode System.

the best results were obtained by running the discharge in bursts of about three minutes at a time, the tube being "re-frozen" and pumped out between runs. The improved collection efficiency with short bursts of discharge was noted by Momyer, who suggested that the fall-off in yield with longer periods might be due either to heating of the collecting electrode driving off the embedded radon, or to the gradual establishment of an equilibrium condition where space charge effects limited the rate of collection. The space charge effect would result from the existence of a large region of high ion density and low potential gradient between the electrodes, and two small regions of low ion density and high potential gradient immediately in contact with them. The collection rate would then be highest before the space charge congregation began to inhibit the ion flow. It was suggested by Momyer that it might be possible to increase the yield by superposing on the D.C. voltage an A.C. ripple of such magnitude that the discharge was alternately struck and snuffed. This was attempted in the present work, but it was found that no significant increase in collection efficiency was obtained, suggesting that the decrease in yield was probably due to heating of the electrodes rather than to the more complicated space-charge mechanism. The frequent "re-freezing" and pumping

out of the discharge tube aided collection efficiency by removing the inevitable air contamination due to leakage.

It was found possible to transfer almost all of the radon to the discharge tube without serious loss in any of the traps, although it might be expected that a proportion of the gas would condense in the  $\text{CO}_2$ -acetone traps, since the temperature of the cooling mixture was about  $10^\circ\text{C}$  below the boiling point of the radon. It was, however, found necessary to allow a period of at least an hour for the radon to diffuse over from the final trap into the discharge tube, and it was noticed that the final yield was increased still further if the tap between discharge tube and final nitrogen trap were opened at intervals during the discharge to allow additional radon to pass over. Comparison of the residual activities remaining in each of the liquid nitrogen traps after removal of the radon led to the deduction that approximately 98% of the radon swept out of the radium solution was eventually collected in the discharge tube.

Using the technique described above, it was found possible to produce sources of up to 0.6 mC. on aluminium foil of thickness 0.2 mgm./cm.<sup>2</sup>. The radon deposit covered a rectangular area of 15 mm. by 2.5 mm.

The possibility that radon tended to leak out of

the foil under vacuum conditions was investigated by taking regular measurements of the  $\gamma$ -activity of the source while inside the spectrometer, and it was found that the activity decayed with approximately the half-life characteristic of radon. It was, however, observed that the counting rate on both scintillation counters rose steadily for some hours after the source was introduced into the spectrometer, and this was attributed to a small leakage of radon resulting in the crystal and nearby surfaces becoming covered with a thin layer of active deposit. It was possible that a leakage of radon too small to be detected as significant in the half-life measurements could have a much more marked effect in the neighbourhood of the crystals themselves. Since the system settled down to an equilibrium condition after a few hours, the source was left in the spectrometer throughout the whole counting period of up to two weeks. Once the system reached the equilibrium condition, correction for the coating effect was automatically made by subtraction of the " $\gamma$ -ray" counting rate taken with the shutter down, since the lowering of the shutter had no effect on the counting rate arising from the radon leakage.

### §3. Verification of the "Surface Layer" Character of the Source.

Experiments were carried out to determine whether the radon constituted a "surface source" or was spread uniformly through the thin foil. After deposition of the source on the foil, comparison of the ranges of the  $\alpha$ -particles of RaC' were made with the source pointing first towards, and secondly away from an  $\alpha$ -particle spark counter of the type described by Connor (45). The design of the instrument is illustrated in fig. (9). The operation depended on the initiation of a spark between two wires at a high potential difference when an  $\alpha$ -particle caused ionisation in the immediate neighbourhood of the wires. The anode and cathode were mounted on two ebonite blocks, the lower block, carrying the cathode, being fixed to the vertical brass plate, while the upper block with the anode wire could be moved vertically by the action of an accurate screw. The anode consisted of a fine tungsten wire of diameter 0.05 mm. stretched horizontally between two insulating pillars, and secured by screws at the side of the upper block. The cathode was a wire of diameter 1 mm., clamped to the fixed ebonite block.

The cathode was connected directly to the negative output of a stabilised power supply, having an output voltage variable up to 4000 volts, and the anode was connected to earth via a resistance capacity potentio-

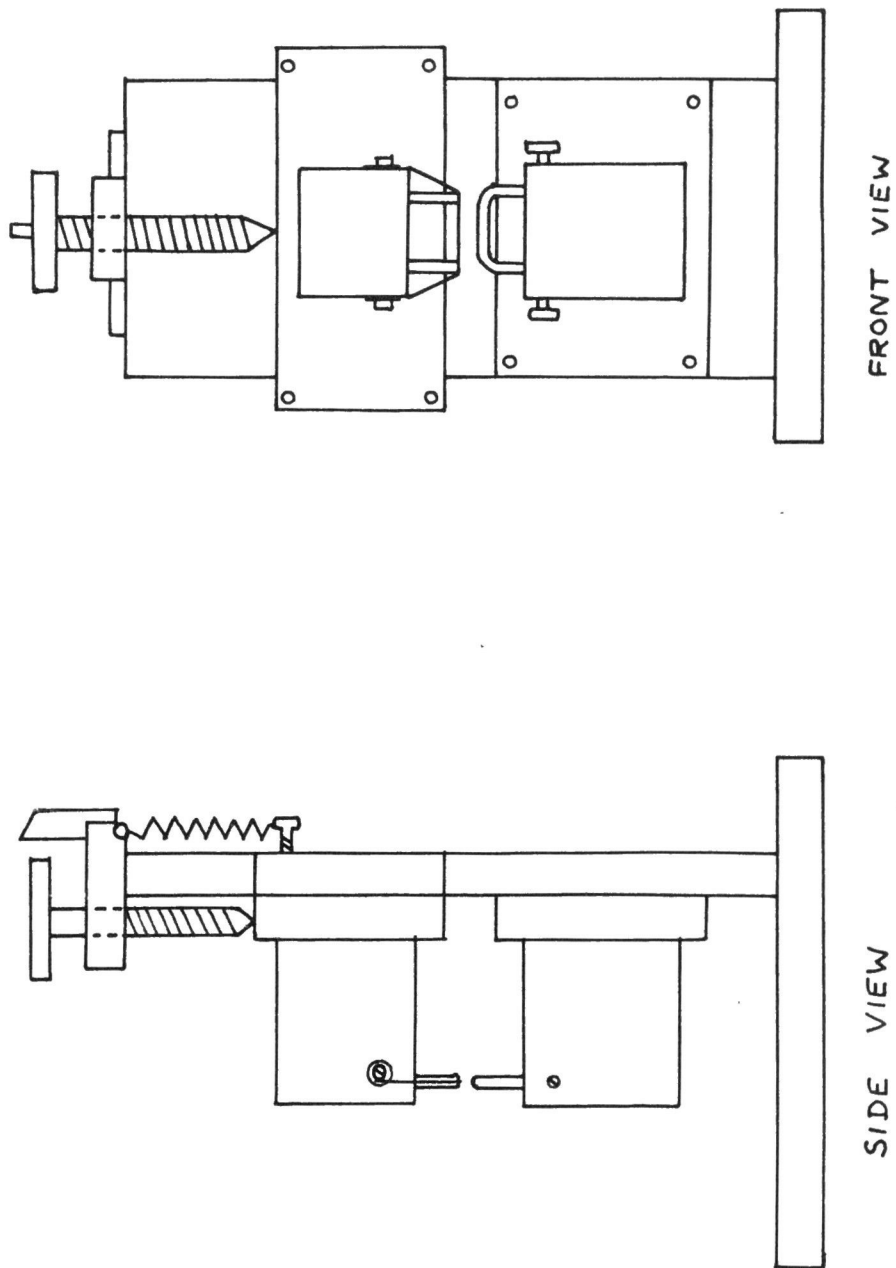


Fig.(9). The  $\alpha$ -particle spark counter

meter. The potentiometer acted as a quench circuit to extinguish the discharge, and provided a known fraction of the voltage surge for application to a scaler. The counting rate/voltage characteristic displayed a plateau covering a voltage range of some 400 volts, over which the dependence of counting rate on voltage was small.

The chief advantages of the  $\alpha$ -particle spark counter for such a measurement were the low background counting rate, and the accuracy of range determination due to the sharply defined sensitive volume of the counter. The source was mounted on a carriage which could be moved relative to the counter by an accurate micrometer screw. Figs. (10) and (11) show the variation of counting rate against the distance of the spark counter wires from the source (a) with the "active" side of the aluminium facing the counter, and (b) with the "active" side away from it. From these graphs the extrapolated ranges of the  $\alpha$ -particles of RaC' were obtained in each case. A strong radon source was used to reduce the counting time for each point to a minimum, thus enabling both sets of data to be obtained within as short a period as possible. This was desirable to reduce the effects of long-term variations in atmospheric pressure.

The extrapolated ranges in air were found to be

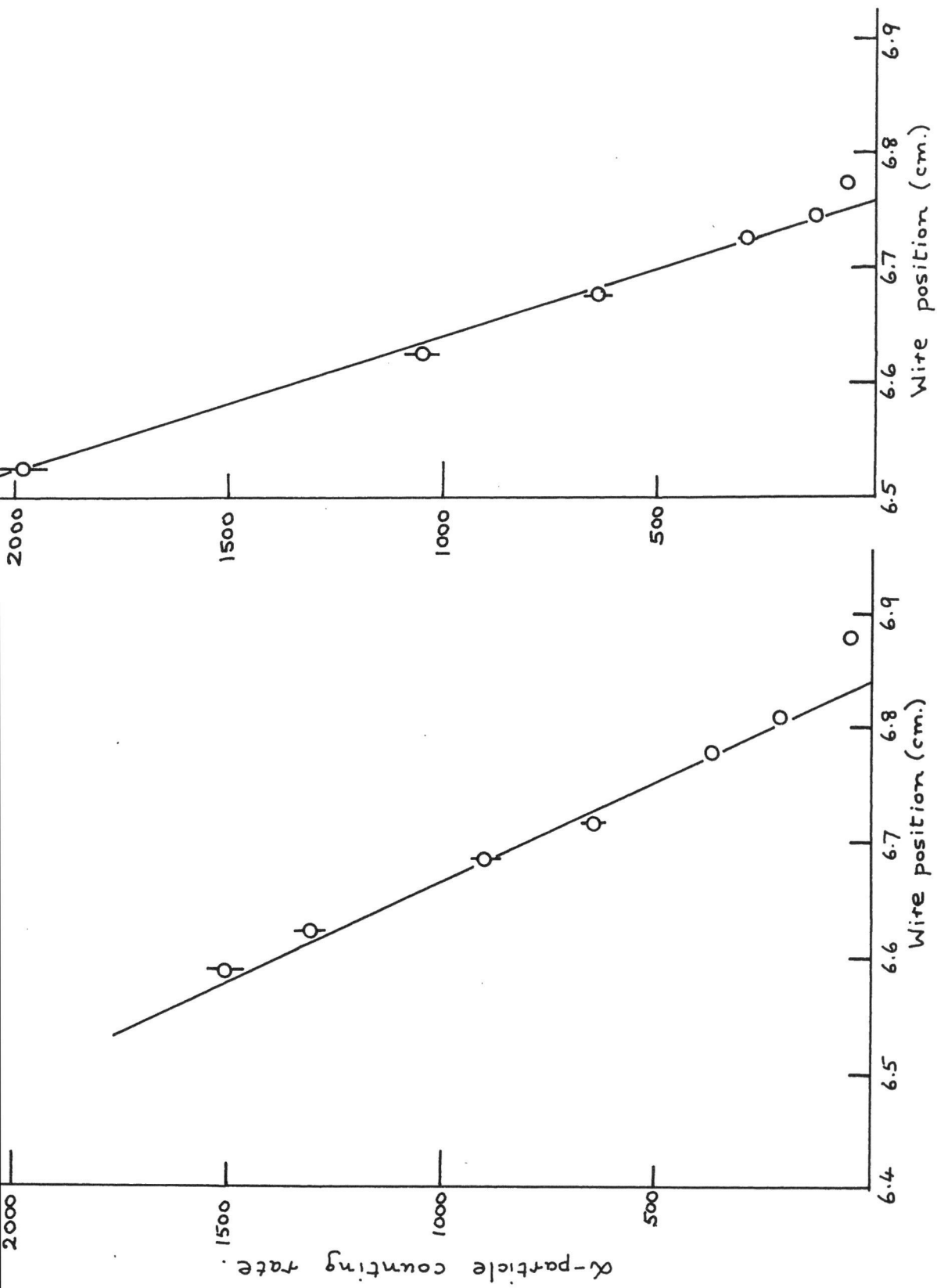


Fig. (10). Active side towards counter.

Fig. (11). Active side away from counter.



(a)  $6.84 \pm 0.01$  cm. and (b)  $6.76 \pm 0.01$  cm. For comparison purposes a third measurement was made with the source side facing the  $\alpha$ -particle counter and a section of aluminium foil of the same thickness as the source backing between the source and counter. The extrapolated range was then found to be  $6.74 \pm 0.01$  cm. Since this corresponds closely with the value obtained previously in the "reverse" position, it was deduced that the source was effectively deposited very close to the surface of the aluminium foil.

CHAPTER IV.The Measurements on the  $\beta$ -ray Spectra  
of RaB and RaC.§ 1. Summary of Techniques.

The experimental investigations fell into three separate sections. These were:

(a) coincidence measurements between the conversion electrons of the strongly converted  $\gamma$ -rays of RaB and the continuous spectrum, the end-point energy of the partial  $\beta$ -spectrum in coincidence with each  $\gamma$ -ray being obtained by Fermi analysis of the coincidence counting rates at chosen points on the continuous spectrum.

(b) several complete surveys, using only one channel, of the energy spectrum of Ra(B + C), which was then split up into component spectra by the technique of repeated Fermi analysis.

(c) use of the degree of resolution provided by the  $\gamma$ -ray counter by setting the multiplier voltage at such a level that only  $\gamma$ -rays above a certain energy were counted, and then finding the end-point of the partial  $\beta$ -spectrum in coincidence with  $\gamma$ -rays of energy greater than the selected value.

## § 2. The Coincidence Measurements on the $\text{RaB} \rightarrow \text{C}$ Transition.

One of the detectors was set on the peak of the required conversion line and the other used to scan the spectrum of the continuous  $\beta$ -emission. In addition to the chance coincidences, which can be estimated from the known single-channel counting rates and an exact knowledge of the resolving time of the coincidence unit (see Chapter II, § 4), the effects of three sources of genuine but unwanted coincidences must be considered. These are (a) coincidences between direct  $\gamma$ -rays striking the detector crystals (b) coincidences between direct  $\gamma$ -rays and the continuous spectrum on either side, and (c) coincidences between  $\gamma$ -rays in the movable detector and conversion electrons of the selected line in the other. These unwanted coincidences were eliminated by taking four separate measurements for each point as follows:

(a) detector (1) counting both  $\beta$ -particles and  $\gamma$ -rays, detector (2) set on peak of conversion line.

(b) shutter lowered to cut off  $\beta$ -particles from detector (1), detector (2) still on conversion line.

(c) shutter raised to allow detector (1) to count ( $\beta + \gamma$ ), detector (2) moved just off conversion line.

(d) shutter lowered, detector (2) off conversion line.

It can be readily shown that the undesired coincidences may be eliminated by combination of the four measurements.

Let  $\beta_1$ ,  $\gamma_1$  be the  $\beta$ - and  $\gamma$ -counting rates in channel (1) and  $\beta_2$ ,  $\gamma_2$ ,  $L_2$  be the  $\beta$ -,  $\gamma$ - and conversion electron counting rates in channel (2), when set on line.

Let  $\beta_2'$ ,  $\gamma_2'$  be the  $\beta$ - and  $\gamma$ -counting rates in channel (2) when set just off line.

Then, using the notation (A)(B) to indicate the number of coincidences between the numbers A and B recorded in each channel, the coincidence rates recorded in the four measurements detailed above may be written as:

- (a)  $(\beta_1 + \gamma_1)(\beta_2 + \gamma_2 + L_2)$
- (b)  $\gamma_1(\beta_2 + \gamma_2 + L_2)$
- (c)  $(\beta_1 + \gamma_1)(\beta_2' + \gamma_2')$
- (d)  $\gamma_1(\beta_2' + \gamma_2')$ .

Taking the combination (a) - (b) - (c) + (d), we see that all other terms cancel, leaving only

$$\beta_1\beta_2 + \beta_1\gamma_2 + \beta_1L_2 - \beta_1\beta_2' - \beta_1\gamma_2'.$$

$\beta_1\beta_2$  and  $\beta_1\beta_2'$  are both equal to zero, since no coincidences (other than chance coincidences) will occur between the particles of the  $\beta$ -continua on each side. Also, since the change in solid angle caused by movement of the second detector just off the conversion line is very small ( $\approx 3\%$ ), we can assume that  $\gamma_2 \approx \gamma_2'$ . The expression then reduces to the term  $\beta_1L_2'$ , corresponding to the required coincidences between the conversion electrons and the  $\beta$ -continuum on the other side.

Since the final result involves the combination of four separate measurements, large counting times were necessary for each in order to attain a reasonable degree of statistical accuracy. It is obviously desirable to reduce the  $\gamma$ -ray background relative to the  $\beta$ -particle counting rate, and this was achieved in two ways. As great a thickness of lead as possible was inserted between source and detector, although too great a thickness restricts the motion of the detectors into the vacuum box. The thickness chosen was such that the conversion electron detector was just able to move in to the peak of the line, while the detector on the other side was just able to move in to within 2.5 mm. of its zero position. The  $\beta/\gamma$  ratio was also increased by using wide source and detector slits (7 mm. and 2 mm. respectively), since in this measurement

a large solid angle is more important than a high degree of resolution. Although the efficiency of the anthracene crystal for  $\gamma$ -ray detection is only a few per cent., whereas the  $\beta$ -particles are counted with almost perfect efficiency, this effect is compensated by the much greater solid angle of acceptance for the  $\gamma$ -radiation. Since the efficiency of counting for the  $\gamma$ -rays increases with multiplier voltage, the position of the plateau of the  $\beta$ -particle counting rate against multiplier voltage was found for each energy, and the voltage set at the minimum value required for plateau conditions.

The line profile of the conversion line was determined carefully before the start of the coincidence measurements, and the movement of the detector was just sufficient to avoid counting the conversion electrons. This ensured that the decrease in  $\gamma$ -ray background due to the variation of the solid angle subtended by the crystal at the source was reduced to a minimum. The accurate measurement of the peak of the conversion line enabled a check to be made on the symmetrical placing of the source. The source holder was turned through  $180^\circ$  and it was confirmed that the peak of the conversion line was detected at the same position of the counter.

The final results for the true  $\beta$ - $e^-$  coincidence

counting rates at each point were corrected for decay and multiplied by the appropriate normalising factors (see Chapter II, § 3). The points were finally plotted on a Fermi diagram, the ordinate being  $(N/F)^{\frac{1}{2}}$ , where  $N$  was the corrected counting rate and  $F$  the Fermi function for the daughter nucleus  $^{214}_{83}\text{Bi}$ . The abscissa,  $\epsilon$ , is the energy expressed in relativistic units, plus one.

Figs. (12), (13) and (14) show typical Fermi plots of the counting rates in coincidence with the K-conversion electrons of the F, G and H  $\gamma$ -rays involved in the de-excitation of the RaC nucleus. The table below shows the energies of these  $\gamma$ -rays as given by Mladjenovic and Slatis (12) and the corresponding  $\beta$ -spectrum end-points determined from the coincidence measurements. The results quoted here have been averaged from several sets of measurements of the end-points corresponding to each  $\gamma$ -ray.

K-conversion line	$\gamma$ -ray energy (keV)	$\beta$ -spectrum end-point energy (keV)
F	241.9	688 $\pm$ 10
G	295.2	694 $\pm$ 15
H	352.0	626 $\pm$ 12

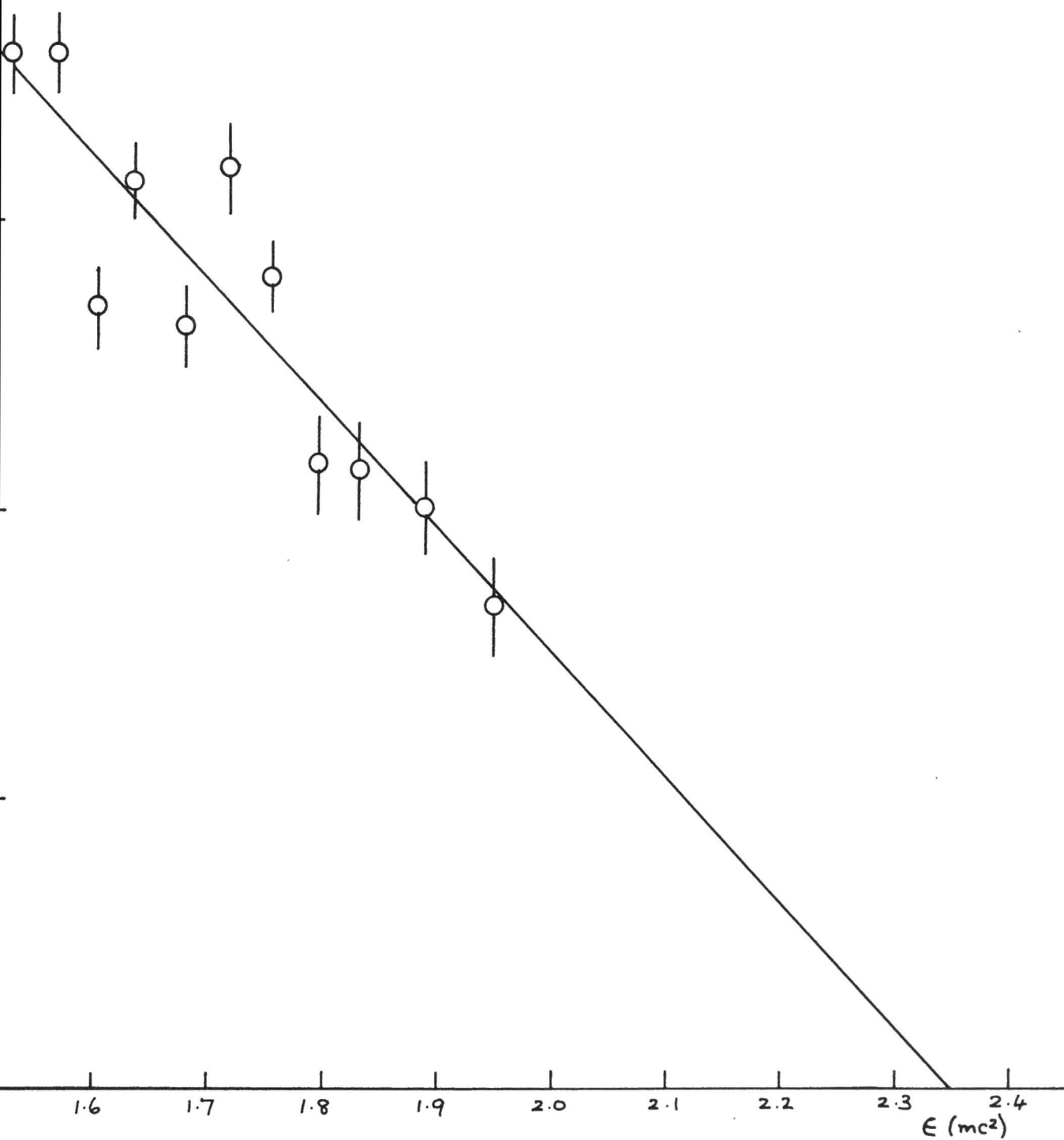


Fig. (12), Fermi plot of partial  $\beta$ -spectrum coincident with F-line.



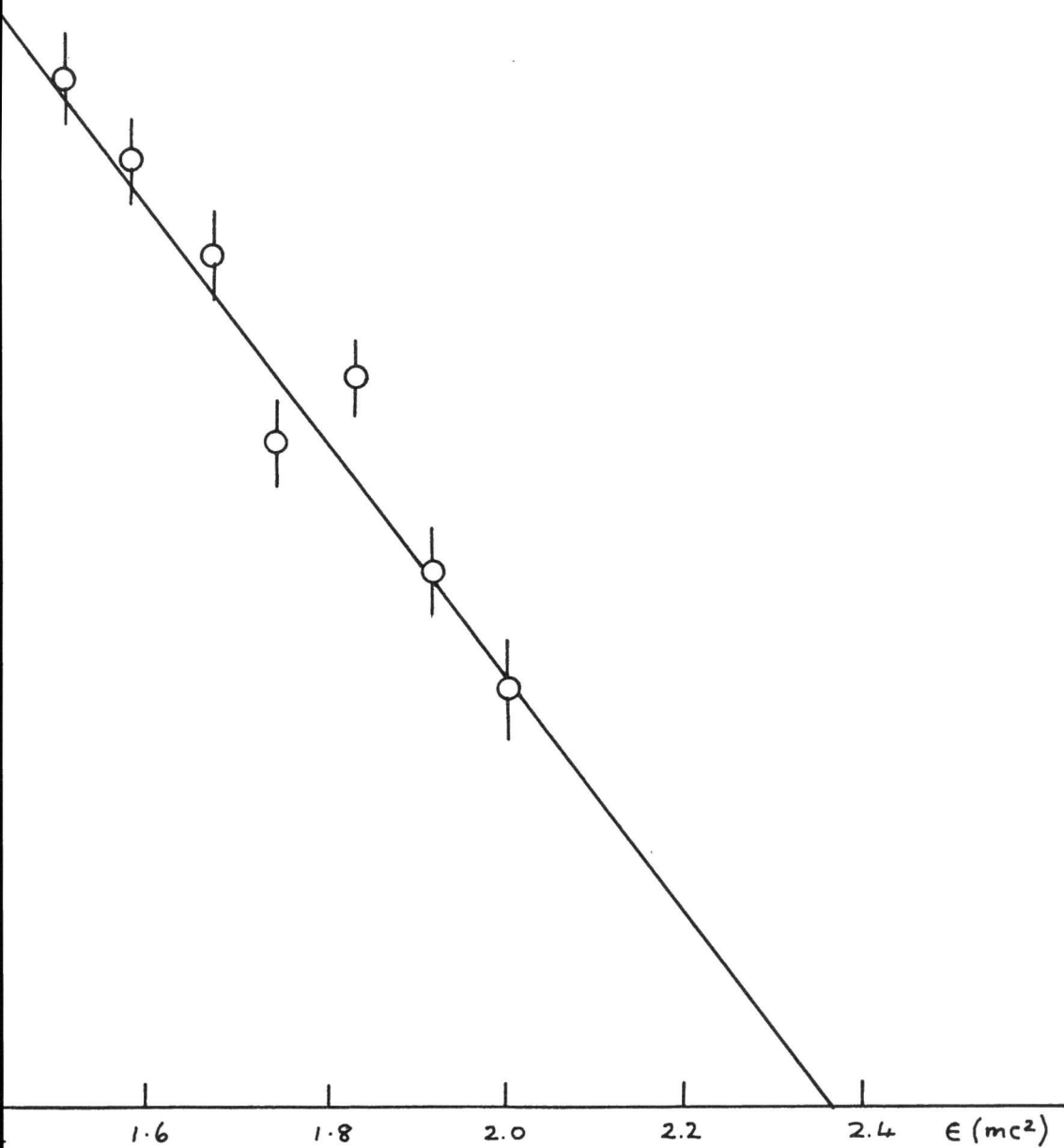


Fig.(13). Fermi plot of partial  $\beta$ -spectrum coincident with G-line.

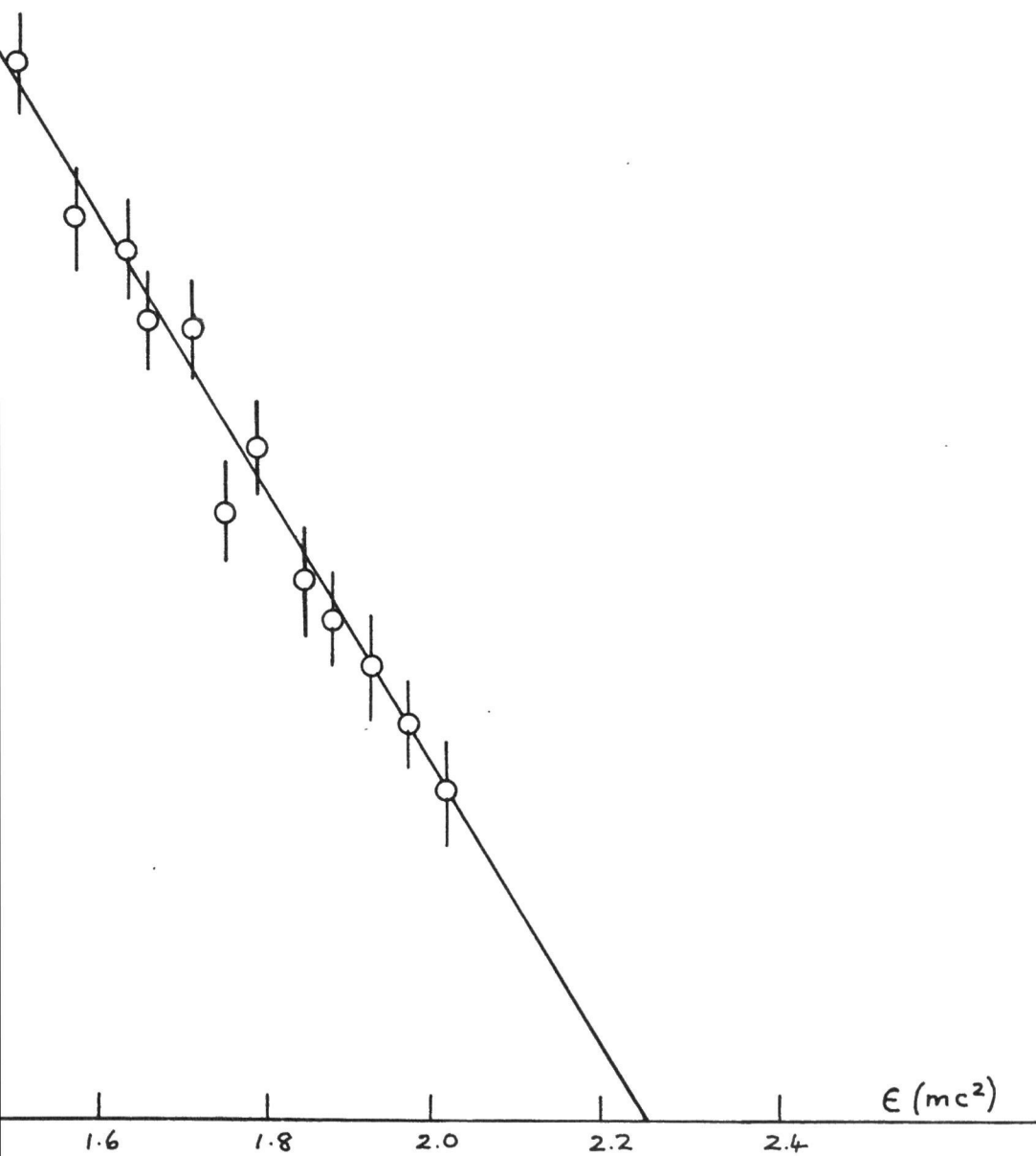


Fig. (14). Fermi plot of partial  $\beta$ -spectrum coincident with H-line.

The results confirm that the first two  $\gamma$ -rays represent competitive de-excitations of a level fed by a  $\beta$ -transition of end-point energy  $690 \pm 9$  keV. The  $\gamma$ -ray corresponding to the H-line, on the other hand, must be involved in the de-excitation of an energy level fed by a  $\beta$ -particle group of maximum energy  $626 \pm 12$  keV. The energy difference between the two end-point energies, 64 keV, agrees within the experimental error with the energy difference of 57 keV between the  $\gamma$ -rays of energies 295 and 352 keV. The level scheme for the RaC nucleus would then appear to be of the form shown in fig. (15) below. A fuller discussion of this decay scheme will be given in Chapter V.

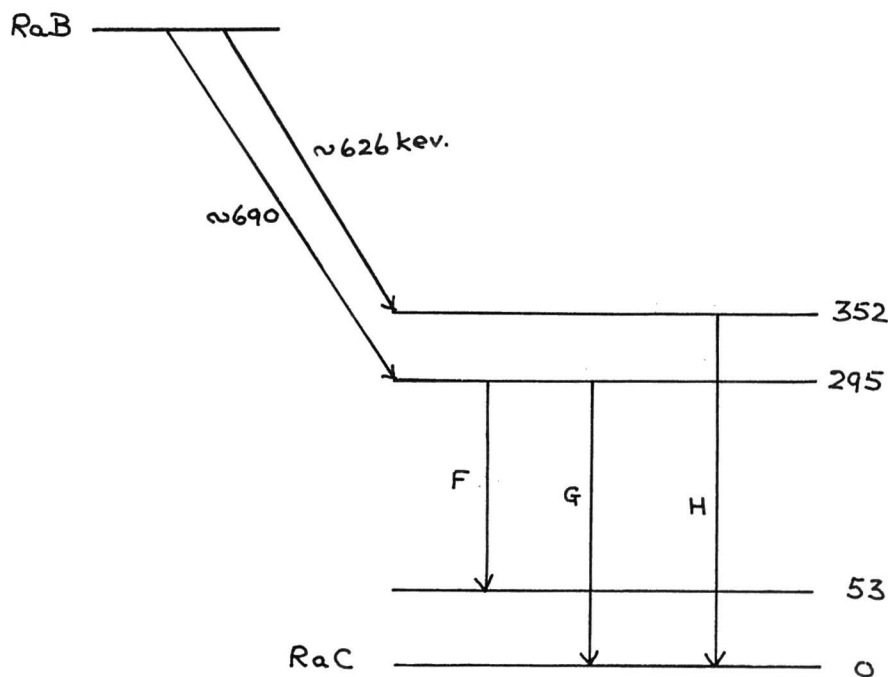


Fig. (15). Level scheme for RaC.



### §3. The Measurements on the Continuous Spectrum.

Measurements were taken of the  $\beta$ -particle counting rates at intervals from  $H_p = 1000$  to 12000 oersteds/cm. Correction was made for the effect of  $\gamma$ -radiation by repeating counts at intervals with the aluminium shutter down, and constructing a graph of the variation of  $\gamma$ -ray counting rate with detector position, from which the required correction could be obtained at each point. On account of the limited momentum range acceptable for each field setting, five values of the magnetic field were necessary to cover the whole spectrum. For the two highest fields, where the portion of the spectrum under observation contained no strong conversion lines, the value of the field strength had to be derived from measurements with the calibrated search coil; the other three fields were measured both by reference to convenient strong conversion lines and by the coil method. Since a higher degree of resolution was desirable in the measurements on the continuous spectrum than was used in the coincidence studies, the source slit width was reduced to 4 mm. and that of the detector slit to 1 mm.

The  $\beta$ -particle counting rates were corrected for decay and normalised for geometry. In addition, since the momentum interval accepted by the detector in any position increased proportionately to the field

strength, each set of counts had to be normalised by division by a factor proportional to the field strength. The good fit of the five separate portions of the final spectrum was a check both on the correctness of the geometrical normalisation factors and the field strengths and on the stability of the source under vacuum conditions.

The division into component spectra was done by the technique of repeated Fermi analysis. The ratio  $N/F$  was calculated for each setting of the detector, where  $N$  was the normalised  $\beta$ -particle counting rate and  $F$  the Fermi function for the corresponding momentum value, obtained from the tables of Feister (46). The values of  $\sqrt{N/F}$  were calculated for all points, and plotted against  $\epsilon$  (the  $\beta$ -particle energy in relativistic units, plus one). The points on the higher energy side of the distribution were plotted down to the point where significant departure from the linear shape indicated the existence of a second partial spectrum of lower end-point energy. The end-point energy ( $\epsilon_0$ ) and slope ( $m_0$ ) of the line corresponding to the highest energy component were then found by the least squares method, assuming an allowed shape for the  $\beta$ -particle spectrum. In practice, for  $\frac{1}{2}\alpha Z > 2\pi R/\lambda$  (where  $\alpha$  is the fine structure constant,  $Z$  the atomic number of the daughter nucleus,  $R$  the nuclear radius and  $\lambda$  the electron wavelength) all first forbidden

spectra should have the same shape as allowed spectra. Since the above relation holds for  $Z > 10$ , the assumption of linearity may be confidently made for almost all of the  $\beta$ -spectra concerned. The formula  $\sqrt{\frac{N_0}{F}} = m_0(\epsilon_0 - \epsilon)$  gave the ordinate due to the highest energy  $\beta$ -component at any energy  $\epsilon$ , and hence  $N_0/F$  could be found at each of the energies corresponding to the other points on the spectrum. The end-point energy of the next partial was calculated by applying the least squares method to the plot of  $\sqrt{\frac{N - N_0}{F}}$  against  $\epsilon$ , again down to an energy such that the presence of a third partial became apparent. The values of the Fermi function used were those for the daughter nucleus  $\text{RaC}'$  ( $^{214}_{84}\text{Po}$ ), but the values of  $F$  for  $\text{RaC}$  ( $^{214}_{83}\text{Bi}$ ) were used when the analysis had reached spectra which were obviously those of the  $\text{RaB} \rightarrow \text{C}$  transition known from the coincidence data.

A complication arose in the determination of the higher energy end-points due to the presence of bremsstrahlung radiation from  $\beta$ -particles striking the metal in the neighbourhood of the detector slit. Since the bremsstrahlung continued to affect the crystal even after the slit had been moved past the position where the highest energy  $\beta$ -particles could enter, the effect was to provide a small background level of counting which persisted beyond the true end-

point of the  $\beta$ -particle spectrum. Since the bremsstrahlung only occurred when the shutter was up, it appeared as though it were a  $\beta$ -particle <sup>component</sup> ~~count~~. An estimate of the intensity of bremsstrahlung near the end-point was obtained by examination of the level portion of the spectrum which continued after the end-point. Since the level of radiation appeared to vary very little with energy in this region, the radiation counting rate here provided a background which could be subtracted from the highest energy partial. It was necessary to consider the bremsstrahlung effect only when dealing with the highest energy partial, as for lower energies the counting rate due to the bremsstrahlung was negligible in comparison with the  $\beta$ -particle counting rate.

The final results quoted for the end-points and relative intensities of the partial spectra of the  $\text{RaC} \rightarrow \text{C}'$  transition were averaged from the results of several runs over the complete spectrum. A typical Fermi analysis is shown in fig. (16), which shows the four higher energy components of the  $\text{RaC}$  spectrum. Fig. (17) shows the two partial spectra associated with the  $\text{RaB} \rightarrow \text{C}$  transition, the portion  $2.14 < \epsilon < 2.42$  being shown in greater detail in fig. (18).

The final results of the measurements on the combined spectrum are given in the table overleaf.

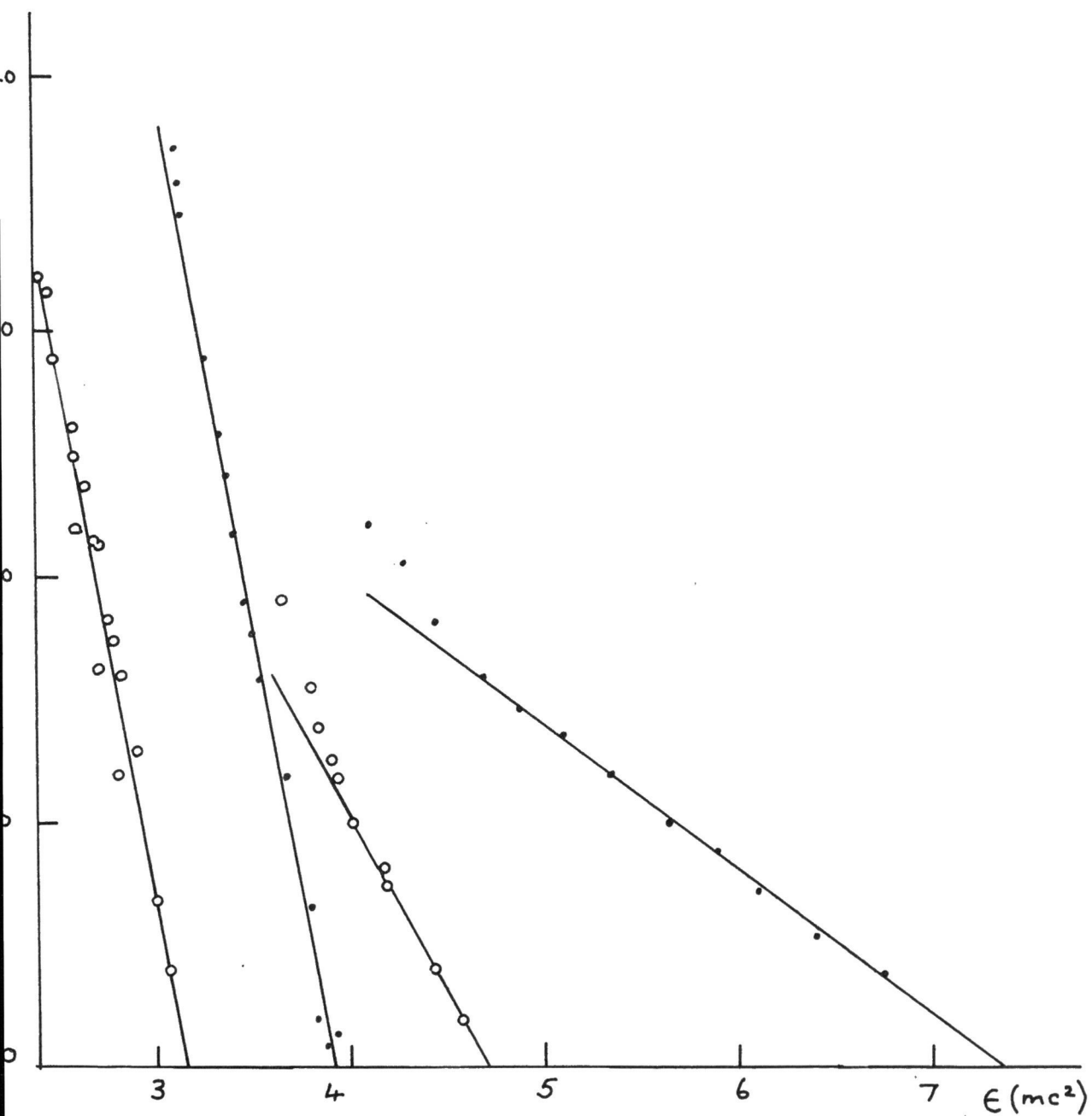


Fig. (16). Components of  $RaC \rightarrow C'$   $\beta$ -spectrum.



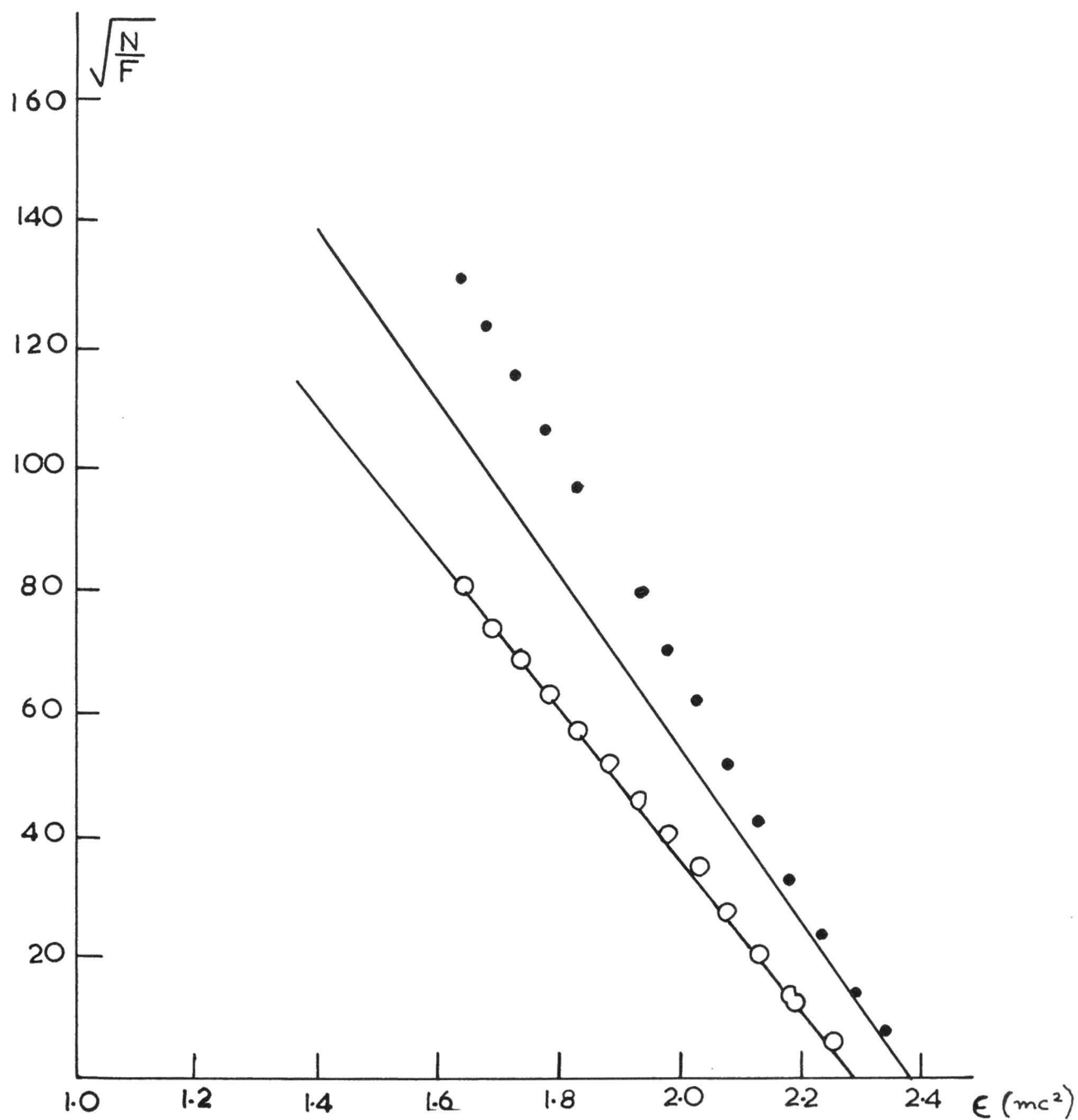


Fig. (17). The partial spectra of the  $RaB \rightarrow C$  transition.

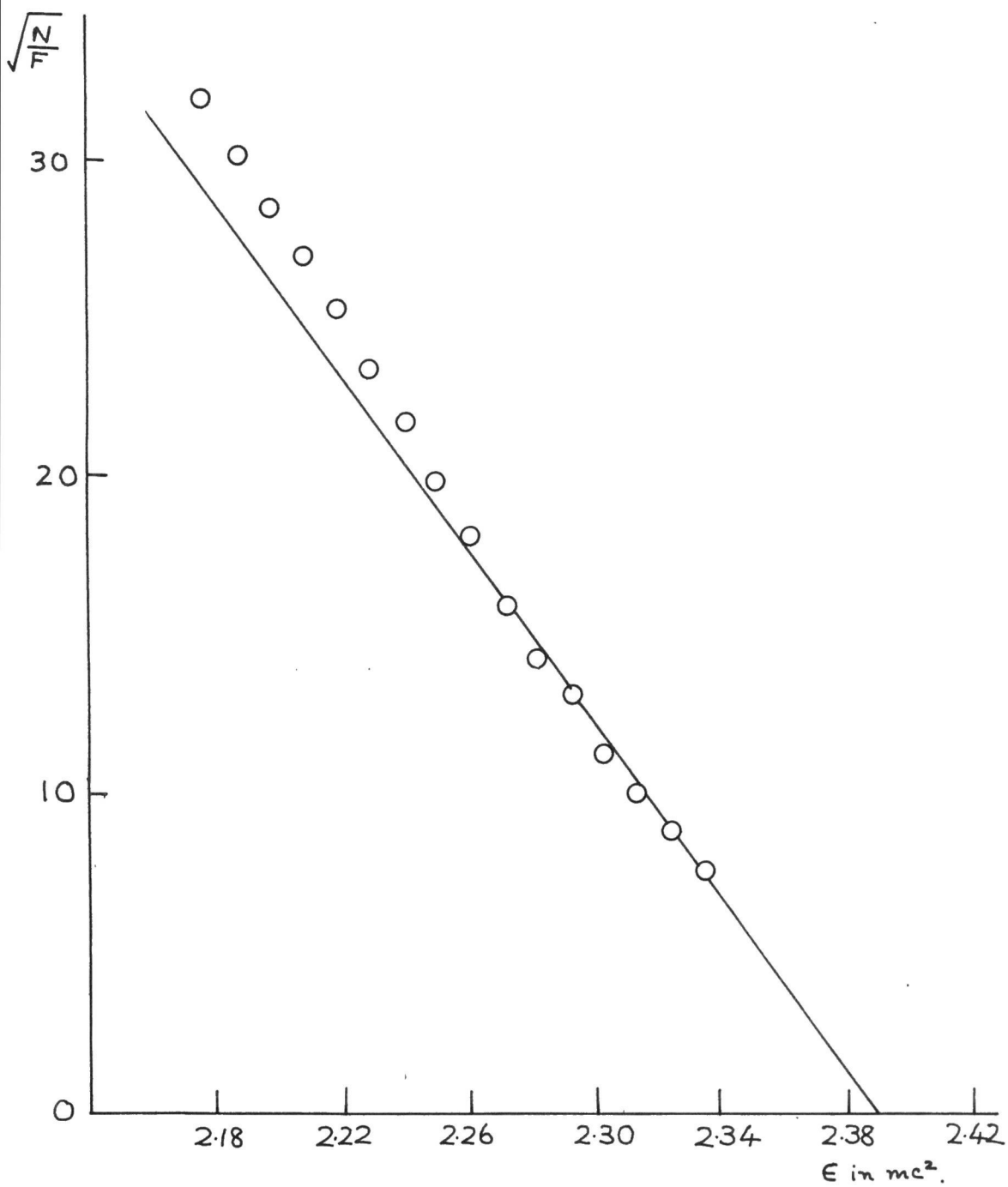


Fig. (18). Higher energy section of fig. (17) in greater detail.

Parent Nucleus	End-point Energy (MeV)	Relative Intensity (%)
RaC	$3.25 \pm 0.02$	24
RaC	$1.88 \pm 0.03$	18
RaC	$1.50 \pm 0.01$	37
RaC	$1.12 \pm 0.02$	21
RaB	$0.70 \pm 0.03$	-
RaB	$0.66 \pm 0.03$	-

The errors quoted for the end-point energies are derived by the formula applicable to the least squares method. The uncertainty in the determination of the end-point energy will obviously be greater when the  $\beta$ -particle group is of low intensity, but an additional error introduced for the lower energy groups is that associated with the repeated subtraction of the  $\beta$ -spectra of higher end-point energies. This source of error will be particularly large for the  $\beta$ -spectra associated with the RaB  $\rightarrow$  C transition. Since, in addition to this effect, another source of uncertainty is introduced in the lower energy regions by the difficulty of distinguishing the profile of the continuous spectrum due to the preponderance of intense conversion lines, the results for the end-point energies of the RaB  $\rightarrow$  C components can be regarded only as rough approximations to the true values.

The relative intensities were found by selecting points at equally spaced momentum intervals and calculating from the parameters of the Fermi plot the value of  $N/F$ , and hence of  $N$ , corresponding to the values of  $\epsilon$ . The quantity  $\sum N$ , summed over the complete partial spectrum then yields a measure of the relative intensity. As this process also decreases in accuracy with decrease of end-point energy, it was not possible to ascribe accurate values to the intensities of the two partial spectra of RaB, although it was clear that these were of roughly equal intensity. The errors in the quoted intensities for the RaC spectra are uncertain, but are not likely to be less than 10% of the intensity value quoted for each partial spectrum.

It is apparent that the four RaC  $\beta$ -feeds found experimentally are insufficient in themselves to account for the extremely complex pattern of  $\gamma$ -disintegration of the nucleus of RaC'. It seems likely that several of the partial  $\beta$ -spectra found arise from a superposition of two or more spectra of closely spaced end-points; in addition there may be  $\beta$ -feeds too weak for detection by the method used. The components actually derived from the analysis were taken as a rough basis for the more complicated decay scheme discussed in Chapter V.

#### § 4. The Coincidence Measurements on the $\text{RaC} \rightarrow \text{C}'$ Transition.

In order to carry out coincidence measurements directly on the  $\gamma$ -rays themselves, it was necessary to determine precisely the multiplier voltage at which a  $\gamma$ -ray of given energy would cease to be counted by the detector. To increase the counting efficiency, the rectangular crystal and its light guide were removed and replaced by a large cylindrical anthracene crystal (of 1 in. diameter), resting on the plane face of a cylindrical light guide. Graphs were obtained of  $\gamma$ -ray counting rate against multiplier voltage for sources of  $^{226}\text{Ra}$ ,  $^{60}\text{Co}$ ,  $^{228}\text{Th}$ , and  $^{137}\text{Cs}$ . Typical graphs (for  $^{60}\text{Co}$  and  $^{228}\text{Th}$ ) are shown in fig. (19). A knowledge of the maximum  $\gamma$ -ray energy for each source enabled a graph to be drawn of "cut-off voltage" against the corresponding  $\gamma$ -ray energy. This graph is shown in fig. (20). From this the "cut-off voltage" for a  $\gamma$ -ray of any given energy could be derived.

The technique employed was to set the multiplier voltage of the  $\gamma$ -ray counter at such a value that the selected  $\gamma$ -ray was just counted, and a Fermi plot obtained for the partial  $\beta$ -spectrum in coincidence with  $\gamma$ -rays of energy greater than the selected value. One of the advantages of this method is that the magnetic field may be set to any value convenient for the

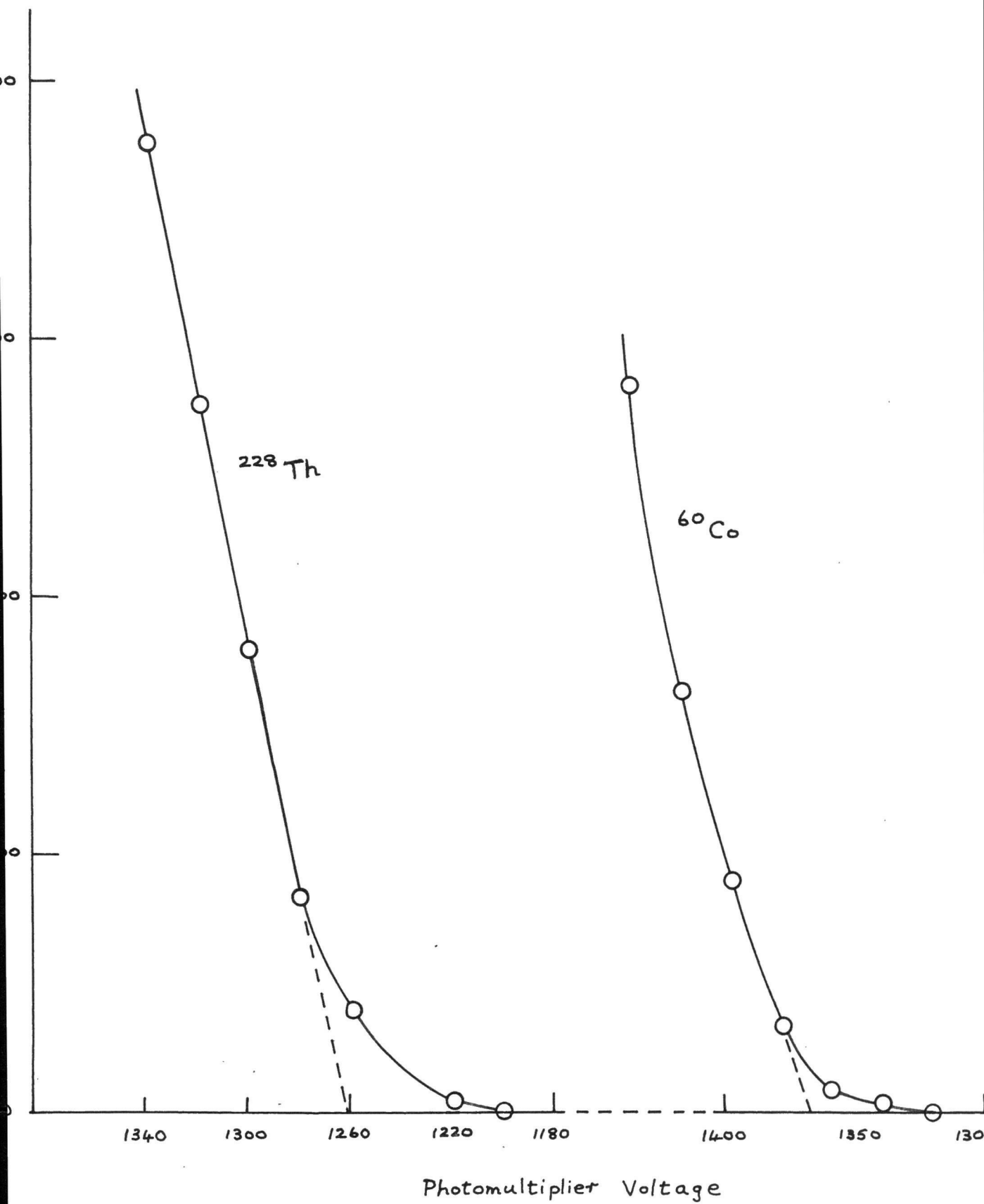


Fig. (19). Y-Ray counting rate v. photomultiplier voltage.

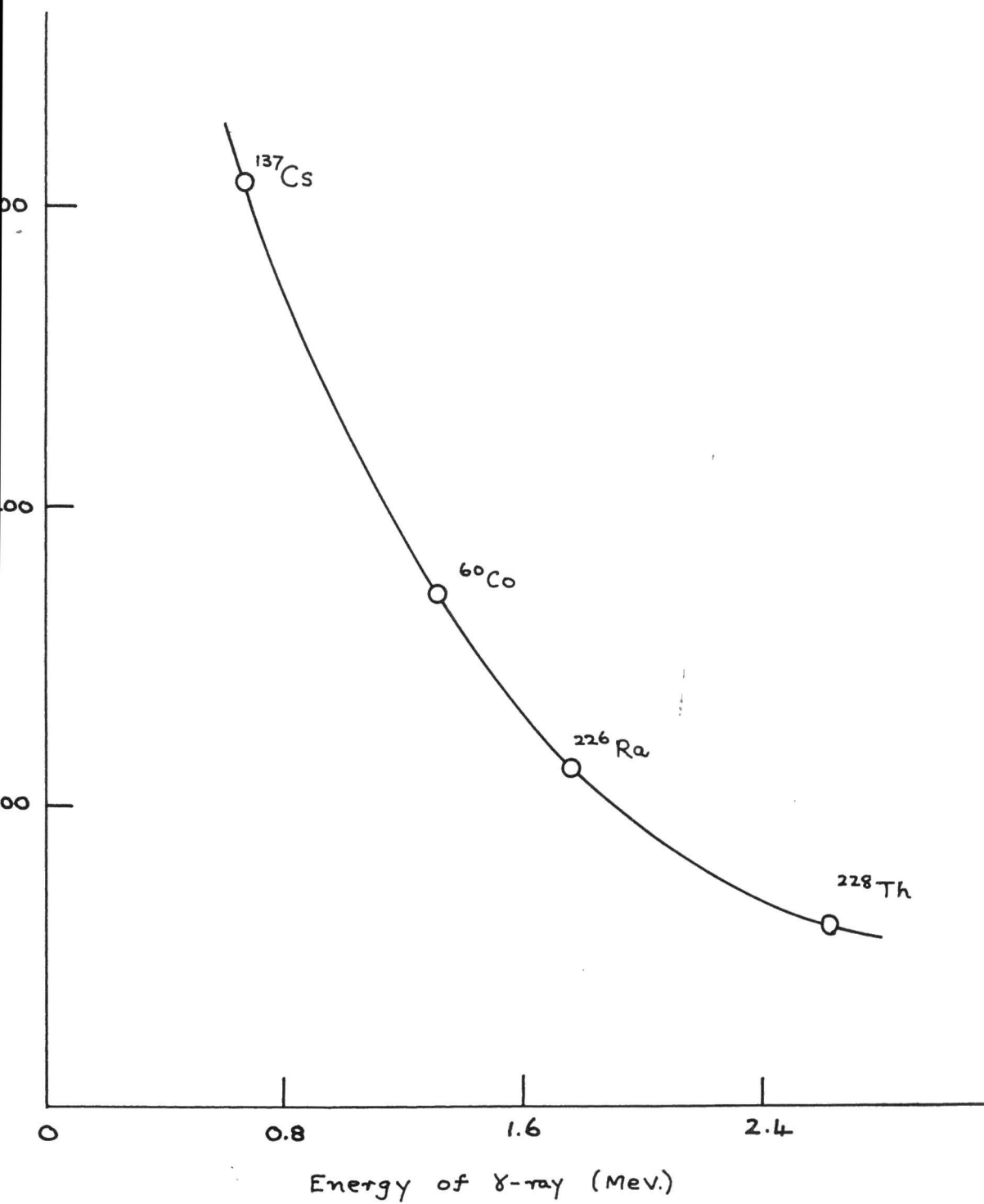


Fig. (20) Cut-off voltage v.  $\gamma$ -Ray energy.

examination of the continuous spectrum, whereas in the previous coincidence measurements the possible field values were restricted by the necessity of focusing the internal conversion line on the second detector.

Fig. (21) shows the Fermi plot of the partial  $\beta$ -spectrum in coincidence with  $\gamma$ -rays of energy  $> 1750$  keV. The end-point energy obtained was  $1.48 \pm 0.02$  MeV. The sum of the energy of the  $\gamma$ -radiation and the maximum energy of the  $\beta$ -feed,  $\overset{3.24}{\cancel{3.25}}$  MeV, agrees well with the value of 3.25 MeV found for the end-point energy of the hardest  $\beta$ -group in the measurements on the continuous spectrum. Taken in conjunction with the result of Johansson (31), that the  $\gamma$ -ray of energy about 1750 keV was not in coincidence with the strong 609 keV  $\gamma$ -ray, the coincidence measurements here suggest that the 3.25 MeV transition leads to the ground state of  $\text{RaC}'$  rather than to the 609 keV excited state.

This conclusion was checked by examination of coincidences between  $\beta$ -particles of energies around 2.9 MeV and the  $\gamma$ -radiation from the 609 keV state. The  $\beta$ -counter was set to count particles of this energy, and counts were taken with the  $\gamma$ -counter voltage adjusted first to count the 609 keV  $\gamma$ -ray, and secondly below the cut-off voltage for radiation of this energy. The results were somewhat inconclusive,



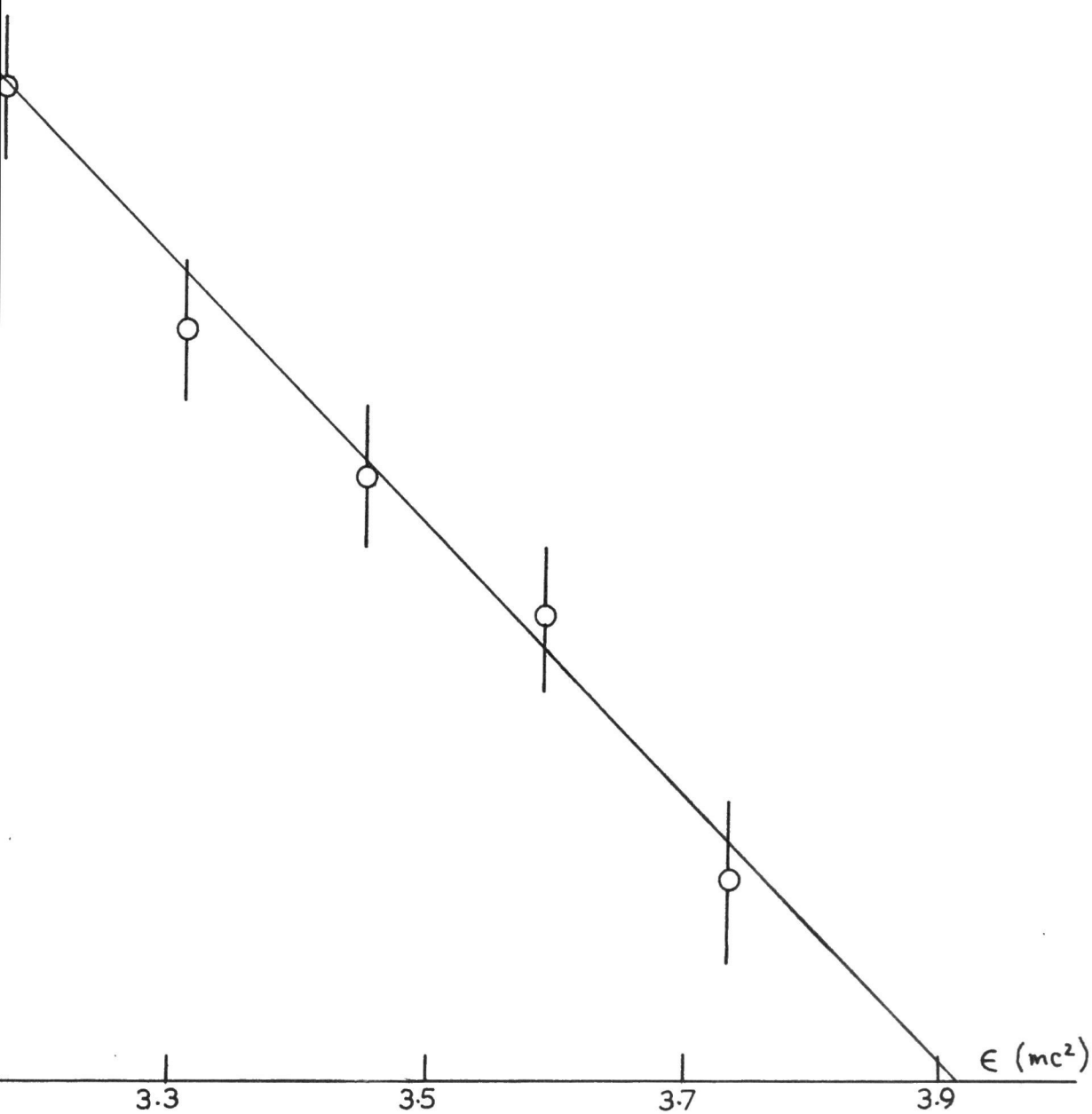


Fig. (21) Partial  $\beta$ -spectrum in coincidence with  $E_\gamma \geq 1750$  kev.

due to the high background of  $\gamma$ -radiation relative to the weak intensity of the  $\beta$ -particles near the tail of the group of end-point energy 3.25 MeV, but no evidence was found of coincidences between the 609 keV  $\gamma$ -ray and the  $\beta$ -particle group of highest end-point energy. This indicates that the  $\text{RaC} \rightarrow \text{C}'$  decay scheme must be constructed on the basis that the total disintegration energy is 3.25 MeV.

## CHAPTER V.

The Construction of Decay Schemesfor RaC and RaC'.§ 1. The RaB  $\rightarrow$  C decay.

The results for the end-point energies of the partial  $\beta$ -spectra in coincidence with the F, G and H  $\gamma$ -rays emitted in the de-excitation of the RaC nucleus are summarised below.

Partial $\beta$ -spectrum end-point energy (keV)	In coincidence with $\gamma$ -ray of energy (keV)	Notation of Ellis for $\gamma$ -ray
688 $\pm$ 10	242	F
694 $\pm$ 15	295	G
626 $\pm$ 12	352	H

The weighted average of the end-point energies for the  $\beta$ -particle group in coincidence with the F and G  $\gamma$ -rays is  $690 \pm 9$  keV. Assuming the decay scheme to be of the form shown in fig. (22) overleaf, the total disintegration energy for the transition between the ground states of RaB and RaC has a value of either 985 keV or 978 keV, depending on the  $\beta$ -branch considered. The average disintegration energy thus appears to be approximately 980 keV, a result in agreement with that of Nielsen et al. (36) in the paper

which appeared after the present investigation had been completed.

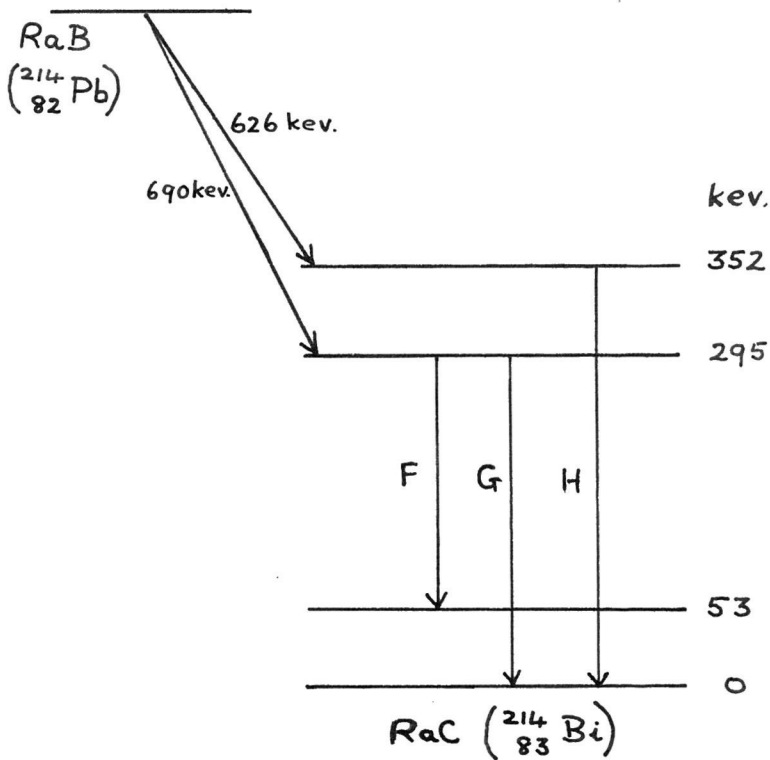


Fig. (22). The  $\text{RaB} \rightarrow \text{C}$  transition.

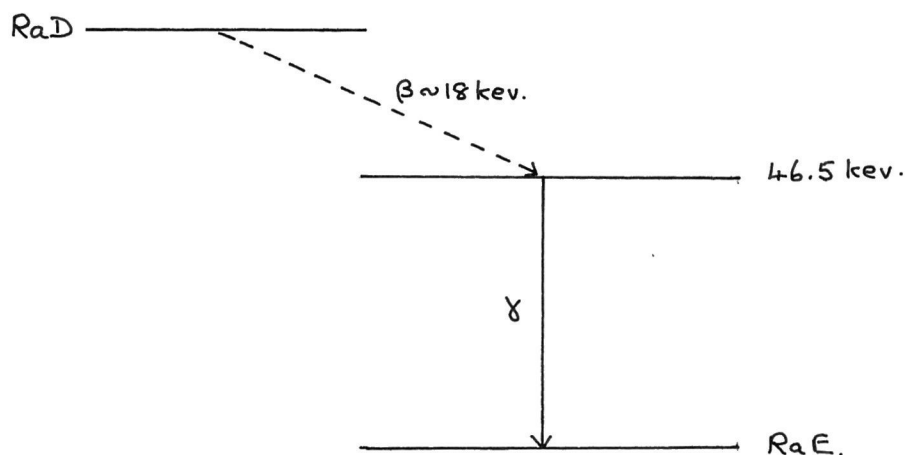
It is interesting to consider the postulated scheme with reference to the determination of spin and parity values of the  $\text{RaC}$  ground state. The lack of agreement in spin and parity assignments for this state has already been discussed (Chapter I). The argument of Feather (29), giving 3 - for the  $\text{RaC}$  ground state was based upon the assumption that the two  $\beta$  - transitions feeding the states at 352 and 295 keV above the ground state were allowed transitions. As

mentioned in the previous chapter, a considerable degree of uncertainty surrounded the determination of the relative intensities of these two  $\beta$ -transitions in the present work, on account of the increasing error introduced by subtraction of the contribution of each of the partial spectra of the  $\text{RaC} \rightarrow \text{C}'$  transition. Thus the inference from the results obtained must be limited to the statement that the two  $\beta$ -groups are of approximately equal intensity.

The degree of forbiddenness of a given  $\beta$ -transition is related to the comparative half-life, which is the product of the partial half-life  $t$  of the  $\beta$ -branch and some quantity  $f$  which is a function of the transition energy and the atomic number of the residual nucleus. Since at the time no other  $\beta$ -particle group was known to occur in measurable intensity, the  $ft$  values for the two transitions were calculated on the assumption that each of them accounted for 50% of the total  $\beta$ -disintegration. The values of the function  $f$  were derived from the graphs of Feenberg and Trigg (47). The results of the calculations are shown below.

End-point energy of $\beta$ -spectrum (keV)	log $ft$
690	5.1
626	5.0

The  $\log ft$  values obtained would normally be taken as indicating that the transitions were allowed, but a further possibility does exist. It is known that a group of highly favoured first forbidden transitions ( $\log ft = 5 - 6$ ) exists for spin change  $\Delta I = 0$  between nuclei near the doubly magic shell (82 - 126). On the other hand, the  $\log ft$  values in similar nuclei for first forbidden transitions with  $\Delta I = 1$  are grouped around 7.5. A typical example of a highly favoured first forbidden  $\beta$ -transition is that of the  $\text{RaD} \rightarrow \text{E}$  disintegration, shown below.



The  $\log ft$  value for the  $\beta$ -transition from the 0 + ground state of the even-even nucleus  $\text{RaD}$  to the 46.5 keV excited state of  $\text{RaE}$  was given by Stanners and Ross (48) as 5.2 - 5.7. The assumption that the  $\log ft$  value for the transition indicates that it is first forbidden ( $\Delta I = 0$ , 'yes'), together with the known M1

character of the 46.5 keV  $\gamma$ -ray, is consistent with the adoption of an assignment of 1 - for the ground state of RaE. This value has been confirmed by Smith (49).

Results published by Krisyouk et al. (50) confirm the existence of a similar feature in the decay  $\text{ThB} \rightarrow \text{ThC}$  ( $^{212}_{82}\text{Pb} \rightarrow ^{212}_{83}\text{Bi}$ ). These authors give a comparative survey of log ft values in the region  $205 \leq A \leq 212$  with particular reference to the existence of first forbidden transitions with low comparative half-lives.

It seems not unreasonable that the decay  $\text{RaB} \rightarrow \text{C}$  should display a similar feature in the  $\beta$ -transitions to the two excited states considered, and since the ground state of the even-even nucleus RaB is classified as 0 +, the two excited states of RaC under consideration will then have the assignment 0 -. The character of the de-exciting  $\gamma$ -radiation from both states was found in the present investigation by deriving the ratios of conversion in the K- and L-shells for the 242, 295 and 352 keV  $\gamma$ -rays from the areas under the corresponding conversion line profiles. The results of this analysis are compared in the table overleaf with the values obtained by Mladjenovic and Slatis (12) and Nielsen et al. (36). The theoretical values quoted for the K/L ratios for M1 and E2 transitions are

taken from Nielsen's paper, and are based on tables by Sliv and Band (51), which take account of the finite size of the nucleus. The values calculated by Sliv and Band show that the approximations made by Rose et al. (52) in neglecting the finite nuclear size lead to considerable error for heavy elements, particularly for magnetic transitions.

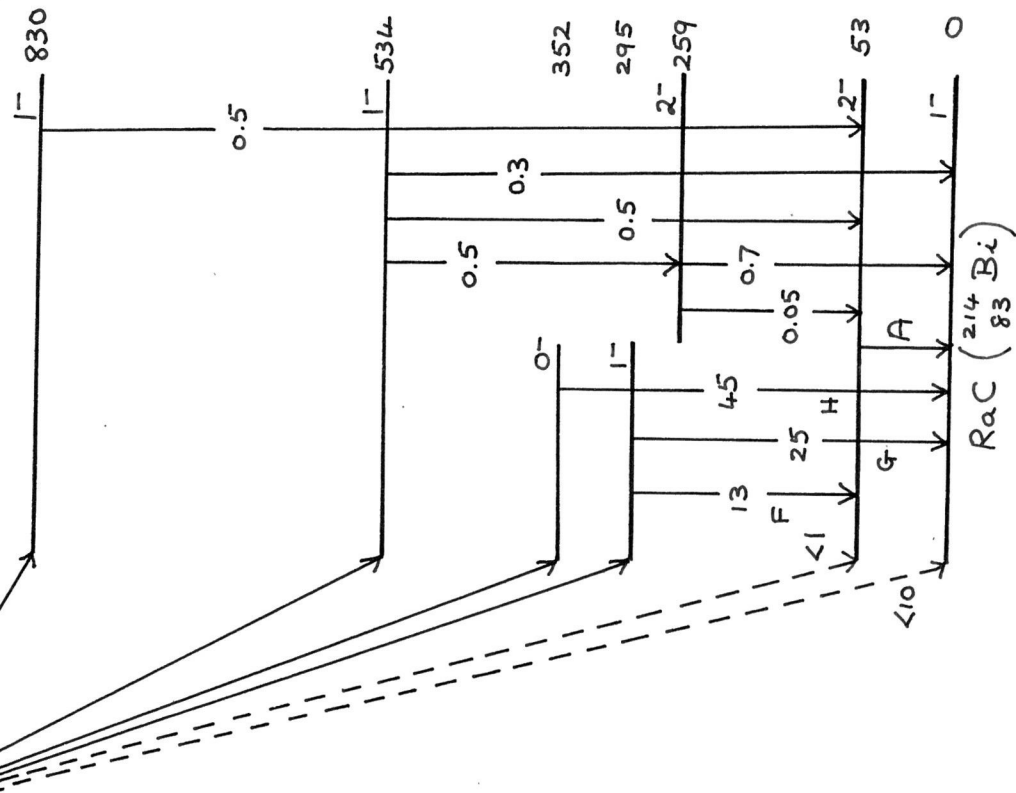
Energy of $\gamma$ -ray (keV)	K/L ratios				
	Mladjepovic and Slatis	Nielsen et al.	Present work	Theoretical values (Sliv and Band)	
				M1	E2
242	4.5	5.3	5.5	5.65	0.9
295	5.5	5.55	5.3	5.7	1.4
352	5.0	5.65	5.4	5.7	1.9

The results of all three sets of measurements indicate that the nature of the radiation for all three  $\gamma$ -rays is almost pure M1. Then, taking the two excited states as  $0^-$ , the ground state must have the assignment  $1^-$ . Once again a close analogy to the  $\text{RaD} \rightarrow \text{E}$  transition is apparent.

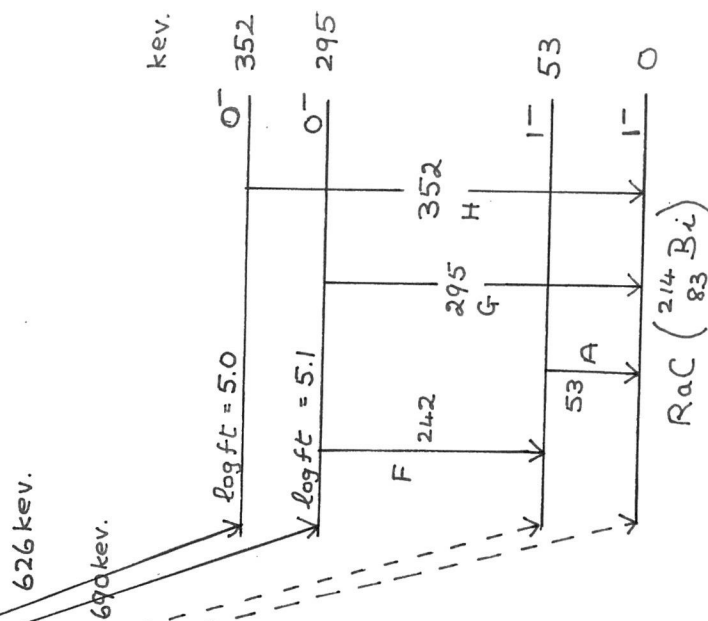
The state at 53 keV is given the assignment  $1^-$  to preserve the M1 character of the de-excitation radiation to the ground state and of the stop-over transition from the 295 keV level.

The adoption of spin one and odd parity for the





(a). Nielsen et al.



(b). Present work

Fig. (23) Comparison of decay schemes for the nucleus of  $\text{RaC} (^{214}_{83}\text{Bi})$ .

RaC ground state is in agreement with the value given by Ricci and Trivero (34), from the  $\log ft$  values calculated for the  $\beta$ -particle groups found in the  $\text{RaC} \rightarrow \text{C}'$  transition. It also agrees with the assignment quoted by Nielsen et al., where the level structure was based on a study of the conversion electron spectra, and of the partial  $\beta$ -spectra in coincidence with the conversion electrons. This scheme is shown in fig. (23), with that of the author for comparison.

Two other weak  $\beta$ -feeds were postulated by Nielsen et al. to account for  $\gamma$ -rays inferred from the conversion electron measurements. The total  $\beta$ -intensity necessary to supply the two levels amounts to only 1.8%, an intensity well below that which could have been detected with certainty in the present Fermi analysis of the continuous spectrum. The upper intensity limits for the ground-to-ground  $\beta$ -transition and the  $\beta$ -feed to the 53 keV state were given by Nielsen et al. as 10% and 1% respectively. The maximum possible intensity for the partial  $\beta$ -spectra in competition with the feeds to the states at 352 keV and 295 keV is thus  $\sim 13\%$ . On the basis of the approximate equality of the latter two feeds, each has to be taken as having a relative intensity of  $\sim 43\%$ . Reduction of the intensities to this value produces only a small change in the values of  $\log ft$ , which remain 5.0 and 5.1

classed as  $0^-$ , the stop-over transition could manifest itself only through the emission of conversion electrons, and the lifetime of the transition would be expected to be much too large to compete with the  $M1$  de-excitation radiation from the 295 keV state to the ground state.

With regard to the existence of the direct  $RaB \rightarrow C$  ground-to-ground state transition, the fact that no trace of this was found in the present investigation may be explained both on the grounds of the low intensity expected for the transition, and the difficulty of separating it from the  $RaC \rightarrow C'$  -transitions of around the same end-point energy. The study of  $\beta - \gamma$  coincidences used in the measurement of the other  $\beta$  -radiations from  $RaB$ , was of course inapplicable here. H. Daniel (53) has reported the existence of a  $\beta$  -transition of end-point energy 1.03 MeV, which is attributed to the  $RaB \rightarrow C$  ground-to-ground transition. The method employed was to study the time variation of the  $\beta$  -radiations of selected energies round about 1 MeV from a freshly prepared source of  $RaB$ . The rate of growth of the components arising from the disintegration of  $RaC$  could be predicted from a knowledge of the lifetimes of  $RaB$  and  $RaC$ , and thus a criterion for distinguishing the source of a  $\beta$  -particle group of given end-point energy was available. From a

knowledge of the components of the RaC  $\beta$ -spectrum, the most energetic component of the  $\beta$ -spectrum of RaB was found to have an end-point energy of  $1.03 \pm 0.06$  MeV, with intensity  $(6.3 \pm 2)\%$ . On this basis the  $\log ft$  value was calculated to be 6.6.

The total disintegration energy obtained by this method agrees within the experimental errors with the value of 980 keV found both by Nielsen et al. and in the present work. The comparative half-life value also is consistent with the assignment 1 - for the RaC ground state, although a value of 0 - is not excluded.

## §2. The RaC $\rightarrow$ C' Transition.

The construction of a decay scheme for the nucleus of RaC' presents a difficult problem owing to the lack of a reliable theoretical model for nuclei in the region a little way from the closed shells. The presence of two protons and four neutrons outside the closed shells ~~makes it unreasonable to found a scheme is sufficient to ensure that a scheme can be built up~~ either on the extreme independent particle model or on the basis of collective excitations which assume predominance only for values of the mass number  $> 225$ . Additional difficulty arises from the complexity and lack of agreement among the experimental data based on the numerous investigations of the radiations involved in the formation and decay of the nucleus. In particular, the consistency of the postulated intensities for many of the  $\gamma$ -radiations from RaC' leaves much to be desired. At the time when the present investigation was started, the data for the  $\beta$ -particle groups of the RaC nucleus were based on relatively crude determinations with poor resolution.

One of the most important foundations for a decay scheme was provided by the long-range  $\alpha$ -particle measurements of Rutherford et al. (1). An attempt has been made by Feather (37) to correlate the excited levels derived from the  $\alpha$ -particle measurements with the known  $\gamma$ -ray energies and intensities. This decay

scheme is shown in fig. (24). Twelve of the postulated states were derived from the long-range  $\alpha$ -particle measurements, and the other eight, shown by dotted lines, were inserted to account for the existence of known  $\gamma$ -rays which could not be fitted into the level scheme of the long-range  $\alpha$ -particles. The 39  $\gamma$ -rays shown in this scheme included all those actually observed in emission at that date, together with nine others, shown as 0% in the diagram, the intensities of which were presumed to be less than 0.2% each. Where necessary the  $\gamma$ -ray intensities were adjusted to give a value for the mean excitation energy in agreement with the value obtained by direct measurement of the  $\gamma$ -ray heating effect. Spin and parity values were assigned from a knowledge of the characters of the  $\gamma$ -radiations and from the degrees of forbiddenness consistent with the intensities of the exciting  $\beta$ -radiations, bearing in mind the proviso that all states involved in long-range  $\alpha$ -emission must have assignments of the form  $(2n) +$  or  $(2n + 1) -$ . While the scheme accounts successfully for many of the known features of the disintegration, considerable disagreement emerges in respect of the values for the internal conversion coefficients of many of the radiations. In addition the degree of forbiddenness of each of the  $\beta$ -transitions from RaC was derived on the assumption that the ground

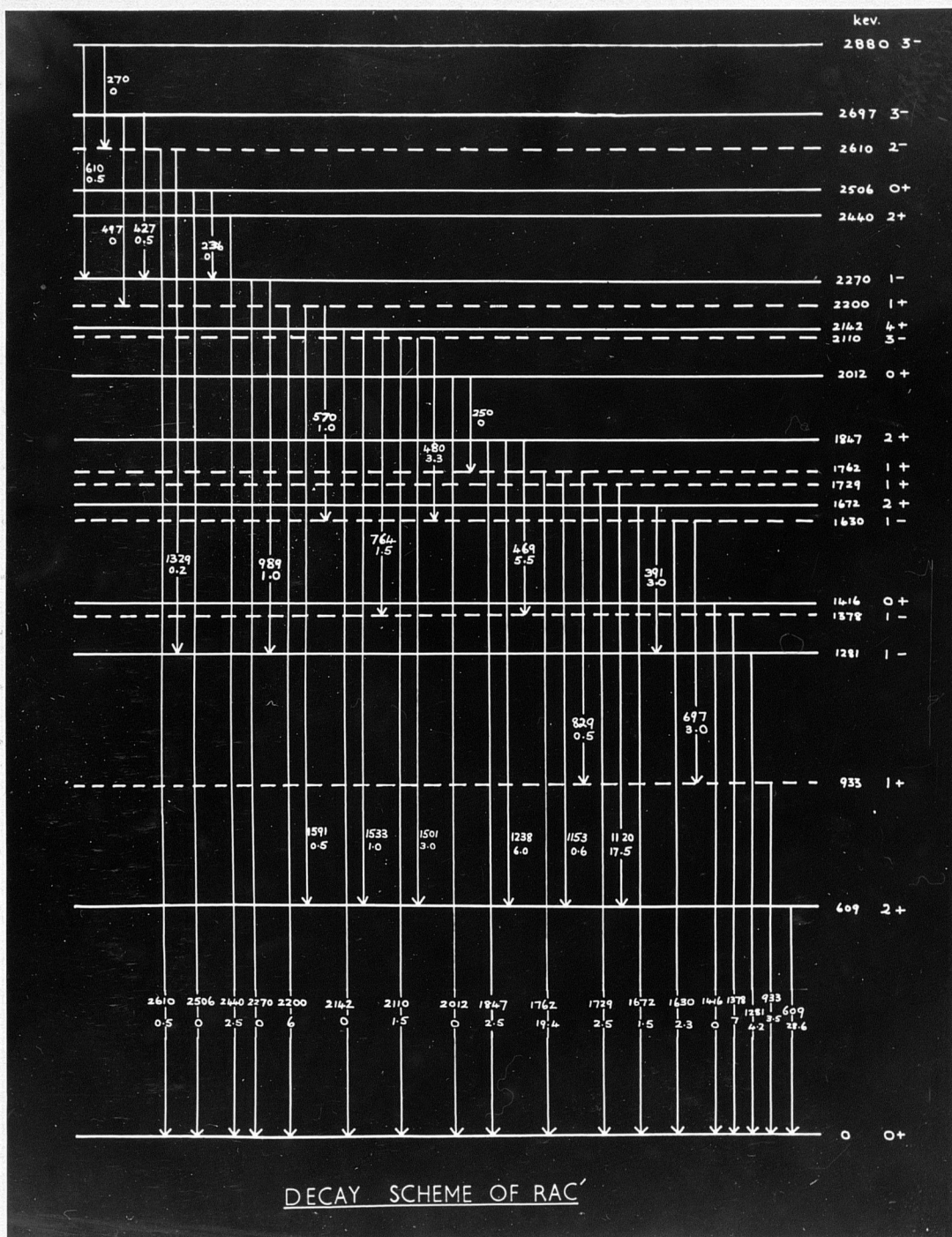


Fig. (24). Decay scheme of  $\text{RaC}'$  (Feather).



state of that nucleus had the assignment 3 -, whereas the measurements detailed in the present work suggest the value 1 - for the RaC ground state.

One of the most recent attempts to construct a decay scheme for RaC' was due to Nielsen (36), and was based on an exhaustive investigation of the conversion lines of the  $\gamma$ -radiations. The decay scheme postulated by Nielsen is shown in fig. (25). The intensities quoted for the  $\gamma$ -radiations were derived from three sources (a) conversion line measurements in conjunction with internal conversion coefficients (b) the relative  $\gamma$ -ray intensities as given by Dzelepov and Sestopalova (16) (c) scintillation measurements of the  $\gamma$ -rays in coincidence with the 609 keV transition, and other  $\beta$ - $\gamma$  and  $e^-$ - $\gamma$  coincidence measurements. From the measured intensity of the 609 keV K-conversion line, and the E2 conversion coefficient, the total intensity of the transitions feeding the 609 keV level was calculated to be 41%. Since the intensity of the  $\beta$ -particle group to the ground state was 23%, the total intensity of the  $\gamma$ -transitions to the ground state parallel to the 609 keV  $\gamma$ -ray was then 36%. Assuming a distribution of the stronger  $\gamma$ -rays in accord with the coincidence measurements, it was found that the ratio of 41:36 between the intensities of the 609 keV  $\gamma$ -ray and all parallel transitions was consistent with





the measurements of Dzelepov and Sestopalova.

Assuming the relative intensities due to the latter, comparison of the percentage intensities obtained with the measured conversion line intensities gave the multipole orders of the radiations. The values for the  $\gamma$ -ray intensities quoted in the diagram were based on the conversion line measurements, assuming pure multipoles in most cases. For the transitions of energies 609 keV and under, the multipole orders were inferred from the K/L ratios, and the intensities from the theoretical conversion coefficients. For some of the weaker transitions, it was not possible to distinguish definitely between M1 and E2 multipole order, especially at high energies, where the conversion coefficients differ by less than a factor of two.

An attempt will be made in the following pages to correlate the decay scheme of Nielsen with the scheme based on the long-range  $\alpha$ -particle measurements, adjustments being made where necessary to bring the required intensities of  $\beta$ -excitation into consistency with the intensities found in the present work. Each of the levels of the two primary decay schemes will be discussed in detail. These states are as follows:  
Ground state (0 +). The spin assignment follows since

$\text{RaC}'$  ( $^{214}_{84}\text{Po}$ ) is an even-even nucleus.

609 keV (2 +). Evident both in the spectrum of the

long-range  $\alpha$ -particles and in the existence of the intense  $\gamma$ -ray of energy  $609.37 \pm 0.16$  keV (26).

933 keV (1 +). This level was suggested by Feather to account for the existence of the 933 keV  $\gamma$ -ray known from the measurements of Ellis, Mladjenovic and Hedgran, etc. Nielsen, on the other hand, considered this  $\gamma$ -ray to represent a transition from a level at 1544 keV to the 609 keV level. The latter interpretation is supported by the measurements of Rowland (54) and Johansson (31), who found that the 609 keV  $\gamma$ -ray was in coincidence with another of energy 935 keV.

1281 keV (2 +). Found from long-range  $\alpha$ -particles. In addition a  $\gamma$ -ray of energy 1281.3 keV was found by Mladjenovic and Slatis (12). The K/L ratio given by these authors was 3.5. The K/L ratios for E1 and E2 radiation are 6.5 and 5.1 respectively. This suggests that the de-exciting radiation is more likely to have E2 character than E1, and thus the assignment 2 + is preferred to the 1- value postulated by Feather. (The possibility of M1 multipole order is excluded, since this would necessitate the assignment 1 + for the excited state, which is incompatible with the existence of the corresponding long-range  $\alpha$ -particle group.)

Again, if we consider the  $\gamma$ -ray intensity expected from the K-conversion line intensity measurements of Mladjenovic and Slătis, we find that the assumption of E1 character leads to a predicted  $\gamma$ -ray intensity  $\sim 14\%$ . With the E2 character, on the other hand, a  $\gamma$ -ray intensity of only  $\sim 4\%$  would be expected; this is in good agreement with the estimate of 4.2% quoted by Feather, and roughly consistent with the relative intensity given by Dzelepov and Sestopalova.

In the decay scheme of Feather, the 1281 keV level was fed by a  $\gamma$ -ray of energy 391 keV (3%). A  $\gamma$ -ray of about this energy can be derived from the measurements of Mladjenovic and Slătis.

Nielsen also found a  $\gamma$ -transition of about the same energy, but suggested that it represented the de-excitation from the 1764 keV level to that at 1378 keV. The intensity given was only 0.4%. The other  $\gamma$ -transition to the 1281 keV state postulated by Feather had an energy of 989 keV, and an intensity of 1%. Although quoted by Ellis, no trace of this  $\gamma$ -ray was found either by Mladjenovic and Slătis or by Nielsen. It is thus possible that the state may be excited entirely by  $\beta$ -radiation from RaC. Analysis of the log ft value for a transition from the 1 - ground state

of RaC to a  $2 +$  state at 1281 keV shows that a  $\beta$ -particle intensity of  $\sim 4\%$  is possible, whereas the adoption of the value  $1 -$  gives too large an intensity for the  $\beta$ -feed. The existence of a  $\beta$ -transition of intensity  $\sim 3\%$  provides better agreement with the intensity measurements in the present work than would the assumption of almost zero direct  $\beta$ -excitation. (See below).

1378 keV ( $2 +$ ). The assignment  $2 +$  is due to Nielsen. Feather gave  $1 -$ , with the possibility of  $\alpha$ -emission, which might be masked by the relatively intense  $\alpha$ -group from the level at 1416 keV. The assignment  $2 +$  is supported by the results of Johansson (31), who classed the de-excitation radiation to the ground state as "rather pure  $E2$ ". The suggestion of Feather was based on the consideration of the ground state of RaC as a  $3 -$  state, which would entail a second forbidden  $\beta$ -transition to the level at 1378 keV. On the assumption, however, that the RaC ground state has an assignment of  $1 -$ , the choice of the same value for the 1378 keV state would imply an allowed  $\beta$ -transition, the intensity of which would then be much too great. If the 1378 keV state is taken as  $2 +$ , on the other hand, the corresponding  $\beta$ -transition becomes first forbidden, and the

intensity is then consistent with the total de-excitation, given by Nielsen as 7%.

In the decay scheme of Feather the state was fed by  $\gamma$ -rays of energies 469 keV (5.5%) and 764 keV (1.5%). According to Nielsen the 469 keV transition had an intensity of only 0.2%. The 764 keV transition corresponds to that of 769 keV which was taken by Nielsen as the de-excitation of the 1378 keV state to the level at 609 keV. The placing due to Nielsen necessitates a  $\beta$ -feed of 6% to the present level, which accords better with the intensity measurements of the  $\beta$ -groups in the present work.

1416 keV (0 +). Known both from the  $\alpha$ -particle data and the presence of internal conversion lines. The 0 + assignment is based on the absence of the direct  $\gamma$ -radiation to the ground state.

1544 keV (1 +). This level was postulated by Nielsen to account for the 935 keV  $\gamma$ -ray in coincidence with the 609 keV  $\gamma$ -transition. The suggested spin and parity assignment was 2 +, 1 + or 3 +. The 2 + value is unlikely as no  $\alpha$ -particle group corresponding to this excitation energy has been detected. The required intensity of the exciting  $\beta$ -transition, based on the intensity (3%) of the 935 keV transition to the 609 keV state, suggests

the assignment  $1 +$  on the basis of comparative half-lives. If  $1 +$  rather than  $3 +$  is adopted, a detectable  $\gamma$ -transition to the ground state would be expected, which may correspond to the 1532 keV transition given by Ellis, although no trace of this was found by Mladjenovic and Slatis.

1630 keV ( $1 -$ ). The existence of this level was postulated by Feather to account for the  $\gamma$ -ray of about this energy found by Ellis. Due to the proximity to the  $\alpha$ -particle group from the level at 1661 keV, it is not possible to say whether or not a level at 1630 keV would also be de-excited by long-range  $\alpha$ -particles. The existence of this level is rendered unlikely by the coincidence results of Johansson (31), who found that (a) the 1620 keV  $\gamma$ -ray was in coincidence with the 609 keV  $\gamma$ -ray, and (b) that the 1620 keV  $\gamma$ -ray was not seen in coincidence with  $\beta$ -particles of energies down to 600 keV. The only conclusion to be drawn from these measurements is that the 1620 keV  $\gamma$ -ray must originate from a level above  $\sim 2650$  keV, and be in coincidence with one of the  $\gamma$ -rays to the 609 keV state from an intermediate level. The possibility that the 1620 keV  $\gamma$ -ray represents a transition from the level around 2880 keV to the 1281 keV level is unlikely, as no evidence exists

for a sufficiently strong  $\gamma$ -transition between the 1281 and 609 keV states, although a weak  $\gamma$ -ray of  $\sim 669$  keV does appear in the decay scheme of Ellis. Since a  $\gamma$ -transition of intensity 3 - 6% occurs between the levels at 1378 and 609 keV, it seems reasonable to postulate a level at 3000 keV from which the 1620 keV  $\gamma$ -ray would reach the 1378 keV level. Assuming the value given by Johansson for the intensity of the 1620 keV  $\gamma$ -radiation (2.8%), the comparative half-life of the  $\beta$ -transition from RaC is indicative of an allowed transition, suggesting the assignment 2 - for the 3000 keV state.

The other basis in the original scheme for the placing of the 1630 keV level was referred to the 695 keV  $\gamma$ -transition of Ellis, which was taken as going to the 933 keV level. Since the 933 keV level has not been accepted, this  $\gamma$ -ray would in any event have to be fitted elsewhere, and Nielsen took a  $\gamma$ -ray of 703 keV energy between the levels at 2117 and 1416 keV. A placing which agrees better with the present intensity measurements on the  $\beta$ -spectra is between the 2430 keV level and that at 1728 keV.

1661 keV (2 +). Quoted by Nielsen to account for 1661 keV  $\gamma$ -ray. This level corresponds to the  $\alpha$ -



particle level at 1672 keV, to which Feather also assigned the value  $2 +$ . In the scheme of Feather, a  $\gamma$ -ray of energy 391 keV was assumed to represent a transition from the 1672 keV state to the level at 1281 keV. According to Nielsen, this  $\gamma$ -ray (given as 387.4 keV) represents a transition between states at 1764 ( $1 +$ ) and 1378 ( $2 +$ ) keV. In view of the close correspondence in energy values obtained by Nielsen, the latter interpretation will be taken.

1728 keV ( $1 +$ ). This level was given the value  $2 +$  by Nielsen, but the absence of detectable  $\alpha$ -radiation suggests that the assignment is more likely to be of the form  $(2n) -$  or  $(2n + 1) +$ . Since the combined intensity of the two de-exciting  $\gamma$ -rays is  $\sim 20\%$ , and no  $\gamma$ -rays leading to this state are shown in either decay scheme, a fairly high degree of excitation by  $\beta$ -radiation is necessary. The only spin assignment which provides the required degree of  $\beta$ -excitation, while retaining the M1 character of the 1120 keV  $\gamma$ -transition to the 609 keV state, is  $1 +$  ( $\beta$ -transition first forbidden,  $\Delta I = 0$ , 'yes'). The existence of the transition from this level to the ground state with intensity 4% (Nielsen) would also tend to favour an assignment of  $1 +$  rather

than  $3 +$ .

1764 keV ( $1 +$ ). Appears in both decay schemes.

1848 keV ( $2 +$ ). Appears in both decay schemes.

2017 keV ( $2 +$ ). This level was classed by Neilsen as  $1 +$ , but the presence of long-range  $\alpha$ -particles necessitates the selection of one of the group  $0 +$ ,  $1 -$ ,  $2 +$  or  $3 -$ . The  $0 +$  value is eliminated by the presence of the 2016 keV  $\gamma$ -ray to the ground state found by Mladjenovic and Hedgran in the Compton spectrum. From consideration of the log ft values for the exciting  $\beta$ -transition, the assignment  $2 +$  appears to be the only value compatible with the total  $\gamma$ -ray de-excitation ( $\sim 5\%$ ).

2117 keV ( $2 +$ ,  $1 +$ ). The spin and parity assignment has been given by Nielsen as  $2 +$  or  $1 +$ , and by Feather as  $3 -$ . Due to proximity to the  $\alpha$ -particle level at 2142 keV, it is uncertain whether or not  $\alpha$ -particles are emitted from this level. Taking the RaC ground state as  $1 -$ , no decision between the values  $2 +$  and  $1 +$  is possible on the basis of degree of forbiddenness of the required  $\beta$ -particle excitation ( $\sim 5\%$ ).

2142 keV ( $3 -$ ,  $4 +$ ). The  $4 +$  assignment was given by Feather, and was based on the assumption that  $\gamma$ -radiations of energies  $\sim 1533$  keV and 764 keV

were involved in the de-excitation. Both of these  $\gamma$ -rays were placed elsewhere in the scheme of Nielsen. No recent evidence exists for the presence of a  $\gamma$ -ray of energy 2142 keV. Assuming that the only mode of de-excitation (apart from the long-range  $\alpha$ -particle group) is a very weak  $\gamma$ -ray of energy 2142 keV, the consideration of comparative half-lives suggests the adoption of either 3 - or 4 + as the spin value.

2204 keV (1 +). The 1 + designation is based upon the M1 multipole order of the de-exciting  $\gamma$ -ray (Nielsen), and is compatible with the comparative half-life for the disintegration from the RaC ground state.

2280 keV (3 -). Based on  $\alpha$ -particle group and on  $\gamma$ -ray to ground state found in Compton spectrum of Dzelepov and Sestopalova. Since the level appears to be fed by two  $\gamma$ -rays from higher energy states, the level of  $\beta$ -excitation required may be very small. The most probable assignment is 3 -, giving a second forbidden  $\beta$ -transition from the ground state of RaC.

2430 keV (2 +).  $\alpha$ -particle level. Also based on  $\gamma$ -ray in Ellis and Mladjenovic and Slätis. The 2 + assignment of Feather still gives the required intensity for the  $\beta$ -feed from the

re-assigned RaC ground state.

2506 keV (3 -, 4 +).  $\alpha$ -particle level. To provide the very low excitation required for this state, a third forbidden  $\beta$ -transition was postulated by Feather. Evidence for the existence of a  $\gamma$ -ray of energy  $\sim 2500$  keV was given by Ellis, but the uncertainty in intensity does not permit a definite spin assignment to the state.

2610 keV (2 -). Based on conversion line measurements by Ellis showing the existence of a 2610 keV  $\gamma$ -ray and of the 1329 keV  $\gamma$ -ray de-excitation to the 1281 keV state. According to Wolfson (14) also, some slight evidence exists for the assumption of a  $\gamma$ -radiation of energy about 2.6 MeV. Mladjenovic and Slatis, on the other hand, found no trace of a conversion line corresponding to the 2610 keV  $\gamma$ -ray. If the level be accepted, the assignment 2 - due to Feather can be retained without altering the degree of forbiddenness of the  $\beta$ -particle excitation.

2697 keV (2 +). Based on long-range  $\alpha$ -particles and on existence of  $\gamma$ -rays of energies 427 and 497 keV (Ellis). H. Daniel (55) quotes evidence for the existence of a  $\gamma$ -ray of energy  $2.72 \pm 0.02$  MeV, which presumably represents the de-excitation

to the ground state. With the altered value for the RaC ground state spin, an assignment of  $2 +$  seems more likely than that of  $3 -$  due to Feather.

2880 keV ( $3 -$ ,  $4 +$ ).  $\alpha$ -particle level. Since the intensity quoted by Daniel (55) for a  $\gamma$ -ray of energy  $2.89 \pm 0.05$  MeV is as low as 0.03% per disintegration, the de-excitation intensity may be low enough to warrant the assumption of a rather high spin value.

In addition to the levels discussed above, it has been necessary to postulate the additional level at 3000 keV, to account for the known data about the 1620 keV  $\gamma$ -radiation. A  $\gamma$ -ray of energy  $3.03 \pm 0.03$  MeV given by Daniel may correspond to the ground state de-excitation from this level. Since the intensity given by Daniel is only 0.07%, the required degree of  $\beta$ -excitation may be taken as the intensity of the 1620 keV  $\gamma$ -ray, namely  $\sim 2 - 3\%$ .

The energy levels derived from the considerations above are shown in the decay scheme in fig. (26). For comparison with the  $\beta$ -spectra obtained experimentally, the structure may be divided fairly readily into groups of closely-spaced levels corresponding to the components of the  $\beta$ -spectrum resolved in the Fermi analysis. Table 1 overleaf relates the end-point energies of these components to the corresponding groups of excited levels.

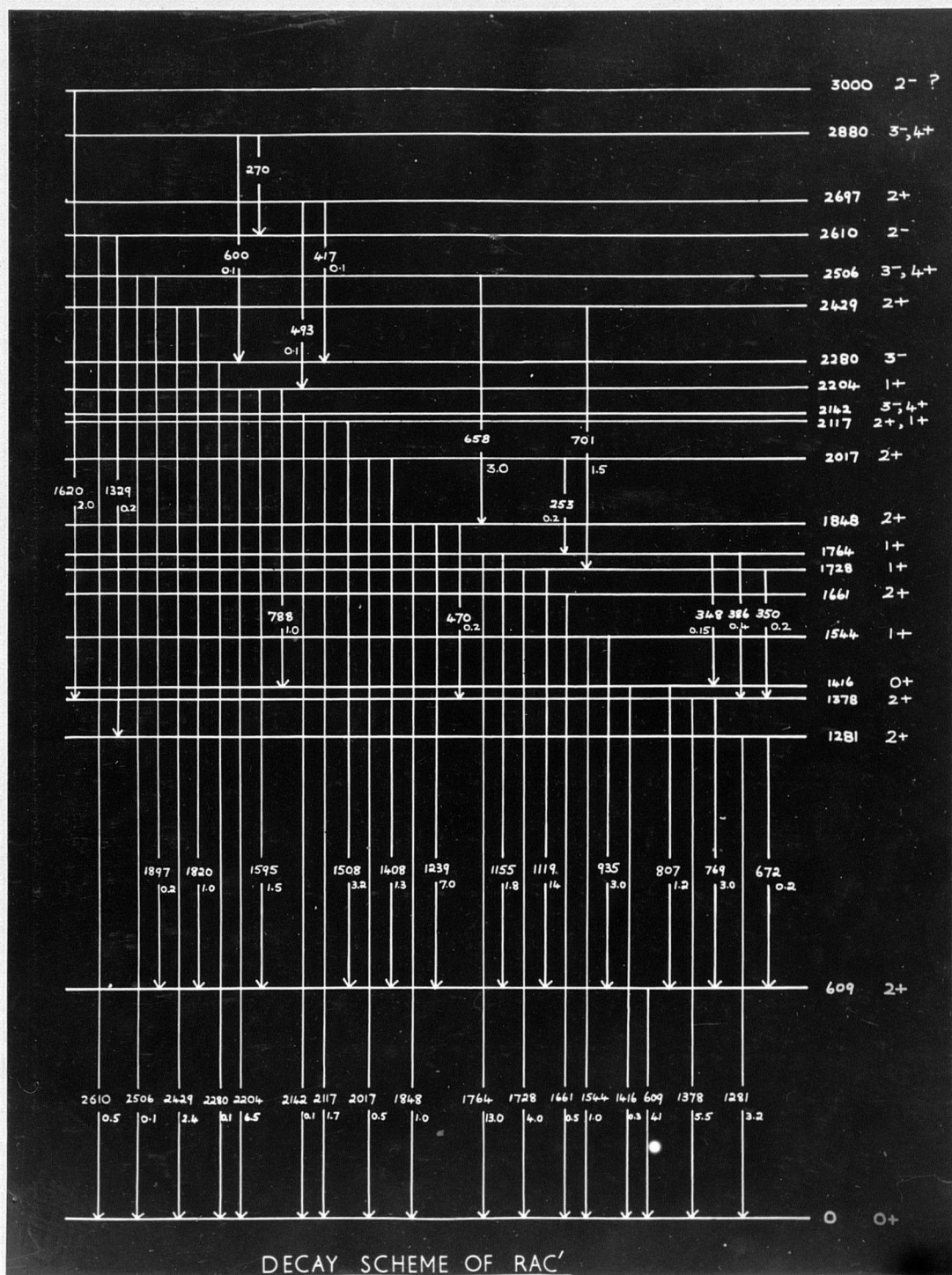


Fig. (26). Suggested decay scheme for  $\text{RaC}'$ .

Table 1.

End-point energy of $\beta$ -spectrum (keV)	Corresponding set of levels (keV)	Intensities after inclusion of partial to 609 keV state (%)
3.25	0	23
1.88	{ 1281 1378 1416 1544	17
1.50	{ 1661 1728 1764 1848	36
1.12	{ 2017 2117 2142 2204 2280	20

The study of the percentage intensities of the  $\gamma$ -radiations and  $\beta$ -particle excitations was based on the data of Nielsen (36) and Dzelepov and Sestopalova (16), which appear to constitute the most accurate sources of information on the relative  $\gamma$ -ray intensities. It is noteworthy that even between these sources considerable divergences do occur, and the



criterion used in the formation of the decay scheme was the measured intensities of the  $\beta$ -spectra.

The results of Ricci and Trivero (34), referred to previously, indicate the existence of a  $\beta$ -particle branch of end-point energy 2.56 MeV and intensity 6% to the 609 keV level. Johansson (31), on the other hand, concluded that such a transition could not have an intensity  $> 2\%$ . If it is assumed that the transition does occur, with  $\sim 4\%$  intensity, this is compatible with the expected first forbidden  $\beta$ -transition from the RaC ground state. The inclusion of the extra  $\beta$ -feed will have the effect of reducing the relative intensity values allocated to the four measured  $\beta$ -spectra, which will then have approximately the intensities shown in table 1.

The intensities of the  $\gamma$ -rays shown in the decay scheme have been derived principally from the measurements of Nielsen, but in a few cases where a somewhat higher intensity appeared to be necessary for conformity with the  $\beta$ -particle intensities, the values of Dzelepov and Sestopalova were used. Some of the weaker  $\gamma$ -rays shown in the scheme of Ellis have also been included, and again the intensities have been chosen as far as possible to agree with the  $\beta$ -particle measurements. The intensity of the strong 609 keV  $\gamma$ -transition has been taken as 41%, after the measurements



of Nielsen. With the values adopted for the intensities of the  $\gamma$ -radiations feeding the 609 keV state, the total incoming radiation provides an intensity level of 37.6%, which when combined with the 4%  $\beta$ -radiation branch to the state gives a total excitation in good agreement with the intensity of the  $\gamma$ -ray to the ground state. After subtraction of the total intensities of the  $\beta$ -radiations to the excited states in the decay scheme, a residual excitation of 23% appears as the intensity of the  $\beta$ -feed to the ground state. This again agrees with the experimental results.

For the levels above about 2400 keV, the  $\beta$ -excitations are likely to have been included in the Fermi analysis under the  $\text{RaB} \rightarrow \text{C}$  part of the spectrum. It seems likely that  $\beta$ -excitations amounting in intensity to about 4 - 5% will have been "lost" in this way, and thus the combined intensities of the remainder will be expected to reach only 96%. The intensities of the groups found experimentally, reduced to take account of this factor, are shown in table 2 overleaf, with the excitations required by the decay scheme for comparison.

Table 2.

Energy levels (keV)	Experimental Intensity (%)	Decay scheme excitations (%)
Ground state	22	22
609	4	4
1281 - 1544	16	13.5
1661 - 1848	35	37
2017 - 2280	19	17
Higher levels	4	6.5

It is interesting to compare the value obtained for the average  $\gamma$ -ray energy from Ra(B + C) with that obtained experimentally from the heating effect of the radiation. On the basis of the level scheme given by Nielsen for the RaC nucleus, the average  $\gamma$ -ray energy is 0.275 MeV per disintegration. With the decay scheme adopted here for the RaC' nucleus, the average  $\gamma$ -ray energy in the RaC' de-excitation is 1.50 MeV per disintegration. The total is then 1.775 MeV per disintegration, which is slightly lower than the value of 1.796 MeV given by Zlotowski (56). It is likely that owing to the uncertainties in intensity of the  $\gamma$ -radiations the relative intensities of several of the higher energy  $\gamma$ -rays have been underestimated in the construction of the decay scheme.

With regard to the general pattern of the level

scheme, relatively few direct disagreements occur with the results of other workers. According to both Demichelis and Malvano (24) and Rowland (54), coincidences occur between a  $\gamma$ -ray of energy 1.38 MeV and the 609 keV  $\gamma$ -ray. The interpretation of the 1378 keV  $\gamma$ -ray as representing a transition to the ground state, as given both by Feather and by Nielsen, has been preferred here, especially since the exhaustive measurements of Nielsen failed to detect the required coincidences. The latter interpretation was also adopted by Daniel and Nierhaus (35).

The comparison with the results of Daniel and Nierhaus for the energies and intensities of the partial  $\beta$ -spectra is also of interest. Table 3 below shows the results obtained by Daniel and Nierhaus, with those of the author for comparison.

Table 3.

Daniel and Nierhaus		Present Work	
End-point energy of partial $\beta$ -spectrum (keV)	Relative intensity (%)	End-point energy of partial $\beta$ -spectrum (keV)	Relative intensity (%)
3.26	19	3.25	22
1.88	9	1.88	16
1.51	40	1.50	35
1.02	23	1.12	19
0.42	9	$\lesssim 1.0$	4

The intensity limit placed by these authors on the intensity of the 2.56 MeV  $\beta$ -transition to the 609 keV state is 4%. It will be seen that while a good degree of agreement is observed between their results and the present work, particularly in respect of the end-point energies derived for the three hardest  $\beta$ -components, some divergence does exist for the intensity ratios, and this is particularly marked for the partial spectrum of end-point energy 1.88 MeV. In the decay scheme of Daniel and Nierhaus (fig. (27)), the total de-excitation intensity from the group of levels at 1281 - 1544 keV was 15.4%. This was derived by averaging over the results of several authors for the  $\gamma$ -ray intensities. No direct  $\beta$ -excitation to the 1544 keV state is shown in the scheme of Daniel and Nierhaus, and the level at 1281 keV is not included, but if it is assumed that the partial  $\beta$ -spectra leading to these states will contribute to the intensity of the 1.88 MeV partial, the relatively higher intensity obtained in the present work accords better with the expected intensity of the feed to this group of levels.

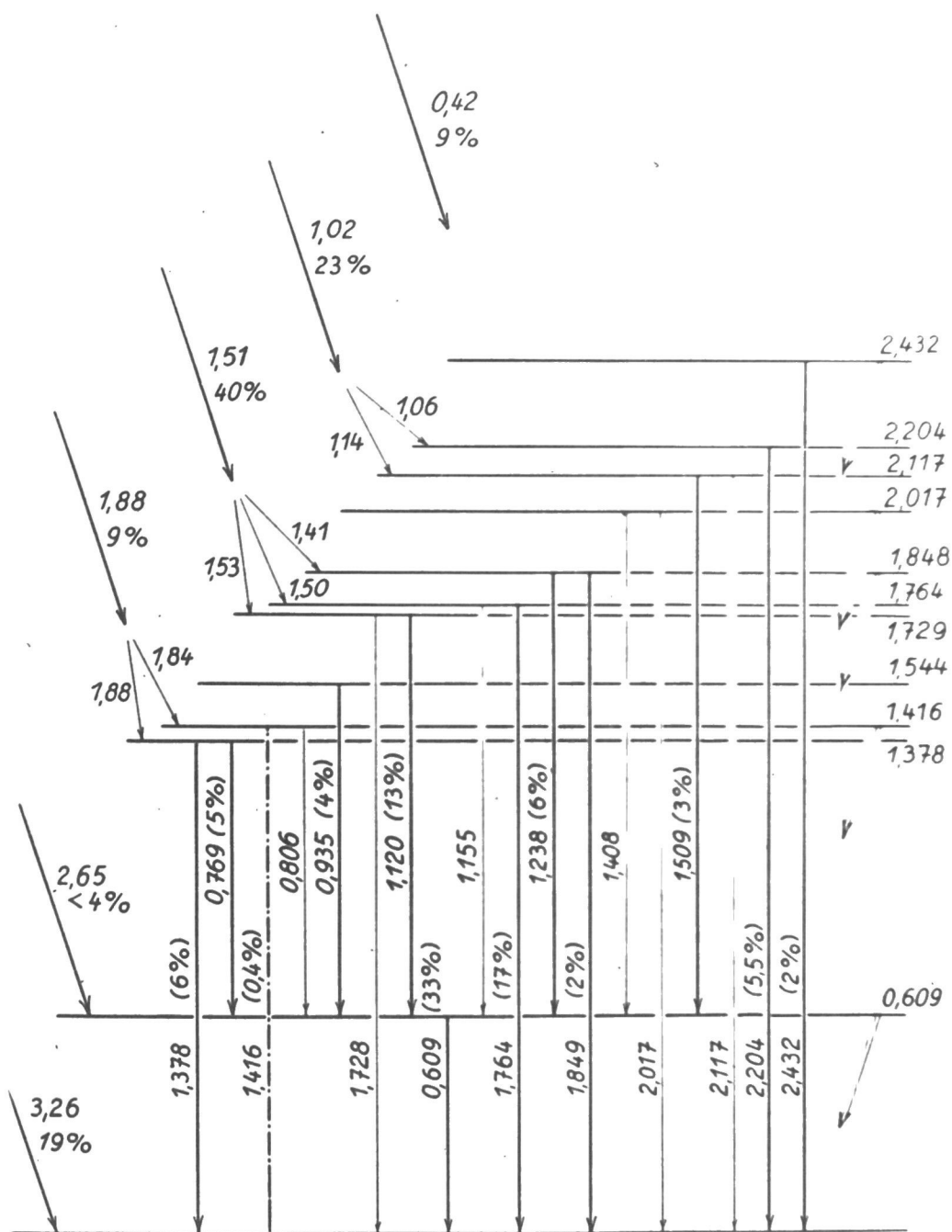


Fig. (27). Decay scheme of  $\text{RaC}'$  (Daniel and Nierhaus).

### § 3. Collective and particle excitations in the nuclei of $RaC$ and $RaC'$ .

One of the primary purposes in obtaining information about the positions and spin and parity characteristics of nuclear levels lies in the possibility of comparing the results derived with those predicted by the various forms of nuclear model. Even if the details of the internucleon interaction were known, the task of constructing exact nuclear wave functions for any but the simplest nuclei would be prohibitive, owing to the complexity of the many-body problem involved. Thus the principal methods of approach to the construction of a nuclear model involve drastic simplifications of the situation which can usefully be employed only in relatively restricted regions of mass and atomic numbers. The principal division of the models employed is into particle models and collective models.

The basic assumption of the particle model is that the interaction of any given nucleon within the nucleus with the remaining nucleons can be represented by a static spherical potential well, the nucleon moving in a field due to all others averaged by the Hartree approximation. With the additional assumption of a strong spin-orbit coupling, the states of the individual nucleons may be characterised by a set of quantum numbers as in the atomic case, and a shell structure derived. (The Pauli exclusion principle is assumed to

hold independently for neutrons and protons). The shape of the potential well and the strength of the spin-orbit coupling can be adjusted to provide agreement with the known values of the 'magic numbers', which are assumed to arise from shell closure.

To provide a basis for calculation of the ground state spins of nuclei, it was proposed by Mayer (57) that the form of the internucleon interaction was such that an even number of neutrons and protons in a given level combined to give a resultant spin of zero, while an odd number coupled to the spin  $j$  of that level. Thus for an odd mass nucleus, the observed spin should be that of the final nucleon. For an odd-odd nucleus such as RaC ( $^{214}_{83}\text{Bi}$ ) the situation is complicated by the necessity of combining the separate spins of the odd neutron and proton. According to the empirical coupling rule of Nordheim (32), if the spins of the odd particles are  $j_1 = \ell_1 \pm \frac{1}{2}$  and  $j_2 = \ell_2 \mp \frac{1}{2}$  respectively, then the resultant nuclear spin is  $|j_1 - j_2|$ , whereas if the spins are  $j_1 = \ell_1 \pm \frac{1}{2}$  and  $j_2 = \ell_2 \pm \frac{1}{2}$  respectively, the spin is  $> |j_1 - j_2|$ . It was remarked by Nordheim that in most cases, but not all, the latter type of combination seemed to give resultant spin values of the order of  $|j_1 + j_2|$ .

For RaC we have 1 proton and 5 neutrons outside the closed shells of magic numbers 82 and 126

respectively. It seems reasonable to assume that the extra proton will occupy the  $6h_{7/2}$  level, since it is known from the measurements of Back and Goudsmit (58) that the ground state spin of the isotope  $^{209}_{83}\text{Bi}$ , which also has one proton outside the closed shell, is consistent with this placing for the extra proton. The spectroscopic notation used is that of Klinkenberg (59), according to whom the first three levels for the odd neutron, in order of increasing energy, are  $6g_{7/2}$ ,  $7i_{11/2}$  and  $5d_{5/2}$ . The combination of the  $6h_{7/2}$  proton with the  $6g_{7/2}$  neutron by the Nordheim rule gives a resultant spin of 0 -. With the neutron in the  $7i_{11/2}$  state, the resultant spin is greater than one, and probably of the order of 10. With the neutron in the  $5d_{5/2}$  state, the resultant spin has the value 2 -.

The high spin value with the  $7i_{11/2}$  placing for the odd neutron would give rise to an isomeric state in  $\text{RaC}$ . There are several well-known examples of isomeric states which arise from the possible competition of states of high spin with states of low spin in odd-odd nuclei. For  $^{176}_{71}\text{Lu}$ , for example, Klinkenberg (60) has concluded that the ground state spin is  $10 \pm 1$ . Evidence has been given by Neumann, Howland and Perlman (61) for the existence of an  $\alpha$ -active isomeric state of high spin value in  $^{210}_{83}\text{Bi}$  (Feather (62)). A general survey covering a large number of nuclear isomers in relation



to shell structure has been given by Goldhaber and Hill (63).

If the high spin value does in fact correspond to an isomeric state in the nucleus of RaC, no trace of the presence of this state would be expected from measurements on the disintegration chain  $\text{RaB} \rightarrow \text{RaC} \rightarrow \text{RaC}'$ , since the degree of forbiddenness of the necessary  $\beta$ -transitions and the multipole order of any  $\gamma$ -rays involved would both be too great for the existence of these radiations in appreciable intensity. The possibility of the manifestation of the state through  $\alpha$ -emission, where the dependence of partial intensity on spin change is less than for the  $\beta$ -transitions, will be much reduced owing to the low overall intensity of  $\alpha$ -particle emission in the chain  ${}^{218}_{85}\text{At} \rightarrow {}^{214}_{83}\text{RaC} \rightarrow {}^{210}_{81}\text{RaC}''$ .

The spin value of 0 - will presumably correspond to an excited level of the type postulated in the decay scheme suggested earlier for the RaC nucleus.

None of the values obtained by the application of the simplest form of the single particle model agrees with the 1 - value based on the measurements in the present work. It must be remembered, however, that the extreme form of the single particle model represents a simplification of the nuclear structure which has had to be modified in several respects by the results of

experiment. One such modification is necessary to account for the fact that high spin values predicted by the particle model are not generally realised in the ground states of nuclei. The assumption is made that during the filling of levels it may be energetically favourable for two nucleons to occupy a level of high spin value, leaving any additional nucleon in a lower level with smaller spin. Another empirical modification has been introduced to explain observed spins such as that of  $^{107}_{47}\text{Ag}$  (Goldhaber and Sunyar (64)), where it was necessary to assume that three nucleons in the  $g_{7/2}$  level should combine to form a resultant spin of  $7/2$ . A similar situation occurs in  $^{23}_{11}\text{Na}$  and  $^{55}_{25}\text{Mn}$ .

Application of the second modification suggests that three of the extra nucleons in  $^{214}_{83}\text{RaC}$  may combine in the  $6g_{7/2}$  level to produce a resultant spin of  $7/2$ , which could combine with the  $7/2$  spin of the odd proton to give the resultant spin of 1, as required by the experimental evidence. A definite prediction of the spin value produced by this mechanism is precluded by the uncertainty as to the exact coupling rules to be applied when the resultant spin of the neutron shell arises from a relatively complicated combination of individual particles. The assumption that the coupling rule of Nordheim is inapplicable in such a

case seems preferable to postulating that the  $1 -$  spin value can be explained by the combination of an odd neutron in the  $6g_{7/2}$  level with the  $6h_{9/2}$  proton, giving a spin of  $1 -$  in direct contradiction to Nordheim's rule. It is of interest to note, however, that the application of this rule does not appear to be as universal as at first supposed (see, for example, Schwartz (65) and Pandya (66)).

It is also of interest to consider whether or not the decay scheme shown for RaC' furnishes evidence for the existence of levels explicable in terms of the collective nucleon motion. According to the theory developed by A. Bohr and his collaborators (67), for nuclei whose equilibrium shape deviates strongly from spherical symmetry, one can distinguish between two different modes of excitation, rotational and intrinsic. The rotational mode is associated with a collective motion which affects only the orientation in space while the internal structure of the nucleus remains unaltered; the intrinsic mode, on the other hand, may be associated either with vibrations of the nuclear shape or with the excitation of individual particles.

The quantization of the rotational motion is illustrated in fig. (28) overleaf. For strongly deformed nuclei possessing axial symmetry, the coupling scheme is distinguished by three constants of the

motion: the total angular momentum,  $I$ , its projection,  $M$ , on an axis fixed in space ( $z$ -axis), and its projection,  $K$ , on the nuclear symmetry axis  $z'$ .

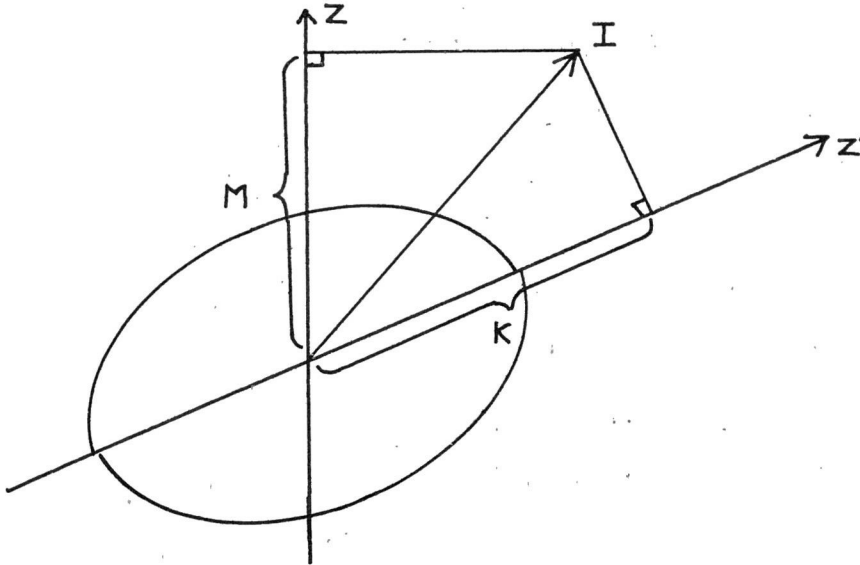


Fig. (28). Quantization of rotational motion.

The states in a rotational band are distinguished by the different values of the angular momentum  $I$ . In an even-even nucleus, the ground state has  $I = 0$  and  $K = 0$ , and the higher states are limited to angular momentum values

$I = 2, 4, 6 \dots$  with even parity, also with  $K = 0$ .

The energies of the states in the band are given, again for an even-even nucleus, by the relation

$$E = \frac{\hbar^2}{2\epsilon} I(I + 1)$$

where  $E$  is the excitation energy, and  $\epsilon$  is a form of the moment of inertia for the rotational motion, and

is dependent on the degree of nuclear deformation.

Although the energies of levels arising from collective vibrational motion of the nucleons are generally of the order of a few MeV, the levels arising from rotational excitation have energies of the same order of magnitude as those originating from the intrinsic particle excitations. The criteria used to distinguish between the modes of excitation are based on the regularities of spins and energies displayed by the rotational bands and also on the essential difference in transition probabilities between the two types of excitation. The E2 transition probabilities within a rotational family are strongly enhanced relative to those associated with a single particle transition.

The ground state of  $\text{RaC}'$  will have both  $I$  and  $K = 0$ . It seems likely that the  $2^+$  level at 609 keV will form the second member of a rotational band built up on the ground state. That this is probable may be seen by comparison of the ratios of de-excitation of the 609 keV state by  $\gamma$ -radiation and long-range  $\alpha$ -emission. According to the measurements of Rutherford, the relative intensity of the  $\alpha$ -particle group arising from the 609 keV level amounts to  $0.43 \times 10^{-6}$  per disintegration. By use of the formula given by Gamow and Critchfield (68) the disintegration constant

100.

for the long-range  $\alpha$ -particle group may be calculated as  $\sim 2 \times 10^5 \text{ sec.}^{-1}$ . Hence from the  $\gamma$ -ray and  $\alpha$ -particle intensity ratio the  $\gamma$ -ray transition probability is  $\sim 1.9 \times 10^{11} \text{ sec.}^{-1}$ . This may be compared with the value given by the formula of Weisskopf (69) for the transition probability for electromagnetic radiation for the single proton excitation case

$$T_{SP}^{EL} = \frac{4.4 (L+1)}{L [(2L+1)!!]^2} \left( \frac{3}{L+3} \right)^2 \left( \frac{\hbar \omega}{137 \text{ Mev.}} \right)^{2L+1} \times (R \text{ in } 10^{-13} \text{ cm.})^{2L} \\ \times S(j_i, L, j_f) \times 10^{-21} \text{ sec.}^{-1}.$$

where  $L$  is the multipole order of the radiation,  $R$  the nuclear radius, and  $S$  a statistical factor depending on the spins  $j_i$  and  $j_f$  of the initial and final states. For the 609 keV radiation in  $\text{RaC}'$  this becomes

$$T_{SP}^{EL} = 1.6 \times 10^8 \times (214)^{4/3} \times (0.609)^5 \times S(j_i, L, j_f) \text{ sec.}^{-1}$$

Owing to the lack of exact knowledge of the initial and final spins of the nuclear levels involved, some uncertainty exists as to the value of the function  $S$ , but it seems probable that it will be around 2. Taking a value of this order, the transition probability is of the order of  $3.4 \times 10^{10} \text{ sec.}^{-1}$ .

It would then appear that the 609 keV  $\gamma$ -transition is faster by about a factor of 5 than would

be predicted on the basis of transitions of a single particle. A summary by Bohr and Mottelson (67(d)) of the "enhancement factors" applicable to E2 transitions in even-even nuclei shows a fairly wide range of values from 10 ( $^{148}_{60}\text{Nd}$ ) to 170 ( $^{232}_{90}\text{Th}$ ). Since the lowest value given is applicable to a transition of only 300 keV, and the enhancement factor tends to increase as the transition energy decreases, the factor obtained above seems reasonable for a rotational transition. In addition, since the degree of enhancement increases with the nuclear deformation, a large value of the enhancement factor would not be expected as near to the closed shells as the nucleus of  $\text{RaC}'$ .

An alternative approach is to examine the ratio of the  $\gamma$ -transition probabilities from a higher state to the two levels considered. According to Bohr and Mottelson (67(d)), for electromagnetic transitions of multipole order  $L$  from a state characterised by the quantum numbers  $I_i$  and  $K_i$  to the members of a rotational sequence characterised by the symmetry axis component  $K_f$  and spins  $I_f, I'_f, \dots$ , the reduced transition probabilities ( $B$ ) satisfy the relation

$$\frac{B(L; I_i \rightarrow I_f)}{B(L; I_i \rightarrow I'_f)} = \left( \frac{\langle I_i L K_i K_f - K_i | I_i L I_f K_f \rangle}{\langle I_i L K_i K_f - K_i | I_i L I'_f K_f \rangle} \right)^2$$

where the quantities on the right are Clebsch-Gordon

coefficients for the addition of angular momenta (c.f. Condon and Shortley (70)). We can now consider the ratio of the transition probabilities for the M1  $\gamma$ -radiations from the state at 1764 keV to the 609 keV state and the ground state, taking the intensity of the 1764 keV  $\gamma$ -transition as 13%. Since the spin value of the 1764 keV state is  $1+$ , the possible values of  $K_i$  are 0 and 1. The substitution of each of these in the expression above leads to predicted values for the intensities of the 1155 keV  $\gamma$ -radiation of 26% and 6.5% respectively. Unfortunately neither of these is in good agreement with the value of 1.8% adopted in the decay scheme. The formula given by Bohr and Mottelson, however, was derived only for the highly deformed nuclei, and it is possible that the lack of agreement is due to the proximity of the present nucleus to the region of closed shells.

If the  $0+$  ground state and the 609 keV  $2+$  first excited state are taken as belonging to a rotational band, the known regularities in the energy spacings of the members of such a band would lead, if the degree of nuclear deformation were sufficiently large, to the expectation of a  $4+$  state at around 2000 keV. According to the empirical curve given by Asaro and Perlman (71), however, the ratio of the energies of the  $4+$  and  $2+$  states for the  $\text{RaC}'$  nucleus would be  $\sim 2$



rather than the value of 3.3 predicted from the application of the extreme level spacing formula given earlier. Thus the  $4 +$  level would be expected to lie around 1200 keV, and no evidence exists for such a level. This is possibly rather surprising, as although the degree of direct  $\beta$ -excitation to such a state would be rather small, it would be expected that the excitation could be provided by  $\gamma$ -transitions from several of the higher states.

It will be seen that despite the exhaustive surveys which have been carried out on the  $\text{RaC}'$  nucleus, particularly in recent years, considerable uncertainty still surrounds the detailed structure of the level scheme. The construction of a scheme with which useful theoretical comparison is possible will depend largely on the provision of more accurate values for the intensities of the  $\gamma$ -radiations and on studies of the  $\beta$ -particle spectra with a higher degree of resolution than was hitherto available. A further possible source of information might lie in the direct measurement of lifetimes of the excited states against  $\gamma$ -ray emission, provided that an extension of present techniques would permit accurate measurement in the region of lifetimes most likely to be encountered in the  $\text{RaC}'$  nucleus.

ACKNOWLEDGEMENTS.

The author is indebted to Professor N. Feather, F.R.S. for extending the facilities of his laboratory, and for his supervision of, and continuing interest in the investigation. Grateful thanks are due to Mr. J. Kyles, M.A. for his participation in, and supervision of the experimental work, and for many helpful discussions and constant encouragement and advice.

In addition, thanks are extended to Dr. R.D. Connor for the loan of the Rosenblum counter used in the range measurements on the  $\alpha$ -particles from the radon source.

REFERENCES.

1. Lord Rutherford, W.B. Lewis and B.V. Bowden,  
Proc. Roy. Soc. A 142, (1933) 347.
2. C.D. Ellis and G.H. Aston, Proc. Roy. Soc. A 129,  
(1930) 180.
3. O. von Baeyer, O. Hahn and L. Meitner, Phys. Zeits.  
12, (1911) 1099.
4. E. Rutherford and H. Robinson, Phil. Mag. (6), 26,  
(1913) 717.
5. C.D. Ellis, Proc. Roy. Soc. A 143, (1934) 350.
6. G.D. Latyshev, Rev. Mod. Phys. 19, (1947) 132.
7. K.C. Mann and M.J. Ozeroff, Canad. J. Res. A 27,  
(1949) 164.
8. G.N. Whyte, Canad. J. Phys. 30, (1952) 438.
9. M. Mladjenovic and A. Hedgran, Physica 18, (1952)  
1242.
10. R.M. Pearce and K.C. Mann, Canad. J. Phys. 31,  
(1953) 592.
11. J.M. Cork, C.E. Branyan, A.E. Stoddard, H.B.  
Keller, J.M. LeBlanc and W.J. Childs, Phys.  
Rev. 83, (1951) 681.
12. M. Mladjenovic and H. Slatis, Arkiv Fys. 8, (1954)  
65.
13. M. Mladjenovic and A. Hedgran, Arkiv Fys. 8, (1954)  
49.
14. J.L. Wolfson, Phys. Rev. 78, (1950) 176.

15. G. Backenstoss and K. Wohllleben, *Zeits. Naturf.*  
10a, (1955) 384.
16. B.S. Dzelepov and S.A. Sestopalova, *Supp. Nuovo*  
*Cim.* 3, (1956) 54.
17. R.H. Fowler, *Proc. Roy. Soc. A* 129, (1930) 1.
18. B.W. Sargent, *Proc. Roy. Soc. A* 139, (1933) 659.
19. M. Miwa and S. Kageyama, *J. Phys. Soc. Japan* 5,  
(1950) 416.
- S. Kageyama, *J. Phys. Soc. Japan* 6, (1951) 285.
- S. Kageyama, *J. Phys. Soc. Japan* 7, (1952) 93.
- S. Kageyama, *J. Phys. Soc. Japan* 8, (1953) 689.
20. A.H. Wapstra, *Physica* 18, (1952) 1247.
- A.H. Wapstra, *Thesis* (1953), Amsterdam.
21. C.D. Ellis, *Inter. Conf. Phys.* 1, (1934) 43.
22. W. Bothe and H. Maier-Liebnitz, *Zeits. f. Physik*  
104, (1937) 604.
23. N. Feather, *Nuclear Stability Rules*, p. 32.
24. F. Demichelis and R. Malvano, *Nuovo Cim.* 9, (1952)  
1106.
- F. Demichelis and R. Malvano, *Nuovo Cim.* 10,  
(1953) 405.
- F. Demichelis and R. Malvano, *Nuovo Cim.* 10,  
(1953) 1359.
- F. Demichelis and R. Malvano, *Nuovo Cim.* 12,  
(1954) 358.
- F. Demichelis and R. Malvano, *Phys. Rev.* 93,  
(1954) 526.

25. N. Feather and H.O.W. Richardson, Proc. Phys. Soc.  
61, (1948) 452.
26. D.E. Muller, H.C. Hoyt, D.J. Klein and J.W.M.  
DuMond, Phys. Rev. 88, (1952) 775.
27. R.W. Gurney, Proc. Phys. Soc. A 109, (1925) 540.
28. L.H. Gray, Proc. Roy. Soc. A 159, (1937) 263.
29. N. Feather, Beta- and Gamma-Ray Spectroscopy  
(ed. K. Siegbahn) p. 748.
30. F. Demichelis and L.A. Radicati, Nuovo. Cim. 3,  
(1956) 152.
31. S.A.E. Johansson, Arkiv Fys. 9, (1955) 561.
32. L.W. Nordheim, Rev. Mod. Phys. 23, (1951) 322.
33. R.W. King, Rev. Mod. Phys. 26, (1954) 327.
34. R.A. Ricci and G. Trivero, Nuovo Cim. 1, (1955) 717.  
R.A. Ricci and G. Trivero, Nuovo Cim. 2, (1955) 745.
35. H. Daniel and R. Nierhaus, Zeits. Naturf. 11a,  
(1956) 212.  
R. Nierhaus and H. Daniel, Zeits. Naturf. 12a,  
(1957) 1.
36. K.O. Nielsen, O.B. Nielsen and M.A. Waggoner,  
Nuclear Physics 2, (1956) 476.  
O.B. Nielsen, Physical Society Conference (Edin-  
burgh), December, 1956. Also private  
communication.
37. N. Feather, Beta- and Gamma-Ray Spectroscopy (ed.  
K. Siegbahn) p. 750.

38. N. Feather, J. Kyles and R.W. Pringle, Proc. Phys. Soc. 61, (1948) 466.
39. J. Kyles, C.G. Campbell and W.J. Henderson, Proc. Phys. Soc. A 66, (1953) 519.
40. J.C. Knight, Thesis, University of Edinburgh (1953).
41. J.D. Cockcroft, C.D. Ellis and H. Kershaw, Proc. Roy. Soc. A 135, (1932) 628.
42. F.H. Wells, J. Brit. Instn. Rad. Engrs. 11, (1951) 491.  
I.A.D. Lewis and F.H. Wells, Millimicrosecond Pulse Techniques, p. 161.
43. P.R. Bell, Beta- and Gamma-Ray Spectroscopy (ed. K. Siegbahn) p. 134.
44. F.F. Momyer, Thesis (1953), University of California. Issued as UCRL-2060.
45. R.D. Connor, Proc. Phys. Soc. B 64, (1951) 30.
46. I. Feister, privately distributed tables.
47. E. Feenberg and G. Trigg, Rev. Mod. Phys. 22, (1950) 399.
48. W. Stanners and M.A.S. Ross, Proc. Phys. Soc. A 69, (1956) 836.
49. K. Smith, quoted by C.S. Wu, Beta- and Gamma-Ray Spectroscopy (ed. K. Siegbahn), p. 343.
50. E.M. Krisyounk, A.G. Sergeyev, G.D. Latyshev and V.D. Vorobyov, Nuclear Physics 4, (1957) 579.
51. L.A. Sliv and I.M. Band, privately distributed tables.

52. M.E. Rose, G.H. Goertzel and C. Swift, privately distributed tables.
53. H. Daniel, Zeits. Naturf. 11a, (1956) 759.
54. R.E. Rowland, Phys. Rev. 99, (1955) 757.
55. H. Daniel, Zeits. Naturf. 12a, (1957) 194.
56. I. Zlotowski, J. Phys. Radium 6, (1935) 242.
57. M.G. Mayer, Phys. Rev. 75, (1949) 1969.
58. E. Back and G. Goudsmit, Zeits. f. Physik 47, (1928) 174.
59. P.F.A. Klinkenberg, Rev. Mod. Phys. 24, (1952) 63.
60. P.F.A. Klinkenberg, Physica 17, (1951) 715.
61. H.M. Neumann, J.J. Howland and I. Perlman, Phys. Rev. 77, (1950) 720.
62. N. Feather, Phil. Mag. 42, (1951) 568.
63. M. Goldhaber and R.D. Hill, Rev. Mod. Phys. 24, (1952) 179.
64. M. Goldhaber and A.W. Sunyar, Phys. Rev. 83, (1951) 906.
65. C. Schwartz, Phys. Rev. 94, (1954) 95.
66. S.P. Pandya, Phys. Rev. 108, (1957) 1312.
67. (a). A. Bohr, Phys. Rev. 81, (1951) 134.  
 (b). A. Bohr, Dan. Mat. Fys. Medd. 26, (1952) no. 14.  
 (c). A. Bohr and B. Mottelson, Dan. Mat. Fys. Medd. 27, (1953) no. 16.  
 (d). A. Bohr and B. Mottelson, Beta- and Gamma-Ray Spectroscopy (ed. K. Siegbahn) p. 468.

67. (e). G. Alaga, K. Alder, A. Bohr and B.R. Mottelson,  
Dan. Mat. Fys. Medd. 29, (1955) no. 9.  
(f). A. Bohr, P.O. Froman, and B.R. Mottelson, Dan.  
Mat. Fys. Medd. 29, (1955) no. 10.
68. G. Gamow and C.L. Critchfield, Theory of Atomic  
Nucleus and Nuclear Energy Sources, p. 174.
69. V.F. Weisskopf, Phys. Rev. 83, (1951) 1073.
70. E.U. Condon and G.H. Shortley, The Theory of  
Atomic Spectra, p. 241.
71. F. Asaro and E. Perlman, Phys. Rev. 91, (1953) 763.



Appendix.

Since the completion of the main body of the thesis, a further paper on the nucleus of  $\text{RaC}'$  has appeared. In this paper, Bishop (72) has attempted the construction of a level scheme on the basis of scintillation studies of the  $\gamma$ -radiations, including measurements on the internal conversion coefficients, angular correlations between cascade  $\gamma$ -rays and transition probabilities derived from the intensities of the  $\gamma$ -radiation in comparison with the known intensities of the long-range  $\alpha$ -particle groups. The decay scheme postulated by Bishop is shown in fig. (29), and it will be seen that considerable similarity exists between this scheme and that advanced in the present work. The main difference between the two schemes is the inclusion in the scheme of Bishop of a level at 830 keV, which has not been suggested by previous workers. The existence of this level was based on measurements of  $\beta$ - $\gamma$  coincidences.

Another divergence is the assignment of the spin value  $0 +$  to the state at 1281 keV. Such an assignment is in conflict with the result of Johansson (31), who assigned an intensity of 2% to the 1281 keV  $\gamma$ -ray in emission. Such an intensity would not be expected for an E0 transition to the ground state.

For the state at 1544 keV, the assignment  $3 +$  was

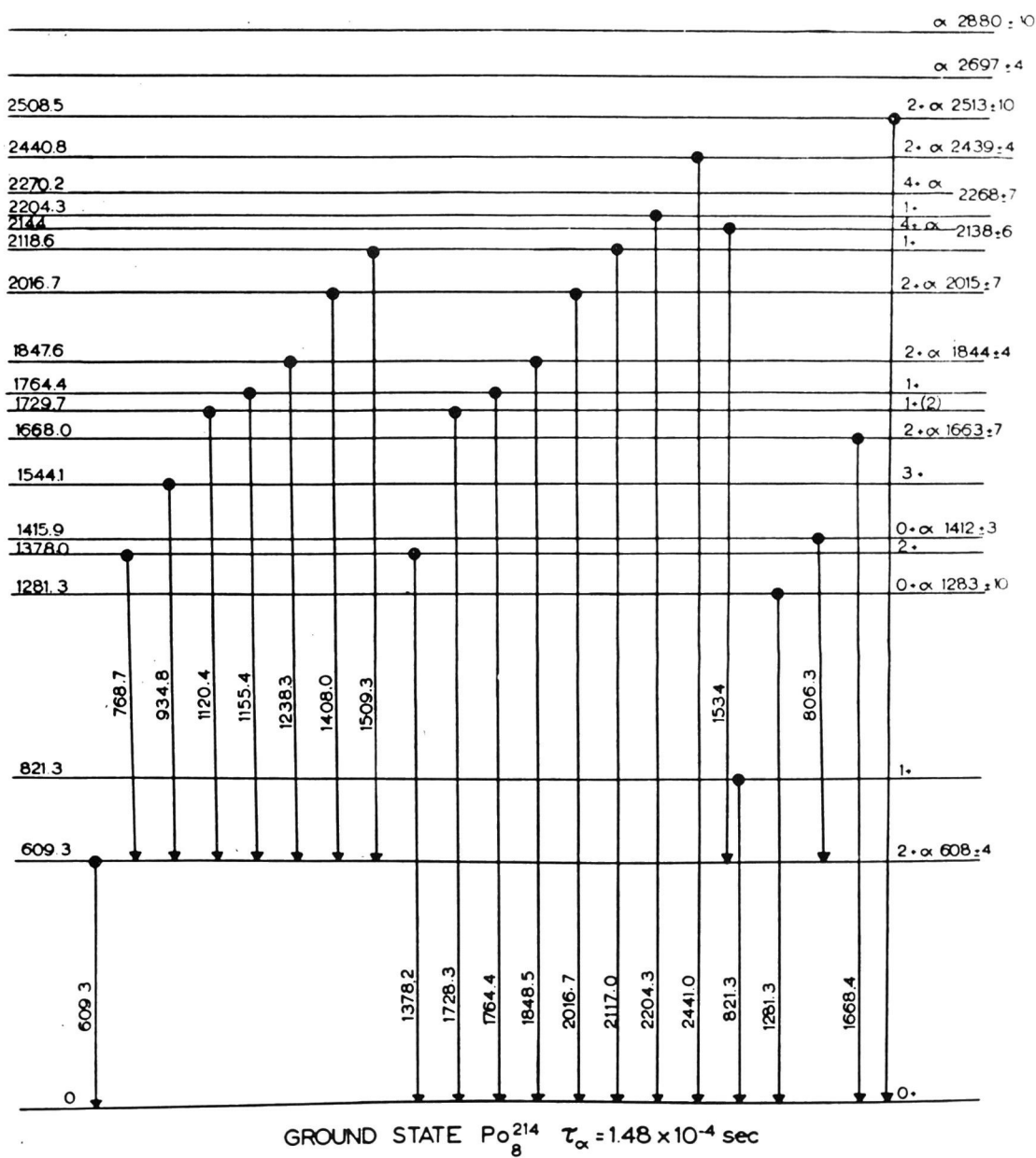


Fig. (29). Decay scheme of  $\text{RaC}'$  (Bishop).

preferred to the  $1 +$  value adopted in the present work. The choice was based on the absence in detectable intensity of the  $\gamma$ -radiation to the ground state.

Evidence was also quoted for the existence of collective effects in the nucleus of  $\text{RaC}'$ . It was found that several of the E2 radiations were faster than expected on the basis of particle transitions. For the 609 keV state, for example, the de-excitation  $\gamma$ -ray was found to be about three times faster than the theoretical value based on the single particle formula. The value of three would appear to be based on a numerical miscalculation, the correct result for the enhancement factor from the given data being about four. Bearing in mind that the  $\alpha$ -particle lifetimes were obtained without taking account of the effect of spin change in the transition, the enhancement factor still agrees well with that derived in the present work.

It was also suggested by Bishop that the 2144 keV state, which was given the assignment  $4 +$ , might be the third member of the rotational band containing the ground state and the 609 keV ( $2 +$ ) level. Since the energy ratio of the third to second state would then be 3.5, this suggestion seems much less satisfactory than the possibility, also advanced in the paper, that the 2144 keV state is the second member of a rotational

band beginning at the 1544 keV level, on the assumption that the spin value of this state is indeed  $1 +$ . Evidence was given to support the suggestion that the 1378 keV state is formed by collective nucleon vibration, as was originally suggested by Alder et al. (73).

The enhancement factor quoted for the E2 transition from this state, in order that the  $\gamma$ -radiation might compete successfully with the  $\alpha$ -particle emission, is of the order of 100.

A further recent contribution to the  $\text{RaC}'$  decay scheme is a paper by Dzelepov et al. (74) on the Compton spectrum of the higher energy  $\gamma$ -rays of  $\text{RaC}'$ . The existence of weak  $\gamma$ -rays of energies 2450, 2684, 2768, 2893, 2992 and 3070 keV was reported. Of these, the  $\gamma$ -rays of energies 2450, 2684, 2893 and 2992 keV could correspond within the energy limits to de-excitations from four of the levels postulated in the present work. It is particularly interesting to obtain some direct confirmation of the level postulated earlier at around 3000 keV. The other two  $\gamma$ -rays, on the other hand, would have to be associated with additional levels which must be added to the already complex decay scheme.

ADDITIONAL REFERENCES.

72. G.R. Bishop, Nuclear Physics 5, (1958) 358.
73. K. Alder, A. Bohr, T. Huus, B. Mottelson and  
A. Winther, Rev. Mod. Phys. 28, (1956) 432.
74. B. Dzelepov, S. Sestopalova and I. Uchevatkin,  
Nuclear Physics 5, (1958) 413.